National Défense
Defence nationale

UNCLASSIFIED

(2)

UNLIMITED
DISTRIBUTION

DRES

AD-A222 658

SUFFIELD MEMORANDUM

NO. 1272

A REVIEW OF LARGE SCALE AND SMALL SCALE UNDERWATER THERMAL EXPLOSIONS

by

M. Rizk

PCN 011SA

April 1990

DEFENCE RESEARCH ESTABLISHMENT SUFFIELD, RALSTON, ALBERTA

Canada

UNCLASSIFIED

DEFENCE RESEARCH ESTABLISHMENT SUFFIELD
RALSTON, ALBERTA

SUFFIELD MEMORANDUM NO. 1272

A REVIEW OF LARGE SCALE AND SMALL SCALE UNDERWATER THERMAL EXPLOSIONS

by

M. Rizk

UNCLASSIFIED

ABSTRACT

This report contains a review of large scale propagating thermal explosions and small scale single drop explosions. The review of large scale propagating thermal explosions identifies potential thermal explosive systems, as well as the experimental conditions and geometrical configurations, conducive to the establishment of thermal detonations.

The review of small scale single drop explosions identifies experimental data relevant to the design of detonating systems of thermal explosives. In addition, the effect of various thermodynamic parameters on the strength of both spontaneous and triggered single drop explosions is predicted qualitatively based on two promising fragmentation mechanisms; a new vapour/gas melt supersaturation mechanism and the water entrapment mechanism. It is shown that the vapour destabilization and nucleation phenomena which constitute the heart of the two fragmentation mechanisms govern single drop thermal explosions. The experimental data, however, is neither conclusive nor sufficient for the development of a predictive model. For some molten metal water systems (Aℓ/water), the data was found to be incomplete and in the case of Fe-$A\ell_2O_3$/water, a system of particular interest, there is no available data. Recommendations are made for new experimental studies to rigorously assess the two fragmentation mechanism and to obtain a better understanding of vapour explosion phenomenon in general.

TABLE OF CONTENTS

LIST OF TABLES

LIST OF FIGURES

LIST OF FIGURES (cont'd)

LIST OF FIGURES (cont'd)

INTRODUCTION

The use of conventional solid high explosives underwater, results in a short lived shock wave that decays exponentially with distance. A steam bubble is then created leading to subsequent pressure pulses of decreasing amplitude (see Figure 1). For some targets (minefields, ice-cap clearing ...), long duration effects and area coverage are more important than short duration localized pulses obtained with solid explosive charges.

Above ground, the detonation of distributed low density explosives (fuel air explosives, ...) forming a cloud covering a large area results in the whole area being subjected to detonation pressures. It may be possible to achieve the same results underwater by detonating a coarse mixture of very hot and cold fluids separated by a vapour film such as a dispersion of molten metal drops in water. The detonation process is illustrated in Figure 2.

It is believed that a triggering shock travelling in a mixture of hot and cold fluids in stable film boiling will collapse or destabilize the film separating the molten drops from the cold fluid [1 & 2]. The molten metal drops will subsequently fragment in the fragmentation region. Due to the increase in heat transfer area, explosive vapourization will take place. The resulting shock catches up with the triggering shock thus enhancing it. Fragmentation of the molten drops further downstream will ensue and the propagating shock may develop into a self-sustained detonation. The energy released behind the shock in this case is thermal in origin as opposed to being chemical origin in conventional explosives. We will therefore refer to mixtures of explosive hot and cold fluid as dispersed thermal explosives.

Thermal explosions can be very energetic. They have been the cause of serious accidents in the metal, paper, liquid gas and nuclear industries. Two of the most serious accidents that took place in Canada are:

a. Quebec Foundry accident (January 1960)
   In this accident 45 kg of molten steel fell into a shallow trough containing 300 ℓ of water. The explosion cracked a 0.5 m thick concrete floor and killed a worker, [3].
b. NRX reactor, Ontario (12 December, 1952)
   The NRX reactor is a water cooled research reactor with a thermal load of 40 MW. During an experiment, a melting aluminum cover fell into the coolant. The subsequent explosion lead to the destruction of the fuel element sheath, releasing radioactive UO_2 into the water. The SPERT-I test reactor accident in the US is also attributed to a thermal explosion.

Thermal explosions can occur in a large number of molten metal/water systems. Only a few were judged suitable for studying their use as distributed underwater thermal explosives namely, tin/water, aluminum/water and Fe-$A\ell_2O_3$/water. In addition, since the thermitic reaction used to produce molten Fe-$A\ell_2O_3$ may also produce molten FeOx, the systems FeOx/water and Fe/water will also be reviewed.

The molten tin/water system was chosen because tin is easy to melt (T_m = 232°C), has been studied extensively and has been observed to explode vigorously. The molten Aℓ/water system was chosen because Aℓ also reacts chemically with water. This chemical reaction could produce stronger or more reproducible thermal explosions. The Fe-$A\ell_2O_3$ was chosen because it is a practical system. Molten Fe-$A\ell_2O_3$ can be

obtained from the thermitic or metallothermic reaction of Aℓ and Fe_2O_3 powders. These powders are safe, cheap, and easy to transport. Molten Fe-$Aℓ_2O_3$ can be prepared in the field without an oven. We note however, that the Fe-$Aℓ_2O_3$ system is more complex than the previous two, and that Fe reacts with steam to form hydrogen.

In this study we will review recent small-scale (or single drop) and large scale molten metal/water experimental studies for the above systems. Special emphasis will be placed on the review of large scale experimental studies in which a shock (or detonation) was observed to propagate in the coarse mixture of molten metal and water. As for small scale or single drop thermal explosions studies they are important because they shed some light on the fundamental mechanisms of thermal explosions. Like chemical reactions in the case of chemical detonations, single drop explosions are considered to be the building blocks of propagating thermal explosions. As such, the parameters affecting single drop explosions are also expected to affect propagating thermal explosions.

Before proceeding with the review, we briefly summarize some of the theories presented in the literature to explain single drop vapour explosions.

THERMAL EXPLOSION THEORIES

Some of the theories are:

(a) hydrodynamic fragmentation;
(b) shell theory;

(c) water entrapment in the melt (homogeneous nucleation);
(d) melt supersaturation with vapour and or gas; and
(e) water entrapment by melt on solid surface cavities (heterogeneous nucleation).

Hydrodynamic Fragmentation

In this theory the relative motion of the hot and cold liquid is assumed to induce hydrodynamic fragmentation of the drop which in turn results in the subsequent explosive vapourization of the water. Fragmentation due to relative motion between the hot and cold fluid occurs at a certain critical Weber number (We_c = 10 to 20),

$$We = \rho V_r^2 \ell / \sigma, \qquad (1)$$

where ρ is the density, V_r is the relative velocity, ℓ is characteristic length (radius) and σ the surface tension.

Fragmentation may result from:

i) Rayleigh-Taylor instabilities [4];
ii) Kelvin-Helmholtz instabilities [5]; and
iii) Boundary layer stripping [6].

These mechanisms have only been shown to cause coarse fragmentation (mm size) and not (μm size) fragmentation, as observed in most thermal explosions [4].

Shell Theory

If We < We_c, hydrodynamic fragmentation does not take place. However, cooling and crystallization of the hot liquid may play a role, especially in the case of molten metal oxides. During solidification, a temperature gradient can develop in the solid phase. If the induced thermal stresses are large enough, fragmentation of the partially solidified particle may take place with subsequent explosive vapourization of the water [7].

Water Entrapment in the Melt (Homogeneous Nucleation Theory)

In this concept, first suggested by Buchanan [8], it is assumed that explosive nucleation of water entrapped in the melt leads to melt fragmentation due to induced stresses in the melt. Melt fragmentation is then followed by explosive vapourization. Water entrapment is assumed to result from cavitation bubble collapse near the molten metal, from vapour dome collapse or other film instabilities [9].

A superheated liquid is a liquid in a (P, V, T) state which is in a region where at least part of it would normally have undergone a phase transition and become a vapour. Figure 3 shows the stable and metastable region (M) on a P-T diagram. Point 0 is the initial stable liquid state. Point 1 is the superheated final state. There is a limit, however, to how much a liquid can be superheated without explosive (or non-explosive) homogeneous nucleation occurring [10 & 11]. We note that in contrast to hydrodynamic fragmentation, homogeneous nucleation is a fast process and usually takes place in less than a millisecond.

Melt Supersaturation with Vapour and/or Gas

A melt supersaturation with gas mechanism was first proposed by Nelson and Buxton [12], to explain molten drop inflation and subsequent quiescent fragmentation observed in some of their experiments. In this mechanism it is assumed that gases dissolve in the melt at high temperatures. As the melt temperature drops, the gas solubilities in the melt decreases, resulting in gas bubble formation with subsequent melt fragmentation due to induced stresses in the melt.

Ward [13] proposed a new vapour/gas melt supersaturation mechanism. In this mechanism it is assumed that for melts above the critical water temperature, both vapour and gases dissolve in the melt. As the melt cools, or if the pressure changes, the melt may become supersaturated with vapour. The vapour precipitates into water droplets. The water droplets are pushed by the solidifying front towards the hot center and nucleate explosively resulting in a thermal explosion.

Water Entrapment by the Melt on Solid Surface Cavities (Heterogeneous Nucleation)

In this concept, it is assumed that trapped vapour/gas and water pockets at cavities on the solid surface act as embryos for bubble formation. Bubble formation induces stresses in the melt and causes subsequent melt fragmentation and explosive vapourization [14]. Heterogeneous nucleation does not require large superheats and occurs much more readily than homogeneous nucleation.

The theories presented above to explain the thermal explosion phenomenon are all plausible. However, none of them have been subjected to systematic or quantitative experimental evaluation.

In the next sections, some of the small and large scale experiments pertaining to the systems of interest will be reviewed in detail. Factors relevant to the design of an experimental program to study thermal detonations will be identified. In addition the validity of the various concepts discussed above will be assessed.

PROPAGATING THERMAL EXPLOSIONS

Propagating thermal explosions have been observed to occur under suitable experimental conditions in the course of large scale experiments on molten metal/water interactions. They have been observed in molten Aℓ/water systems, molten tin/water systems and molten Fe-$Aℓ_2O_3$/water systems.

Molten Tin/Water Systems

Board and Hall [15] carried out a study to investigate the propagation of small scale thermal interactions in molten tin/water using high speed photography to observe the progress of the interaction.

In a first set of experiments, a single mass of molten tin (50 g) at 800°C was poured onto a shallow crucible and immersed in water. The system pressure originally 13 kPa was suddenly raised to ∿0.1 MPa by rupturing a diaphragm connecting the apparatus to the atmosphere. The vapour film collapsed within 1 ms of the diaphragm rupture. The explosion took place within the next 250 μs. The maximum generated pressure pulse was 0.4 MPa, with a positive duration of 1 ms.

Board and Hall [15] noted the existence and collapse of a series of 10 vapour domes on the vapour film just before the explosion. The collapse of such vapour domes can lead to the formation of liquid jets which will penetrate the tin at estimated velocities of ∿100 m/s giving rapid fine scale mixing. Board and Hall [15] surmized that the jets cause molten tin fragmentation which in turn generates a thermal explosion. To interpret the propagation phase of the explosion they propose that the pressure pulse due to a small localized interaction increases the pressure in the surrounding liquid sufficiently to collapse the film on an adjacent tin drop. Thus triggering the next localized explosion and soon.

Board and Hall [15] conducted a second series of experiments to investigate the hypothesis that the propagation of a thermal explosion is a result of self driven vapour film collapse. In these experiments, 200 g of molten tin were poured into an aluminum trough, 30 cm long with a shallow V cross section, immersed in an open water vessel at 80°C.

At low tin temperatures (∿650°C), a thermal interaction occurred spontaneously near one end of the crucible. At higher tin temperatures (∿750°C), there was no spontaneous interaction but interaction could be initiated via an impulse applied to one end of the crucible by a steel rod. In both cases the propagation phenomena were the same. The weak interaction at one end resulted in a localized but much more vigorous vapour dome growth and collapse. During the growth phase of the dome a second interaction was initiated 10 to 15 cm away, near the center of the crucible. During the growth of the latter region a third interaction was initiated at the far end. The time interval between interactions was 2.5 ms. The pressure pulses generated were ∿70 kPa in magnitude and quite long (∿3 ms). Film collapse occurred

only in cold areas at ends and center of the trough where a guide tube contacted the trough.

Board and Hall [15] suggested that the discontinuous propagation sequence is due to the open geometry of their apparatus resulting in weak coupling between the neighbouring tin areas. They therefore proceeded to study the propagation of a thermal interaction in a confined geometry. The apparatus in this series of experiments consisted of a narrow tank (20 cm long x 3 cm wide x 15 cm high, with one perspex face) filled with water at 80°C. A mass of tin 200 g at 700°C was poured in the tank. Tapping of the tank base near one end resulted in a minor and localized interaction at the tin/water interface. However, 10 ms later a vigorous explosion began and propagated 15 cm along the tank at $\sim 5 \times 10^3$ m/s before the pressure dropped and the explosion propagation stopped. The tin at the other end of the vessel exploded 5 ms later. This test series showed that in a confined geometry and under appropriate conditions the continuous propagation of an explosion through self-driven vapour blanket collapse is possible.

In 1979, Hall et al., [16] conducted a new experimental study to further investigate the continuous propagation of a thermal explosion in a confined geometry consisting of a long and narrow tube. The water vessel used in this series of experiments is shown in Figure 4. It consists of a 2.8 cm diameter, $\sim$100 cm long tube. The tube was made either of 3 mm thick steel or of 3 mm thick borosilicate glass for visualization experiments. A small furnace located above the water vessel was used to melt the tin. A small detonator (0.1 g PETN) was used to trigger the explosion in some of the tests. The water temperature was varied between 85°C and 95°C. The tin temperature was varied between 600 and 750°C and the amount of tin released was either 75 ml or 180 ml. Four Kistler type 603B pressure transducers located on the

apparatus walls were used to record the strength of the explosion. Two high speed cameras (10 x 10^3 frames per second) and a video camera were used for flow visualization in some of the experiments.

Eight tests in all were conducted, five of which were successful (T2, T4, T5, T7 and T8). A summary of the experimental results is given in Table I. In all tests, whether the explosion was triggered spontaneously by contact with cold water (20°C) at the bottom of the tube or by means of a detonator, the pressure records indicated a pressure spike of large amplitude (8 MPa to 11 MPa) with short rise time (<50 μs) characteristic of a shock wave, as shown in Figure 5. The pressure spike is followed by a pressure plateau at 3-4 MPa. In general, the shock front propagation velocity ranged from 300 m/s to 60 m/s with the larger values near the bottom of the tube.

Flow visualization showed that the molten tin mass breaks into 3-5 mm drops upon entry (comparable with the Weber break up scale, $\sigma/gD\rho$, where σ is the surface tension) and appears to reclump later on. When the shock front reaches the tin, the tin seems to be unaffected by the shock. Tracking of features behind the shock front was difficult, but suggests flow velocities of 20 m/s. The tin clumps appear to reach these velocities in ∿400 μs.

The Chapman-Jouguet (C-J) plane at which the flow reaches the velocity of sound could not be directly observed. However, its distance behind the shock front could be inferred from one of the experiments in which the glass tube break was observed to follow within 15 cm of the front without affecting its propagation. This suggests that the break lies beyond the C-J plane and that the reaction zone length is less than 15 cm. Hall et al., [16] note that in a few detonation models, the C-J plane is assumed to occur when the pressure is half

that of the shock peak. If this is the case, most pressure traces in this test series with 50/50 tin/water volume ratios indicate a reaction zone length of 1.5 cm to 3 cm.

The post explosion debris were of two types. Debris found external to the apparatus were very fine with a diameter <30 μm. Debris found in the tube were collected in honeycomb like clumps and had a foam like appearance. In general, as will be discussed in the section on small scale experiments; 1) the size of the debris are a measure of the explosion strength (the smaller their size, the stronger is the explosion); 2) the foam like appearance of the debris and their porosity suggest that the melt fragmentation results from the nucleation of water droplets (water entrapment or vapour/gas supersaturation mechanisms).

Experiments to study the propagation of large-scale thermal interactions in molten tin/water were also carried out by Fry and Robinson [17 & 18] at the Winfrith Atomic Energy Establishment. Only the tests in which continuous or coherent propagation of the thermal interaction was observed will be discussed.

Fry and Robinson [17] used a narrow, 8 mm wide, water vessel (glass walled on 2 sides) to provide more confinement (see Figure 6). High speed cine-films were used to observe the progress of the interaction in the tests. A detonator located at one end of the catch tray was used to trigger the explosion. Two tests were successfully conducted (T107, T109). The results are summarized in Table II.

In each test, 6 kg of molten tin at 800°C was poured in the water at ∿85°C. In the first test, for which only one detonator was used, there was an observable delay in the explosion. The resulting

shock wave front propagated at 81 m/s. The maximum generated pressure was 1.7 MPa. The pressure rise time was 320 μs. In the second test, for which two detonators were used there was no observable delay. The shock wave front propagated at ∿120 m/s, generating a maximum pressure of 3.4 MPa with a pressure rise time of 320 μs. The records in Figure 7 show the pressure recorded from pressure transducers 50 mm apart. The propagation velocity was observed to vary linearly with P_{max}, characteristics of a shock front (Figure 8). Since no perturbations were observed ahead of the front, Fry and Robinson surmized that the front velocity was at least sonic.

The post-explosion debris were pitted in appearance. Their sizes ranged from 2 mm to less than 45 μm. Gas absorption techniques were used to measure the surface area (10-200 m^2/kg) which was found to be much larger than that indicated by the size distribution. The debris were thus highly porous, indicating that fragmentation was due to the nucleation of water droplets in the melt (water entrapment or vapour/gas supersaturation mechanism).

In summary, Fry and Robinson [17] and Board and Hall [15] obtained continuously propagating vapour explosions along a film of molten tin in water. The maximum generated pressures, however, were low (∿3 MPa). Using a long tube instead, Board and Hall [19] was able to obtain propagating vapour explosions (shock or detonation wave) with much higher peak pressures (11 MPa). It is surmized, that the confined geometry of the steel tube is more conducive for the propagation of vapour detonation.

Molten Aℓ/Water Systems

Although many large scale experimental studies have been carried out on this system, only Fry and Robinson [17 & 18] carried out experiments to study the propagation of large scale thermal interactions in molten aluminum/water mixtures. They used high speed cine-films to observe the progress of the interaction.

In the first test series, an open rectangular vessel (450 mm x 4000 mm x 80 mm) was used. In the two tests discussed in their paper [17], the water temperature ranged from 8 to 10°C. The molten aluminum (∿800°C) had a mass of 3 kg in the first test and 7 kg in the second.

In these two tests, a spontaneous trigger appeared to initiate the vapour explosion event. The vapour explosion was then observed to propagate through the mixture. The propagation front could not be defined properly but was recognized by the definitely blurred region behind it. It could also be identified with the passage of a pressure wave through the mixture. In general, there was no increase in pressure ahead of the front suggesting that it must be sonic at least. The pressure front propagation velocities were 76 m/s and 120 m/s, respectively. The peak pressures were 1.2 MPa and 6 MPa with corresponding rise times between 1600 μs and 800 μs.

In a second series of tests, Fry and Robinson [17] used a partially roofed cylindrical vessel (300 mm is radius and 200 mm high) to provide strong confinement. The vessel walls were made of steel or perspex. Pressure transducers located on the walls of the vessel were used to measure the strength of the explosion. Two tests are discussed. In the first test, a mass of 7 kg of molten aluminum at 790°C was dropped into water at 6°C contained in a steel cylindrical vessel.

In the second, a mass of 7 kg at 800°C was dropped in water at 14°C contained in a perspex vessel. In both tests, the interaction was triggered by a very strong pressure pulse from a detonator attached underneath the center of the base of the vessel.

In the first test, the propagation velocity of the pressure front was observed to be 409 m/s, and the maximum generated pressure was 40 MPa with shock rise time of 90 μs. In the second test, the propagation velocity was 301 m/s, and the maximum generated pressure was 21 MPa with a rise time 106 μs. It is to be noted that the propagation velocities and maximum generated pressure are much higher in a partially roofed cylindrical vessels than in the open rectangular vessels used in the first series.

In a third series of tests, the experiments were carried out in vessels that were made very narrow (8 cm) in comparison with the depth (45 cm) and width (∿40 cm) (see Figure 6). The front and rear walls were transparent. A catch tray ∿5 cm above the base was used to collect the molten aluminum. The interaction was triggered by firing a detonator, attached to the side wall of the vessel, to produce an interaction propagating horizontally through the metal/water mixture on the tray. Two tests are discussed (T120 and T122). In these tests aluminum charges of 5 kg at 820 and 807°C are dropped in water at 24 and 18°C, respectively. The observed shock wave front coincided with a rapid increase in pressure to 40 and 60 MPa respectively, and propagated at a velocity of ∿350 m/s. Figure 9 shows the recorded pressure transducers signals from test T120.

The variation of the velocity of the pressure front with the peak pressure, (P_{max}) from these experiments are also included in

Figure 8. It can be observed that it has the characteristics of a shock front. Whether the shock wave front also has the characteristics of a detonation front has not been established, but the front propagation velocity appears to be at least sonic.

The post-explosion debris were pitted in appearance with size ranging from 2 mm to 40 μm. Gas absorption techniques indicated a rather large debris surface area (1000 m^2/kg) with respect to the one calculated by assuming spherical globules. That seems to indicate that the debris are porous, thus suggesting that fragmentation in the case of self-sustained propagating shock wave results from the nucleation of water droplets in the melt.

Table III gives a summary of the Winfrith experiments, involving Aℓ/water mixtures, with coherent interactions propagating continuously. In brief, the Fry and Robinson [17 & 18] experiments indicate that a coarse mixture of molten aluminum drops (0.1 to 1 cm in diameter) in water is detonable. Use of a triggering detonator in confining cylindrical or rectangular geometry generally results in the propagation of stronger shocks with higher propagation velocities. The maximum generated pressure can be quite high (∿60 MPa), with corresponding pressure rise times less than a millisecond.

Molten Fe-$Aℓ_2O_3$/Water

Molten Fe-$Aℓ_2O_3$ mixtures can be obtained from the combustion of Aℓ-Fe_2O_3 thermitic powder mixtures. The thermitic powders are cheap, safe, easy to transport and can be ignited in situ. Most of the experiments conducted to date using Aℓ-Fe_2O_3 powders have been carried out at the Sandia Laboratories in Albuquerque.

Buxton & Benedick [20] carried out a series of large scale experiments to investigate the thermal to mechanical work conversion ratio in molten Fe-Al_2O_3/water mixtures. Their apparatus consisted of an open tank lying on crushable honeycomb blocks. The mechanical work generated by the thermal explosion was calculated by measuring the impulse on the bottom and estimating the potential energy of the ejected fuel debris and water. The melt quantity varied between 10-20 kg, and had temperatures of ∿3000K. The temperature of the untreated water was varied from ambient to near saturation. Fifty experiments were conducted.

Spontaneous explosions were observed to occur in all cases even when the water was near saturation temperature. The explosion probability however was somewhat reduced at high temperatures due to the increased film stability. Detonators (0.6 g PETN explosive) were also used to trigger the thermal explosions in some tests. Triggered explosions were observed to be no different from spontaneous ones.

The generated pressure spikes were high (∿20 MPa), and the pressure rise time was less than a millisecond, but no propagation front could be identified from the high speed camera (3000 and 5000 fps) records.

As the mass of water was increased, the thermal/mechanical conversion ratio (thermal energy available/mechanical work from explosion) was found to rise from 0.2% to 1.4%. Increased confinement using a vessel cover also increased the conversion ratio.

Photographs of the sieved debris showed that in general the debris are mossy. Some spherical particles were hollow as though they contained gas or vapour pockets. Some of the mossy material was found

to be an agglomerate of both α-iron and aluminum oxide suggesting that they both participated in the explosion. In small scale experiments molten Fe/water mixtures do not explode spontaneously. Buxton and Benedick [20] therefore surmize that the molten Al_2O_3 ($T_m \sim 2300K$) exploded first subsequently triggering the Fe/water thermal explosion.

The instrumentation used in the open geometry test series by Buxton and Benedick [20] was rather rudimentary. A fully instrumented intermediate scale series of experiments (EXO-FITS) was carried out by Mitchell et al., [21]. The apparatus consisted of a rectangular parallelepiped, of square cross-section (60 mm x 600 mm x 760 mm), with an open top, made out of 6.3 mm thick plexiglass (see Figure 10). The melt quantity was varied from 0.6 to 5.3 kg at a temperature of ∿2727°C. The water/fuel ratio could be varied from 20 up to 50. The water was untreated with the temperature ranging from 9°C to 27°C. Three high speed cameras were used to photograph the event. Two ran at 9000 frames per second (fps) and one at ∿200 fps.

Mitchell et al., [21] observed that, in general, the fuel intermixes for about 0.2 seconds. The resulting average diameter of the molten globules is between 10 and 20 mm. A spontaneous perturbation near the base of the apparatus generally triggers the thermal interaction which then develops into a shock that propagates towards the top of the vessel at a speed of 200-600 m/s. The generated pressure spikes are high and narrow with a peak of 20 to 150 MPa, and rise times less than a millisecond. The pressure spike is usually followed by a lower sustained pressure tail at ∿10 MPa. Characteristic pressure traces are shown on Figure 11. Figure 12 shows various interface and wave front positions.

It is known that for chemical detonations there is both a density and diameter effect on the detonation velocity in cylindrical charges. Mitchell et al., [21] assumed that the melt-coolant charge diameter corresponds to the average diameter measured from the outlines of the melt/water mixture and that the apparent fuel density corresponds to the melt mass divided by the total melt/water mixture volume. Figure 13 shows the effect of average charge diameter on the propagation velocity of the explosion front. Just as in chemical detonations, the front velocity increases with the average charge diameter. Figure 14 shows that the propagation velocity peaks at a specific density (i.e., a specific melt/water ratio). The authors note that this dependence of velocity on density is analogous to that observed in oxygen rich and oxygen deficient chemical explosive mixtures. The authors therefore suggest that there is a strong analogy between chemical and thermal detonations.

A parametric study of the effect of melt entry velocity, fuel mass and pressure showed that spontaneous explosions were suppressed if:

i) the velocity at entry was larger than 6 m/s; and
ii) the fuel mass was less than 1.8 kg.

The thermal explosions could be triggered once again however, if a detonator (0.6 g PETN) was used to initiate them.

Mitchell et al., [21] also carried out a series of experiments (FITSA) in an enclosed vessel as part of the fully instrumented test series. Use of the enclosed vessel allowed all fuel debris from the thermal explosions to be collected and analyzed, and the initial pressure to be varied. In this series of tests, the melt Fe-Al_2O_3 was

maintained at 2727°C and its mass was varied from 1.94 kg to 5.58 kg. The water was untreated and the water temperature ranged from 10°C to 25°C. The initial pressure ranged from 0.083 to 1.09 MPa. Five tests were conducted (FITS1A to FITS5A).

The authors observed that no spontaneous explosions took place at an initial pressure equal or larger than 1.09 MPa. The thermal explosion could however, be triggered if a detonator (0.6 g PETN) was used to initiate it (FITS5A).

The debris data from the thermal explosion of tests FITS3A (initial pressure 0.083 MPa) and FITS5A (1.09 MPa) exhibited a bimodal distribution with a peak near 300 μm and another near 38 μm (the smallest sieve used). The water temperature was 24°C and melt mass 5.28 kg in both tests.

Figure 15 shows the debris surface area as a function of the average sieve size as obtained using gas absorbtion or BET techniques. The authors observe that the surface areas calculated assuming that the debris consist of solid spherical particles are two order of magnitude smaller than those measured (5000-25000 m^2/kg) suggesting that the debris are highly porous with extensive crack formation. In addition, the debris from FITS5A (P_{max} = 130 MPa) were at least twice as porous as those from FITS3A (P_{max} = 70 MPa).

Mitchell and Evans [22] used the fully instrumented test apparatus to study the effect of larger melt masses (i.e., to study the effect of scaling on propagating thermal explosions). In this series of tests, the melt mass and temperature were held at 18.7 kg and ∿3100K, respectively. The water temperature was varied between 36°C

and 46°C. The water/melt mass ratio was varied between 1.5 and 15. Nine tests were carried out (FITS1B to FITS9B).

It was observed that for water/melt mass ratios (M_w/M_f) less than 1.5 no steam explosion took place. For M_w/M_f = 1.5, there was no steam explosion pressure peak but a large steam generation pressure rise followed possibly by hydrogen combustion as shown in Figure 16. For M_w/M_f > 1.5, a significant steam explosion pressure peak and associated pressure plateau were observed, as illustrated in Figure 17. As in the intermediate scale experiment, the explosion was preceded by fragmentation of the melt into 1-2 cm diameter globules and the pressure front propagated quickly (200-600 m/s) through the mixture. For M_w/M_f > 12, double explosions separated by ∿120 ms occurred in some instances.

One test was carried out at a water temperature of ∿99°C near the saturation temperature. Several trigger like perturbations were observed but did not result in a propagating thermal explosion due to the increased film stability.

Marshall et al., [23] also carried two series of experiments to study the thermal explosions of Fe-Al_2O_3 melt. The first coarse mixing (CM) test series was carried out to study melt quiescent fragmentation as it enters water at near saturation conditions. The second alternate contact mode test series (ACM) was carried out to study what happens when water enters a pool of molten Fe-Al_2O_3.

The apparatus used in the CM test series was the EXO-FITS apparatus (Figure 10). The initial pressure was 0.082 MPa, the melt mass was 18.5 kg, at a temperature of ∿3000K. The melt entry velocity ranged from 2.4 to 6 m/s and the coolant to fuel mass ratio ranged from

6 to 58. In some tests the removable crucible bottom of the melt chamber was allowed to fall with the melt. Twelve tests were conducted. Ten with water near saturation and two with subcooled water. Thermal explosions were observed to occur in both tests with subcooled water.

In general, when the water was near saturation, violent surface interactions occurred upon melt entry and the melt was dispersed. The surface interactions were attributed to the large amount of hydrogen released by the Redox reaction of steam and iron. These tests showed that the probability of a thermal explosion when Fe-$A\ell_2O_3$ melts are dropped in water near saturation is small but not zero.

In the ACM test series, 10 kg of iron/aluminum thermite were prepared in a graphite crucible. Water was gently poured in the crucible. Two tests were conducted. In the first, 0.5 ℓ of water were poured into the crucible and a violent explosion ensued. In the second, water was introduced after 4.5 seconds from completion of the thermite burn and there was no explosion. The authors assume that a solid crust had formed on top of the melt. These experiments show that explosions can occur in the alternate contact mode.

In summary, the large scale studies performed at Sandia National Laboratories have shown that propagating thermal explosions may take place in coarse mixture of molten Fe-$A\ell_2O_3$/water, for melt globules 10-20 mm in size, subcooled water and M_w/M_f mass ratio ranging from 1.5 to 15. The generated shock waves are characterized by high and narrow pressure peaks (20-150 MPa) followed by a sustained pressure tail. The effects of apparent melt density and melt-coolant charge diameter on the propagation velocity of the explosion are similar to that in a mixture of oxygen rich and oxygen deficient explosives in chemical detonations. It can therefore be concluded that Fe-$A\ell_2O_3$/

water mixtures are detonable and that the induced pressures are relatively large.

Summary and Discussion

It can be concluded that in order to obtain a self sustained propagating shock wave, the molten material has to be in a prefragmented state before it is initiated either by a spontaneous instability or a triggered pressure pulse. The droplet diameters for which propagating thermal explosion fronts have been observed range from ∿0.1 to ∿2.0 cm.

The initiation of propagating thermal explosions by a small spontaneous trigger in some of the molten metal/water systems considered shows that a fragmentation mechanism effective at low shock strength does exist [16]. At high water temperature, however, a stronger trigger must be used to initiate propagating thermal explosions. There seems to be no major differences between the strength of triggered and spontaneously initiated explosions.

The propagation of quasi-steady self sustained shock wave fronts is favoured in confined geometries such as narrow and long cylinders and cylinders with a covered top. There seems to be no major differences between intermediate and large scale propagating thermal explosion [20].

The propagating shock front is generally characterized by a high (9-100 MPa) and narrow (50-900 μs) pressure spike followed by a pressure plateau of (∿2-20 MPa). The velocity of propagation of the self sustained shock front is at least sonic. The effect of factors such as apparent melt density and average charge diameter on the front

velocity is similar to that observed in chemical detonations. The reaction zone length and the C-J plane have not been directly observed. However, Board and Hall [19] inferred from one of their tin/water experiments that the reaction length is this system is less than 15 cm. The above observations strongly suggest that the quasi-steady, self sustained, supersonic (at least sonic) shock wave front propagating in a cloud of dispersed molten metal drops and water is in fact a thermal detonation.

The molten metal debris are mossy or coral like in appearance with bubble like cavities in some instances (Aℓ/water). Their sizes range from ∿10 μm to 500 μm. The debris appearance suggests a fragmentation mechanism based on the nucleation of water droplets in the melt (water entrapment or vapour/gas supersaturation mechanisms).

If propagating thermal explosions are ordered according to their strength, the strongest ones have been observed in the Fe-$Aℓ_2O_3$/water system (P_{max} = 150 MPa), followed by the Aℓ/water system (P_{max} = 40 MPa) and finally the tin/water system (P_{max} = 9 MPa). The corresponding debris surface area measured using gas absorption techniques is also largest for the Fe-$Aℓ_2O_3$/water system (10000 to 25000 m^2/kg), followed by the Aℓ/water system (∿1000 m^2/kg).

Table IV gives a brief summary of the experimental conditions (melt temperature, water temperature, etc.), and explosion characteristics (maximum generated pressure, rise time, etc.), of the strongest explosions observed to date in each of the three systems reviewed.

The experimental facts presented above indicate that the potential use of coarse mixture of molten metal and water as distributed

underwater thermal explosives is therefore worth investigating with the Fe-Al_2O_3/water system presenting the best potential.

We note, however, that in all the experimental studies the molten material intermixed before the explosion. The initial coarse mixture size distribution was unknown and the initial mixture density could be inferred at best. No systematic study of the effect of these factors on the characteristics of the thermal detonation has been carried out. The effect of some other factors such as dissolved gas content in water, initial pressure etc., which are expected to particularly affect thermal detonation have not been examined. Except for tin/water systems [17], the effect of the strength and duration of the initiating shock in the case of triggered propagating thermal explosions has also not been investigated.

SINGLE DROP THERMAL EXPLOSIONS

Single drop thermal explosions are the building blocks (like chemical reactions in chemical detonations) of propagating thermal explosions or thermal detonations. More specifically, studies of single drop thermal explosions may lead to an understanding of the mechanisms of thermal explosion and eventually to the development of predictive models for propagating explosions. It is reasonable to assume that the governing parameters for single drop explosions also affect propagating thermal explosions and that the initiation of single drop explosions is related to the initiation of propagating thermal explosions. Studies of single drop thermal explosions also provide an experimental data base that can be of direct use in the design and control of experiments on propagating thermal explosions.

In this section, we will review experimental studies that have been carried, in various laboratories, on the thermal explosions of single molten drops of tin, Aℓ, Fe, FeOx and $Aℓ_2O_3$. (No studies, however, seem to have been carried to date on the thermal explosion of single drops of Fe-$Aℓ_2O_3$ in water.) We will then thoroughly analyze the available experimental data. Two promising thermal explosion theories; the water entrapment theory and the vapour/gas melt supersaturation theory, will be evaluated by critically examining whether they can predict the effect of various thermodynamic parameters on the strength and limiting behaviour of thermal explosions. Finally, new experimental studies to further our understanding of thermal explosions will be proposed.

Molten Tin/Water System

We first consider molten tin/water systems. The effect of various parameters on the strength of thermal explosions in this system have been thoroughly investigated.

One of the parameters considered because of its expected major effect on the explosion strength is the water temperature. Asher et al., [24] used a small flask filled with degassed water to study the effect of water temperature on the explosion strength (see Figure 18). The ambient pressure was provided by a Helium blanket. About 15 g of molten tin at 700°C was released through an orifice at the top of the flask. The water temperature was varied between 15°C and 65°C, at various ambient pressures (0.06 to 0.14 MPa). The strength of the explosion was assessed from the percentage disintegration (PD) by weight of the tin.

As shown in Figure 19, the PD at a given temperature were not reproducible. However, an envelope could be drawn around the experimental points, to define an inner area or interaction zone in which thermal explosions occurs and an outer area in which there are no explosions. In general, as the water temperature (T_w) was raised, the PD first increased, reached a maximum and then rapidly decreased. At a well defined cutoff maximum water temperature (COT_w^{max} = 60°C at atmospheric pressure), thermal explosions ceased to take place.

Shoji and Takagi [25] also investigated the effect of the water temperature on the strength and probability of spontaneous thermal explosions. They released a 5 g molten tin drop into distilled water. The ambient pressure was provided by an air blanket. The strength of the explosion was assessed by measuring the explosion pressure, some 20 mm below the explosion center.

Figure 20 shows the variation of the strength and probability of explosion of a molten tin drop (T_{mi} = 700°C) with water temperature (0-100°C). The results of Shoji and Takagi [25] and Asher et al., [24] are similar. However, Shoji's cutoff maximum water temperature at atmospheric pressure (COT_w^{max} = 80°C) is 20°C larger. We note that Shoji et al. (1983) used a different blanket gas (air as opposed to Helium) to maintain the ambient pressure.

Shoji and Takagi [25] suspected that the vapour explosion phenomena is related to the boiling regimes. They therefore carried out a second study [26] in which they monitored the temperature of the molten tin. They were able to record not only the initial tin temperature (T_{mi}) but also the tin quench temperature (T_Q) at which the film is destabilized (see Figure 21) and the tin explosion temperature

(T_{ve}), for various bulk water temperatures (0°-80°C) and corresponding degrees of water subcooling ($\Delta T_{sub} = T_{boiling} - T_w$). As shown in Figure 22, thermal explosions only occurred within a domain of melt and water temperatures (i.e., thermal interaction zone or TIZ) bounded from above by the quench temperature (T_Q) or minimum stable film boiling temperature and from below by a melt/water interface temperature, T_I, equal to the homogeneous nucleation temperature of water (T_{HN}). Thus, spontaneous thermal explosions can only take place if two conditions are met: i) the film surrounding the molten drop has to be unstable; and ii) the melt/water interface temperature (T_I) has to be higher than the homogeneous nucleation temperature of water (T_{HN}). Shoji and Takagi [26] also observed that for initial melt temperatures (T_{mi}) lying above the T_Q line there was a delay in the explosion since the melt had to cool first. No delay was observed for melt temperatures within the TIZ.

The cutoff maximum water temperature (COT_w^{max}) as determined by the intersection of T_Q and T_{HN}, is seen to correspond to the cutoff at ∿80°C shown in Figure 20. Thus the COT_w^{max} appears to correspond to conditions of stable film boiling and a melt/water interface just below T_{HN}, which explains why explosions cease altogether, at this limit. Moreover, since T_{HN} is very sensitive to the type and amount of dissolved gas in the water [10], one would expect different blanketing gases to result in different intersection points and therefore different COT_w^{max}. This explains the different value of COT_w^{max} obtained by Asher et al., [25] in their experiment with a helium blanket.

A second parameter expected to have a major effect on the explosion strength is the melt temperature, (T_{mi}). Figure 23 shows the

effect of raising the initial melt temperature (300° to 850°C), on the strength and probability of thermal explosions, for a fixed water temperature (T_w = 30°C). There is a cutoff minimum melt temperature ($COT_{mi}^{max} \sim$ 300-400°C) below which thermal interactions are non-violent. As the initial melt temperature (T_{mi}) increases the explosion strength increase until a maximum of ~0.2 MPa at (T_{mi} = 700°C) is reached. We note that COT_{mi} seems to correspond to a melt/water interface temperature (T_I) just below T_{HN}, as shown in Figure 22.

Various other authors also investigated the effect of water and melt temperature on tin/water thermal explosions. Miyazaki et al., [27] let a water droplet (5 mm diameter) fall from various heights (i.e., for various Weber number, $We = \rho V_r^2 \ell/\sigma$) onto a molten tin drop whose temperature was monitored. The ambient pressure was provided by an Argon blanket. Figure 24 shows their results. The shape of the thermal interaction zone (TIZ) for various Weber numbers is similar to that of Shoji and Takagi [26]. For We ≥ 25, corresponding to drop heights h ≥ 5.5 cm, (i.e., for good thermal contact) the TIZ ceases to depend on Weber number and the cutoff maximum water temperature (80°C) is identical. However, the observed COT_{mi} is only 290°C, which is less than that observed by Shoji et al., [26]. This may be due to the different blanketing gas, argon, used by Miyazaki et al., [27]. The authors noted that in general vapour explosions take place in less than a millisecond and can clearly be distinguished from purely hydrodynamic break up due to collisions which takes several milliseconds.

In their study of the effect of water and initial tin temperature on molten tin/water vapour explosions, Tso et al., [28] released 3 g molten tin drop at various temperatures (250° to 900°C) into water maintained at various temperatures (0° to 100°C). They estimated the

strength of the explosion from the percentage disintegration by weight (PD). Based on the extent of fragmentation they were able to subdivide the thermal interaction zone (TIZ) into four zones, as shown in Figure 25:

a. Zone A corresponds to 100% fragmentation. The debris have coral like features and their size range from a few μm to 5 mm;
b. Zone B corresponds to a lesser percentage of fragmentation than Zone A. The debris have localized pockets of coral like appearance;
c. Zone C corresponds to the transition zone between fragmentation and non-fragmentation. The molten drop subdivides into globules with cavities on one side and a smooth side where the metal first contacted the water; and
d. Zone D corresponds to the domain of no explosions. The globules are round and shiny.

Tso et al., [28] suggest that the hollows and coral like appearance of the melt are due to the nucleation of water droplets enclosed in the melt. We recall, that explosions of maximum strength were observed by Shoji and Takagi [25] for a melt temperature of 700°C and a water temperature of ∿45°C (Figure 20). This point falls well within Zone A of maximum explosion strength.

Fröhlich and co-workers [29 & 30] considered the alternate contact mode in which a mass of liquid water (0.125 to 1 g at 20°C) is ejected at various velocities through a small water outlet (diameter 1 to 10 mm) into a crucible filled with molten tin at various temperatures (247° to 327°C) (see Figure 26). For melt temperatures below ∿267°C, which the authors consider to be the homogeneous nucleation

temperature of water, no explosions were observed. Figure 27, shows that the probability of thermal explosion increases with discharge velocity and decreases with water outlet diameter. For high discharge velocity (>5 m/s) and smaller outlet diameter (0.5 mm to 1 mm), the probability of explosion is 100%. These results were interpreted as follows: for high water injection velocities (>5 m/s), the film is stripped away. The jet breaks up into droplets. If the droplets are smaller than a critical size (which they estimated to be ∿157 μm from heat transfer consideration), they are heated through to the center to a temperature above T_{HN}. Vigorous flash vapourization result in an explosion. In general, the strength of the explosions does not depend on the mass of water but rather on the number of droplets less than the critical size. Thus, these results indicate that the explosive nucleation of water droplets plays a direct role in vapour explosions.

A third parameter expected to have a major effect on thermal explosions is the ambient pressure. Asher et al., [24] investigated the effect of increasing ambient pressure (0.06 to 0.14 MPa) on the explosion strength of molten tin. The ambient pressure was provided by a Helium blanket. Figure 19 shows that as the pressure is raised, for fixed melt initial temperature (T_{mi} = 700°C) and water temperature (T_w = 40°C), the explosion strength goes through a maximum at ∿0.12 MPa.

Raising the ambient pressure affects not only the explosion strength but also the cutoff maximum water temperature. Figure 28 shows that as the pressure is raised, COT_w^{max} also goes through a maximum. In addition it shows that for a water temperature less than 60°C, there are two cutoff pressures COP^{min} and COP^{max} corresponding to

COT_w^{max}. The two cutoff pressure can also be clearly seen in Figure 29.

Figure 29 also shows two sets of curves: a first set (solid line) for distilled water with the ambient pressure provided by nitrogen; and a second (dashed line) for distilled water, with the ambient pressure provided by air. The curves are similar but not identical, demonstrating that the type of blanketing gas does have an effect on vapour explosions even for distilled water. Thus the different ambient pressures at which an explosion of maximum strength takes place in the experiment by Shoji and Takagi [25] and Asher et al., [24] may be attributed to the different blanketing gases used.

A fourth parameter expected to have a major effect on the explosion strength is the gas concentration in the water. Asher et al., [31] investigated the effect of various gases (N_2, O_2, N_2O and CO_2) on the strength of thermal explosions, for various water temperatures (15 to 65°C). Figures 30a to 30d show that as the amount of gas dissolved in the water increases, the explosion strengths, as characterized by the percentage disintegration (PD), steadily decreases. For large amounts of gas in dissolution (CO_2 and N_2O), explosions can be altogether suppressed. The COT_w^{max} also decreases with increasing gas content in the water.

The effect of increasing the amount of a given type of gas dissolved in water (CO_2), at a fixed water temperature (20°C), on the percentage disintegration is shown in Figures 31a and b. In general, as the gas concentration is raised, the PD decreases somewhat, until a well defined cutoff maximum gas concentration ($COC_{CO_2}^{max}$ = 100 ml/kg) is reached at which thermal explosion are suddenly suppressed. The cutoff maximum gas concentration in the water seems to increase with

increasing gas solubility. Thus for CO_2, which is more soluble in water than N_2O, the cutoff maximum gas concentration is larger (100 ml/kg for CO_2 versus 75 ml/kg for N_2O).

In summary, the effect of various parameters on spontaneous tin/water explosions has been examined extensively by various authors. The maximum explosion strength of single drop is relatively low ($\sim$0.3 MPa). In general the vapour explosion phenomena takes place in much less than a millisecond. There is some evidence, that vapour explosions are due to fragmentation caused by the explosive nucleation of water droplets in the melt. This would explain the fast pressure rise times.

Small scale tin/water explosion triggered by a shock are not much different from spontaneous explosions [29, 30, 31, 32 & 33]. It is suggested that the rarefraction tail following the shock that initiates the vapour explosion in this case. However, no systematic study of the effect of various parameters (trigger strength, duration, water temperature, etc.) on triggered single drop thermal explosions of molten tin have been carried out to date.

Molten Aluminum/Water System

Anderson and Armstrong [34] have conducted an experimental program to study small-scale aluminum/water vapour explosions. Two systems were considered. In the first system, water was injected into a large mass of molten aluminum. In the second system, molten aluminum was injected into a large mass of water.

In one series of experiments, low and high velocity jets of water (20°C) were injected both above and below the surface of a mass

of aluminum (0.13 kg at ∿1000°C). The jets were at least 0.5 mm in diameter and had a velocity of ∿400 m/sec. No explosions were observed. We recall that Fröhlich et al., [29] using the same system with molten tin did observe vapour explosions.

In a subsequent series of tests, a small mass of water (0.7 g) at 20°C in a small glass sphere was dispersed into 1 kg of molten Aℓ at ∿900°C using an exploding wire. Explosions were observed for wire of energies higher than ∿380 joules. Since higher exploding wire energies produce smaller water droplets upon dispersion, it may be surmized that there is a threshold water droplet size above which there are no explosions. Above this threshold size, the water droplets cannot be heated to above the homogeneous nucleation temperature.

Two well instrumented test series were conducted using the second system. In the first test series, a molten mass of Aℓ (∿10-30 g or 1-2 cm in radius) at 800°C was dropped and collected at the bottom of a relatively large vessel (15 cm x 10 cm x 10 cm) containing water at 20-37°C. An exploding wire (5-10 cm away) was used to shock the melt and the bubble surrounding it. Below a threshold trigger pressure of 5 MPa (measured ∿5-10 cm away from a 80 J discharge) there were no explosions. Above the threshold the generated pressure pulses (measured 5-10 cm from the explosion source) were of the same magnitude as the initiating trigger pulse.

In the second test series, a much smaller water tank was used (3.8 mm x 5 cm x 2.5 cm deep). The bridgewire energy was varied between 200 and 720 J. The purpose of this test series was to look for evidence of a chemical reaction between the aluminum and the vapour, as would be indicated by light emission. Of the twenty-five tests conducted only three tests indicated some chemical reaction (light emis-

sion). The measured pressure and force from those tests were not significantly different from those without light emission. Interestingly, in one of the tests with no light emission (aluminum temperature = 800°C, water temperature = 30°C, trigger energy = 1500 J and droplet mass = 28 g) the maximum pressure generated was 22 MPa. However, allowing the molten aluminum drop to collect at the bottom of the vessel may lead to water/gas being trapped in the roughness of the vessel bottom. Heterogeneous nucleation of this entrapped water when subjected to the negative pressure tail of the trigger pulse may account for this high pressure.

Nelson and Buxton [12], using the arc melting apparatus shown in Figure 32, also investigated thermal explosions in Aℓ/water. A bridgewire or a minidetonator 5 cm away from the 8 g Aℓ drop was used to produce triggering pulses with maximum pressures of 1-2 MPa and 20 MPa, respectively, at the drop position. The water temperature was 23°C, and an argon blanket was used to provide the ambient pressure. Thermal explosions did not occur. The apparent discrepancy between these results and those of Anderson and Armstrong [34] are likely due to the different experimental conditions. The droplet collected at the bottom of the water chamber in the latter experiments could account for the different observations, as discussed above. The melt temperatures may also have been very different since these were not monitored by Nelson and Buxton. Moreover, the molten drop was heated in argon in one set of experiments and allowed to fall freely in a vapour/air atmosphere in the other set of experiments.

In brief, experimental studies have shown that thermal explosions can occur in single drop aluminum/water systems, if a shock of adequate strength (≥5 MPa, 5 cm away) is applied. Maximum generated pressures as high as 22 MPa have been measured. Nucleation, either

homogeneous or heterogeneous, appears to play a role in the explosion process. In some cases oversaturation of the molten sample with gas may explain molten drop inflation and fragmentation [12]. Molten Aℓ drop explosions caused by a free falling drop in water without the effects of heterogeneous nucleation at the bottom of the vessel should be investigated to resolve the apparent discrepancy between the two sets of experiments.

Molten Fe/Water System

Nelson and Buxton [12] carried out a series of small scale experiments to investigate vapour explosions in steel melts. Their apparatus is shown in Figure 32. The water at 7 to 47°C was de-ionized. The steel mass (∿25 g) was maintained at ∿1493°C (i.e., ∿200°C above melting). Fifty-five experiments were carried out. It was observed that in all cases, the molten specimens were in film boiling. Film boiling lasted up to 8 seconds, after which specimen freezing occurred. In no case was transition to nucleate boiling observed. When no pressure transients were applied the melt specimens usually solidified without interaction. When pressure transients were applied (1 atmosphere overpressure, exploding wire 1-2 MPa or mini-detonator ∿20 MPa), the specimens first inflated and in a few cases fragmented. Explosions as such never occurred. The extent of fragmentation was observed to depend on the delay time between specimen flooding and pressure triggering. The fragmentation extent was in general much larger when the specimens were melted in an argon and 0.6% steam atmosphere as opposed to a pure argon atmosphere which suggests that steam dissolves in the melt and influences the fragmentation mechanism.

Since the vapour film did not collapse and the water did not penetrate the drop, fragmentation of the specimen cannot be explained by any of the mechanisms in which the cold liquid plays a major role. Nelson proposed a mechanism of fragmentation based on the growth or nucleation of gas bubbles in the hot liquid. According to Nelson, the solubility of gases in molten metals in general decreases with temperature (in some case it increases). Figure 33 shows how the weight percentage of hydrogen in an iron-hydrogen specimen is affected by a drop in temperature. Three sources of gas were identified in the system considered [12]; the gas impurities present initially in the melt specimen, the ambient gas in which the specimen is melted, and the quench liquid gases. According to Nelson, fragmentation of the melt may result if the overpressures due to oversaturation are high enough.

Nelson [36] also carried out another series of experiments using single drops (~5 mm in diameter) of molten stainless steel, carbon steel and pure iron produced by induction melting. The molten drops were surrounded by large bags of hydrogen produced by the oxidation of the iron by the vapour (Redox reaction). Peak trigger pulses of 0.5 MPa and 4 MPa were used. Only one experiment with a trigger pulse of 4 MPa produced a steam explosion. In general however, thermal explosions were not triggered.

In summary, Nelson's small scale study of vapour explosions in molten Fe/water systems has shown that thermal explosions in this system do not occur spontaneously. Triggering pressure pulses (≥4 MPa) in general only initiate vigorous drop fragmentation. The fact that fragmentation strength increases when the drop is heated in gas with a small percentage of steam instead of pure gas is consistent with the vapour/gas melt supersaturation mechanism [13]. It might therefore be worth investigating whether a thermal explosion would occur in this

system, if the amount of steam in the heating atmosphere is sufficiently large.

Molten FeOx/Water System

The molten FeOx/water system is the only system in which triggered single drop explosions has been studied systematically. Nelson and co-workers [9, 37, 38 & 39] carried out three series of small scale experiments to study vapour explosion in molten FeOx/water systems.

In a first series of experiments Nelson et al., [37] used the floodable arc melter shown in Figure 32 to study the effect of molten fuel composition on the thermal explosion of a 15 g drop of FeOx at 1727 to 2027°C. No spontaneous explosions were observed. In triggered explosions (explosive wire 1-2 MPa and minidetonator 10-20 MPa), the melt was observed to first fragment into millimeter diameter drops; then, several milliseconds, later into micrometer diameter drops. This fragmentation was followed by the major pressure-producing event. Vapour explosions ceased to occur for O/Fe ratios of 1.1 and below. Nelson suggests that iron oxides with O/Fe ratios of 1.1 and below react with steam and generate hydrogen which stabilizes the film. The reaction of steam with the melt also reduces the percentage steam that dissolves in the melt. According to the vapour/gas melt supersaturation theory the explosions cease to occur when the amount of steam that dissolves in the melt becomes negligible.

In a second series of experiments, Nelson et al., [38] used the laser melting apparatus shown in Figure 34 to study the effect of the trigger pressure amplitude on the thermal explosion of 2.8 mm diameter, $FeO_{1.19}$ molten drops, at a temperature of 1957°C. In general, drops

released from heights >8 mm, that pull along a small bag of air, did not explode spontaneously. However, for a trigger pressure >0.4 MPa, the drops explode promptly, ∿150 μs after the bridgewire is fired. For triggering pressures between 0.2 and 0.4 MPa, the explosion is delayed, sometimes as long as 100 ms. Below 0.2 MPa the explosion cannot be triggered.

The pressure produced by the explosions, a few MPa (50 mm away from the drop), are three to four times larger than the trigger pulse. They can be as large as 50 MPa at the drop. The debris are mossy (few μm) suggesting that nucleation plays a role in the explosion. The short delay to explosion for trigger pressure above 0.4 MPa also indicate that the thermal explosion may be due to the nucleation of the water droplets entrapped in the melt. (The larger negative pressure tail that accompanies large pressure triggers may also play a role in triggering the nucleation event.)

In a third series of experiments, Nelson et al., [39] used the laser melting apparatus (Figure 34), in a pressure controlled chamber to investigate the effect of ambient pressure and water temperature on the minimum trigger pulse, and the effect of ambient pressure and melt temperature on the explosion strength. In all tests the oxygen partial pressure was maintained constant at ∿0.02 MPa so as to maintain the O_2/Fe ratio constant in the melt. The ambient pressure was varied by using argon gas.

The ambient pressure affects the water subcooling ($\Delta T_w^{sub} = T_{boiling} - T_w$), and is therefore expected to have a major effect on the film stability and the corresponding threshold pressure trigger (ΔP^{th}) required to destabilize the film. Figure 35 shows that as the

ambient pressure is raised ΔP^{th} first decreases very rapidly down to a minimum of 0.1 MPa, then stabilizes at this value for ambient pressures ranging from 0.2 to 0.8 MPa and finally at ∿0.8 MPa starts increasing with ambient pressure. Thus, as expected, the ambient pressure has a marked effect on the film stability.

Raising the water temperature also affects the film stability and should have a major effect on ΔP^{th}. Figure 36 shows that as the water temperature is raised from a minimum of 0°C, ΔP^{th} increases first slowly and then rapidly. T_w was observed to have a similar effect on the film stability in the case of spontaneous thermal explosions. As shown in Figure 22, T_Q first decreases slowly with T_w and then rapidly.

Nelson et al., [39] also investigated the effect of ambient pressure on the explosion strength. Their data is shown in Figure 37 for a narrow trigger pulse range between ∿0.7 and 0.8 MPa. It is seen that the peak generated pressure goes through a maximum of ∿4 MPa at 0.8 MPa ambient pressure. This effect of ambient pressure on the strength of triggered thermal explosions is similar to that on spontaneous tin/water thermal explosions, shown in Figure 29.

Another parameter expected to have a strong effect on the explosion strength is the melt temperature. Nelson et al., [39] investigated the effect of melt temperature (1497 to 2497°C) on the strength of FeOx/water explosions for a given trigger pressure. Their data points are shown in Figure 38. It can be observed that the explosion strength goes through a maximum of ∿2.4 MPa at a melt temperature of 2127°C. Thus, the effect of melt temperature on the strength of triggered thermal explosions of FeOx/water is very similar to its effect on tin/water spontaneous thermal explosions as shown in Figure 23. It is

interesting to note that the explosion strength starts to decrease at a temperature in the neighbourhood of the dissociation temperature of steam (∿1927°C).

The water temperature is also expected to strongly influence the strength of triggered thermal explosions but this influence has not yet been investigated.

Molten $A\ell_2O_3$/Water System

The thermal explosion of drops or coarse mixture of aluminum oxide and water has not been studied extensively. Only one study on the thermal explosion of single drops of $A\ell_2O_3$ in water was found [40]. In this study, drops of molten alumina were prepared by the laser melting of 2.4 mm diameter alumina spheres attached to 0.25 m diameter sapphire fiber supports. The molten alumina spheres at ∿2054°C were then dropped in water. They could be made to explode by firing a bridgewire. Since the superheats was small the pressure generated by these explosions were weak (<2 MPa). These pressure pulses may not be representative of the ones that could be obtained at the higher superheats which can be obtained by the thermitic ($A\ell$-Fe_2O_3) reaction (2727°C).

Summary

Single drop thermal explosions of molten metals (i.e., tin, aluminum and iron) and of oxides (i.e., iron oxides (FeOx) and alumina ($A\ell_2O_3$)) have been reviewed.

For molten tin, thermal explosions were observed to occur spontaneously, within a domain bounded from below by the water homogeneous

nucleation temperature and from above by the tin quench temperatures (T_Q). This suggests that the phenomena of vapour film stability and water nucleation play a major role in spontaneous explosions. Furthermore, for tin temperatures above the quench temperature there is a few milliseconds delay in the spontaneous thermal explosion. Thus in order to achieve propagating explosions on command, the molten tin temperature should be higher than T_Q.

For molten Aℓ, $Aℓ_2O_3$ and FeOx (for an O/Fe mole ratio of 1.1 and above) a pressure trigger (bridgewire or detonator) was required to initiate the explosion. For molten Fe, explosions could not be in general initiated. The threshold initiating pressure pulse (ΔP_{th}) is strongly dependent on the thermodynamic parameters that determine the stability of the vapour film surrounding the drop and on the melt.

The strength of single drop thermal explosions, as indicated by the percentage disintegration by weight or by the maximum generated pressure, vary with the melt. The thermal explosion of single drops of molten aluminum is the strongest followed by that of $FeO_{1.19}$, $Aℓ_2O_3$ and tin. A similar ordering in strength was observed for propagating thermal explosions.

The strength of single drop thermal explosions, (spontaneous and triggered) is also strongly dependent on a number of thermodynamic parameters namely: i) the initial melt temperature; ii) the water temperature; iii) the ambient pressure; and iv) the dissolved gas content. However, the effect of these parameters has not been systematically investigated (except for tin and $FeO_{1.19}$ molten drops).

Table V lists the threshold pressure pulse, for the prompt initiation of the thermal explosion of single drops of aluminum, aluminum

oxide and iron oxide ($FeO_{1.19}$). Table VI lists the experimental conditions of the strongest single drop thermal explosions observed in each of the following systems, Aℓ/water, $FeO_{1.19}$/water, $Aℓ_2O_3$/water, tin/water, and Fe/water.

Discussion of Results

Single drop thermal explosions take place in much less than a millisecond. Thus vapour explosions can clearly be distinguished from purely hydrodynamic breakup due to collisions which takes several milliseconds [27]. The time scale of single drop thermal explosions favours drop fragmentation mechanisms that are based on the homogeneous nucleation of water in the melt. The foamy appearance and high porosity of the molten drop debris also favours such models. Of the thermal explosion theories, only two: i) the vapour/gas melt supersaturation model; and ii) the water entrapment model, are based on the water homogeneous nucleation phenomenon.

In the vapour/gas melt supersaturation model, for melt temperatures above the critical temperature of water, vapour is assumed to dissolve in the melt. The amount of vapour that dissolves depends on the vapour solubility in the melt and the partial pressure of the vapour in the film surrounding the molten drop. When the film becomes unstable, the melt surface gets cooled, effectively causing the vapour to precipitate into water droplets. The droplets in the hot core then nucleate explosively, resulting in a thermal explosion. A decrease in the ambient pressure may also cause the water droplets to nucleate explosively. There are three main steps in this mechanism: i) vapour dissolution in the melt; ii) vapour precipitation which is governed by the film stability; and iii) water droplet nucleation. In general enhancing any of those intermediate steps, enhances the thermal explo-

sion strength and whenever any of those steps can no longer take place explosion cease to occur.

In the water entrapment model it is assumed that water jets are formed when the film becomes unstable. These jets penetrate the melt and break up into water droplets, whose explosive nucleation results in a thermal explosion. The composition of the water droplets in the melt is identical to that of the water solution surrounding the molten drop. There are two main steps in this mechanism: i) water entrapment governed by the film stability; and ii) water droplet nucleation.

In this section, we give an interpretation of the effect of various thermodynamic parameters on the strength of thermal explosions based on these mechanisms. Triggered explosions are then discussed. Finally, various thermal explosion limits (i.e., COT_w^{max}, the cutoff maximum water temperature, COP^{min}, the cutoff minimum ambient pressure, COC_{gas}^{max}, the cutoff minimum melt temperatures) are examined and whenever possible identified.

The experimental data (see Figure 22) suggests that thermal explosions are governed by two phenomena, namely; the stability of the film surrounding the molten drop and the water homogeneous nucleation. The approach adopted is to predict the effect of the ambient pressure, the water temperature, the gas concentration in the water, and the melt initial temperature, from a knowledge of their effect on the two above mentioned phenomena.

The film stability depends on two parameters: i) the partial pressure of the gas in the film P_I, ($P_I = Kc_{gas}$ where K is Henry's constant) and ii) the degree of water subcooling ΔT_w^{sub} ($\Delta T_w^{sub} = T_{boiling}$

$(P_0) - T_w)$. In general an increase in P_I causes the film stability to increase. The effect of P_I on the film stability is however substantial only for large P_I and corresponding large gas concentrations in the water [12, 38]. For spontaneous thermal explosions, the quench temperature T_Q, i.e., the melt temperature at which the film becomes unstable, is a measure of the film stability; lower T_Q correspond to more stable films. T_Q is a unique function of ΔT_w^{sub}. Figure 22 shows that T_Q decreases with ΔT_w^{sub} and that at low ΔT_w^{sub} the rate of change of T_Q is largest. It is to be noted that ΔT_w^{sub} can be raised either by reducing T_w or by raising the ambient pressure P_0. For pure or distilled water, the effect of raising the ambient pressure is identical to the effect of lowering T_w for the same ΔT_w^{sub}. However, in most experiments a gas blanket is used to maintain the ambient pressure. Therefore, for a given ambient pressure, the gas concentration in the water may cover a range of values with a maximum of P_0/K, (where K is Henry's constant) under equilibrium conditions. As the ambient pressure is raised the gas concentration in the water increases. Thus the effect of ambient pressure and gas concentration are linked. We shall assume that at low pressures, the amount of gas dissolved in the water is small. As the pressure is raised the film stability at first decreases. Then as the pressure is raised further, c_{gas} becomes substantial, its effect dominant and the film stability starts to increase. This suggests that for large gas concentrations in the water, the quench curve (see Figure 22) would be shifted downwards, as P_I is raised. This expected trend has not yet been examined experimentally.

A water droplet will only nucleate if it is heated through by the melt to above its threshold homogeneous nucleation temperature

(T_{HN}). The water homogeneous nucleation temperature depends on two parameters, the ambient pressure P_0 and the gas concentration in the water c_{gas}. As shown in Figure 39, T_{HN} increases with ambient pressure and decreases with c_{gas}. However, the effect of ambient pressure and gas concentration are linked. At small gas concentrations, the effect of c_{gas} is dominant, causing T_{HN} to decrease [10]. Then, the pressure is raised further the effect of P becomes dominant, causing T_{HN} to increase. Thus the homogeneous nucleation threshold is affected by the gas concentration in the water for small gas concentrations, while the film stability is affected by the gas concentration in the water for large gas concentrations.

The thermal explosion strength is related to the extent of the molten drop fragmentation, which is expected to depend on the nucleation event explosive strength. It has been shown [12], that the nucleation event explosive strength for a water droplet containing gas in dissolution decreases as c_{gas} increases. We make the assumption that this effect is substantial mainly at large gas concentrations.

Based on the above general considerations it is possible to predict the effect of various thermodynamic parameters namely; the water temperature, the ambient temperature, the melt temperature and the gas concentration in the water (or the gas partial pressure in the film), on the explosion strength using the vapour/gas melt supersaturation model or the water entrapment model. The effect of these parameters on the film stability and the water nucleation phenomena do not depend on the explosion model. However, the explosion model dictates the effect of changes in film stability, the nucleation event threshold and the nucleation event explosion strength on the molten drop thermal explosion strength.

Vapour/Gas Melt Supersaturation Model

We begin by examining the effect of water temperature on the explosion strength. The amount of gas (c_{gas}) dissolved in cold distilled water, at a near atmospheric gas blanket ambient pressure, is relatively large. In addition, since ΔT_w^{sub} is large, the vapour film surrounding the molten drop is unstable. As the water temperature (T_w) is raised both ΔT_w^{sub} and c_{gas} decrease. ΔT_w^{sub} being still relatively large its effect on the film stability is minimal. As c_{gas} decreases however, the amount of vapour in the film surrounding the drop increases. Thus, the amount of water vapour that dissolves in the melt increases, leading to an increase in the number of precipitated water droplets. Since c_{gas} is still relatively large, T_{HN} is only marginally affected if any. More water droplets nucleate and the net result is an increase in the explosion strength. As the water temperature is raised further, the water becomes almost pure, so that the percentage vapour that dissolves in the melt does not change much. The vapour film stability however, increases rapidly since ΔT_w^{sub} is now small. This causes the melt to be cooled less efficiently and results in a decrease in the number of precipitated water droplets. In addition, T_{HN} increases at small c_{gas}. The net result is a decrease in the explosion strength. The predicted increase in explosion strength with water temperature for lower water temperatures and the subsequent decrease at higher temperatures is consistent with the observed effect of T_w on the percentage melt disintegration by weight as shown in Figure 19, and on the maximum explosion overpressure as shown in Figure 20.

The effect of ambient pressure on the explosion strength can also be predicted. For distilled water at a low gas blanket ambient pressure initially and at a given temperature corresponding to a small

ΔT_w^{sub}, the film is almost stable while the water is almost pure. As the ambient pressure is raised ΔT_w^{sub} and c_{gas} start to increase. At first, c_{gas} is small and the percentage vapour that dissolves in the melt does not change much. The vapour film stability however decreases rapidly since ΔT_w^{sub} is small. This causes the melt to be cooled more efficiently and results in an increase in the number of precipitated water droplets. In addition, T_{HN} may start to decrease since c_{gas} is small and increasing. There is an increase in the number of droplets that nucleate and the net result is an increase in the explosion strength. As the pressure is raised further however, the amount of gas pushed into solution becomes appreciable. The percentage vapour that dissolves in the melt decreases. Moreover, the film stability increases. The melt is not cooled as well resulting in a decrease in the amount of vapour that precipitates. Since c_{gas} is now relatively large, the effect of P on T_{HN} becomes dominant, causing T_{HN} to increase. The net result is a decrease in the explosion strength. The predicted increase in explosion strength with ambient pressure for lower pressures and the subsequent decrease at higher pressures is consistent with the observed effect of P_0 on the maximum explosion overpressure as shown in Figure 29.

The initial melt temperature also affects the explosion strength. As the melt temperature is raised, above the critical temperature of water (375°C), water droplets over a wider range of sizes are heated above T_{HN}, which causes the explosion strength to increase. However, as the melt temperature is raised further, the film thickness increases substantially. This causes the melt to be cooled less effectively and results in a decrease in the number of precipitated water droplets which in turn leads to a drop in the explosion strength. The predicted increase in explosion strength with initial melt temperature

at lower melt temperatures and the subsequent decrease at higher melt temperatures is consistent with the observed effect of T_{mi} on the maximum explosion overpressure as shown in Figure 23.

Finally, we shall consider the effect of the amount of gas in dissolution in the water on the explosion strength. For water containing substantial amounts of gas initially, increasing the gas concentration increases the partial pressure of the gas in the film and thus decreases the percentage vapour that dissolves in the melt. Since c_{gas} is quite large, the film also becomes more stable. The melt is not cooled as well leading to a reduction in the number of water droplets that precipitate. T_{HN} is not much affected. The net result is a decrease in the explosion strength, which is consistent with the effect of c_{gas} on the percentage melt disintegration by weight as shown in Figures 30 and 31.

The vapour/gas melt supersaturation model can thus be used to qualitatively predict the general effect of the thermodynamic parameters on the thermal explosion strength. This model depend on vapour dissolving in the melt. There is some evidence that vapour dissolves in molten iron and plays a role in the melt fragmentation since the addition of a small amount of steam to the gas in which the iron is melted significantly increases the fragmentation extent [12]. However, there has been no systematic experimental investigation of the solubility of water vapour in various melts. The decrease in explosion strength of iron oxide near the water vapour dissociation temperature also suggests that the vapour plays a role in thermal explosions, but the effect of water vapour dissociation on the explosion strength has not been examined. If vapour dissolution in the melt is the main contributing factor for vapour explosions, it should be possible to obtain

explosions by rapidly quenching the melt, even in the absence of surrounding water.

Water Entrapment Model

The alternate model based on water entrapment can also be used to predict the effect of various thermodynamic parameters on the strength of spontaneous thermal explosion. The effect of water temperature on the explosion strength as shown in Figures 19 and 20, can be understood based on similar arguments to those given above for the vapour/melt supersaturation model. As the water temperature is raised the water subcooling and the amount of dissolved gas in start to decrease. For large ΔT_w^{sub} the effect of increasing the temperature on the film stability is small. However, the decrease in c_{gas} causes the droplet nucleation event to become more explosive resulting in an increase in the explosion strength. As the water temperature is raised further so that ΔT_w^{sub} becomes small the vapour film stability, increases rapidly. This reduces the amount of water entrapped in the melt. In addition T_{HN} starts to increase. The net result is a decrease in the explosion strength.

The effect of ambient pressure on the explosion strength is also predicted to be similar for the two models. As the ambient pressure is raised, the water subcooling and the amount of gas pushed into dissolution start to increase. At first ΔT_w^{sub} is small thus the film stability decreases rapidly and more water gets entrapped in the melt. In addition T_{HN} starts to decrease. The net result is an increase in the explosion strength. As the pressure is raised further the effect of ΔT_w^{sub} on the film stability diminishes while the corresponding

increase in c_{gas} causes a substantial increase in film stability. Moreover the entrapped water has now a larger gas concentration. The nucleation event explosive strength is considerably reduced. The net result is a decrease in the thermal explosion strength. This is consistent with the experimentally observed effect of P_o on the maximum explosion overpressure as shown in Figure 29.

The predicted effect of the initial melt temperature on the explosion strength is the same for the two models, based on identical arguments.

The effect of the amount of gas in solution in the water on the explosion strength is also predicted to be the same for the two models. For an initially large gas concentration in the water, as c_{gas} is raised, the film stability increases. Thus less water gets entrapped in the melt. Moreover, as a result of the larger gas concentration in the entrapped water droplets, the nucleation event explosive strength decreases. The net result is a decrease in the explosion strength. This is consistent with the effect of c_{gas} on the percentage melt disintegration by weight as shown in Figures 30 and 31.

Triggered Thermal Explosions

For triggered thermal explosions, the film surrounding the molten drops is stable at the temperatures and pressures considered. To initiate a thermal explosion, a pressure trigger above a certain threshold value ΔP_{th} is used. ΔP_{th} is a measure of the extent of the film stability and depends on the melt and the thermodynamic parameters. ΔP_{th} is expected to depend like T_Q on ΔT_w^{sub} and P_I. Figures 35 and 36 show the effect of P_o and T_w on ΔP_{th} for a molten

drop of $FeO_{1.19}$. The effect of P_I however has not been examined yet. For a given molten drop if the pressure trigger is maintained constant at ΔP_{th}, the effect of the various thermodynamic parameters on the explosion strength should be similar to their effect on spontaneous thermal explosions. Indeed, Figure 37 shows, that for a fixed ΔP_{th}, an increase in the ambient pressure P_0, causes the explosion overpressure to increase at lower P_0, and then decrease at higher P_0. This effect is similar to that observed for the spontaneous explosion of tin as shown in Figure 29. In addition, Figure 38, shows that an increase in the initial melt temperature T_{mi} cause the explosion overpressure to increase at lower T_{mi} and then decrease at higher T_{mi}. This effect is also similar to that observed for the spontaneous explosion of tin, as shown in Figure 23. The effect of water temperature on the explosion strength at fixed ΔP_{th} has not been examined yet. The effect of P_0 and T_{mi} on the explosion strength can also be qualitatively predicted by the vapour/gas melt supersaturation model and the water entrapment model, based on similar arguments as in spontaneous explosions. It is however to be noted that for melt temperatures above 1975°C, the dissociation of the vapour in the film contributes to the decrease in the explosion strength in the vapour/gas melt supersaturation model for the system considered.

Explosion Limits

Figure 20, shows the effect of the water temperature on the explosion strength of molten tin for a fixed air gas blanket pressure. As seen in Figure 20, when the water temperature is raised, a maximum cutoff water temperature (COT_w^{max}) of 80°C is reached, at which thermal explosion stop altogether. A water temperature of 80°C corresponds to the intersection of T_Q and T_{HN} (see Figure 23). Thus at COT_w^{max}, the

film is stable and the melt/water interface temperature is just below T_{HN}.

The cutoff water temperature depends on the gas blanket used. With a helium gas blanket, COT_w^{max} is only 60°C as shown in Figure 19. This can however be explained based on the amount of gas dissolved in the water. Helium gas is less soluble than air in water. Thus more air than helium will dissolve in the water. As discussed above, the homogeneous nucleation temperature (T_{HN}) decreases with gas concentration while T_Q is virtually unaffected for low concentrations. Thus, the intersection point of T_Q and T_{HN} for the water/helium system corresponds to a smaller COT_w^{max}.

The ambient pressure also influences the cutoff maximum water temperature COT_w^{max}. For distilled water, as the gas blanket pressure is raised, the amount of gas pushed into dissolution increases. At first, the gas concentration in the water is small. Thus, T_{HN} decreases while T_Q is essentially unaffected. This causes COT_w^{max} to increase (see Figure 22). As the pressure is raised further however the gas concentration in the water becomes appreciable. This causes the film stability to increase and shifts the quench curve T_Q downwards. Moreover, T_{HN} starts to increase with P. These two effects combine to cause a decrease in COT_w^{max}. Figure 28, shows the limit explosion curve COT_w^{max} as a function of ambient pressure for a helium gas blanket. As predicted COT_w^{max} increases with P_o at lower pressures and decreases with P_o at higher pressure. In addition, Figure 28 shows that in general there are two cutoff pressures: i) a minimum cutoff pressure (COP^{min}) corresponding to a very small gas concentration in

the water and a higher value of T_{HN}; and ii) a maximum cutoff pressure (COP^{max}) corresponding to a larger gas concentration in the water and a lower value of T_{HN}. At both COP^{min} and COP^{max}, the film is stable and the melt/water interface is just below T_{HN}, so that explosions cease to take place. The two cutoff pressures above can also be observed in Figure 29, for molten tin with an air gas blanket.

The above considerations assumed a low gas concentration in the water. For water containing appreciable amounts of gas, the effect of the dissolved gas is somewhat different. In this case the explosion domains are mainly controlled by the curve T_Q (see Figure 22), since the effect of c_{gas} on T_{HN} is small. For a fixed melt explosion temperature above T_{HN}, and a fixed water temperature, explosions will take place as long as the film is unstable. T_Q however is shifted downwards as c_{gas} is raised. In the limit, a gas concentration is reached COC_{gas}^{max} at which the film is stable, so that explosions cease altogether. Unlike COT_w^{max}, COP^{min} and COP^{max}, COC_{gas}^{max} corresponds to conditions of stable film boiling only. The cutoff maximum gas concentration COC_{gas}^{max} also depends on the type of gas dissolved in the water. The higher the gas partial pressure P_I in the film, the more effective the given gas will be in supressing explosions. P_I can be expressed as $P_I = K\, c_{gas}$, where K is Henry's constant. Thus more soluble gases (i.e., smaller K) are less effective in suppressing explosions. We would therefore expect COC_{gas}^{max} to increase with gas solubility. This is consistent with the COC_{gas}^{max} of 90 ml/kg for gas CO_2 and the COC_{gas}^{max} of only 75 ml/kg for the less soluble N_2O gas (see Figures 31(a) and 31(b)).

There is also a minimum cutoff melt temperature COT_{mi}^{min} below which explosion will not occur. Figure 23, shows that COT_{mi}^{min} for tin/water explosions lies between 300°C and 400°C. As indicated by Shoji et al., [25], this is consistent with a melt/water interface temperature just below T_{HN} as shown in Figure 22. Thus COT_{mi}^{min} is equal to T_{HN} and at this limit even if the film is unstable explosions cannot take place.

CONCLUSIONS AND PROPOSED RESEARCH

Propagating thermal explosions have been observed in three systems: the tin/water system; the Aℓ/water system; and the Fe-$Aℓ_2O_3$/water system. The tin/water system is a simple, single component, unreactive system. The Aℓ/water system is a single component, reactive system (Aℓ and steam react) that yields stronger propagating explosions. The Fe-$Aℓ_2O_3$/water system is a multicomponent, reactive system that yields the strongest propagating explosions and is the most interesting from a practical point of view since no external heat source is needed to produce the melt.

Most experimental studies of propagating thermal explosions to date have been carried out by the Nuclear industry. The aim of these studies was to investigate what happens when a large mass of molten reactor simulant material falls into water and to evaluate the thermal to mechanical conversion ratio of the thermal explosion. In general, the large mass of molten material intermixed before the explosion. The initial coarse mixture size distribution was therefore unknown, and the initial mixture density had to be inferred. No systematic study of the effect of these parameters on the characteristics of the thermal deton-

ations have been carried out. Furthermore, in the case of propagating thermal explosions in confined geometries, the apparatus was not long enough for steady state thermal detonations to be established. The effect of various parameters (e.g., such as dissolved gas content in water) which affect thermal detonations were not examined in any detail.

It is therefore recommended that an experimental program to investigate the explosive performance of thermal explosives be developed. The aim of this experimental program will be two fold:

a. to examine the detonability and performance of melt-coolant explosive mixtures for well defined initial conditions (initial density, coarse mixture size distribution, dissolved gas content in water, etc.); and
b. to provide a data base for the development and evaluation of quantitative models of propagating thermal detonation.

Experimental data on single drop explosions can be used in developing potentially promising systems for obtaining propagating thermal explosions. The determination of the quench curve and the homogeneous nucleation curve, corresponding to the upper and lower bounds for spontaneous explosions, and the explosion delay time have been identified as important single drop experimental data. However, the only system for which such data are available is the tin/water system.

Whereas the wealth of small scale test data for the spontaneous thermal explosion of single drops of molten metal (namely tin) in water indicate under which conditions an explosion occurs, the experimental data for thermal explosions initiated by an external trigger is

extremely limited. The FeOx/water system is the only system that has been investigated systematically todate. However, the effect of the water temperature and water gas concentration on this system thermal explosion strength has not been examined. Moreover, the effect of both maximum trigger pressure pulse and impulse on the explosion event has not been studied yet. A systematic investigation of triggered thermal explosions in the following system of interest: i) Aℓ/water; ii) Fe/water; iii) $A\ell_2O_3$/water; and in particular iv) the thermitic system Fe-ℓ_2O_3/water need also be carried out.

We were able to predict qualitatively the effect of various thermodynamic parameters on the explosion strength based on two models: i) the gas/vapour melt supersaturation model; and ii) the water entrapment model. Thus both models look promising. In the gas/vapour melt supersaturation model the assumption was made that for melt temperatures above the critical temperatures of water, vapour dissolves in the melt. However, although there are indications that vapour dissolves in molten iron [12], it has not been shown to dissolve in other systems of interest. Further work is therefore needed to examine the solubility of vapour in the various melts. In addition, to establish that such a mechanism results in thermal explosions, it is important to investigate whether thermal explosions occur upon rapid quenching of the melt when in contact with water vapour and in the absence of liquid water. In the alternate water entrapment model, our predictions were based on the assumption that the gas concentration in the water has a marked effect on the nucleation event explosive strength. A rigorous assessment of this model awaits therefore, new quantitative data on the effect of c_{gas} on the nucleation event explosive strength, for the systems of interest. More experimental data is therefore needed to rigorously assess these two promising fragmentation mechanisms and to develop a predictive model of single drop thermal explosions.

In conclusion, previous studies have resulted in a much better understanding of propagating and single drop thermal explosions, but much research remains to be done if one is to harness or control the energy released. The effect of various parameters on thermal explosions (triggered and spontaneous) can be described by the water entrapment and vapour/gas melt supersaturation mechanism, by noting that the nucleation and film destabilization phenomena constitute the heart of both mechanism. Considerations based on these two phenomena can therefore be used to guide the experimental, analytical and numerical effort needed to establish an understanding of thermal explosions.

REFERENCES

1. Board, S.J. and Hall, P.W., (1975), "Detonation of Fuel Coolant Explosions", Nature 245, pp. 319-321.

2. Cronenberg, A.W., (1980), Nuclear Safety, Vol. 21, No. 3, May-June.

3. Vaughan, G.J., (1980), "The Metal/Water Explosion Phenomenon A Review of Present Understanding", UK Atomic Energy Authority, Vol. 177, (SRDR-177).

4. Chu, Cho-Chone C., (1986), "One Dimensional Transient Fluid Model for Fuel-Coolant Interaction Analysis", Ph.D. Thesis, 1986, University of Wisconsin-Madison.

5. Chandrasekhar, S., (1971), Hydrodynamic and Hydromagnetic Instabilities, Oxford Press, pp. 481-512.

6. Fishburn, B.D., (1974), "Boundary Layer Stripping of Liquid Drops Fragmented by Taylor Instability", Acta Astronautica 1, pp. 1274-1284.

7. Usynin, C.B. and Khramov, N.I., (1985), Combustion, Explosions and Shock Wave, pp. 111-114.

8. Buchanan, D.J., (1974), "A Model for Fuel Coolant Interaction", J. Phys. D: Appl. Phys., 7, pp. 1441-1457.

9. Nelson, L.S. and Duda, P.M., (1988), "Photographic Evidence for the Mechanism of Fragmentation of a Single Drop of Melt in

Triggered Steam Explosion Experiment", J. Non-Equilbr. Thermodyn, Vol. 13, pp. 27-55.

10. Ward, C.A., Balakrishman, A. and Hooper, F.C., (1970), "On the Thermodynamics of Nucleation in Weak Gas-Liquid Solutions", Journal of Basic Engineering, pp. 695-704.

11. Forest, T.W. and Ward, C.A., (1977), Journal of Chemical Physics, Vol. 66, No. 6.

12. Nelson, L.S. and Buxton, L.D., (1978), "Steam Explosion Triggering Phenomena: Stainless Steel and Corium-E Simulants Studied with a Floodable Arc Melting Apparatus", NUREG/CR-0122, SAND77-0998, Sandia National Laboratory, US.

13. Ward, C.A., (1988), Private communication, (Professor, Mechanical Engineering Department, University of Toronto, Canada).

14. Ward, C.A., Johnson, W.R., Venter, R.D., Ho, S., Forest, T.W. and Fraser, W.D., (1983), "Heterogeneous Bubble Nucleation and Conditions for Growth in a Liquid-Gas System of Constant Mass and Volume", Journal of Applied Physics 54(4), April.

15. Board, S.J. and Hall, R.W., (1974), "Propagation of Thermal Explosions - Tin/Water Experiments", Report No. RD-B-N-2850, Central Electricity Generating Board, UK.

16. Hall, R.W., Board, S.J. and Baines, M., (1979), "Observation of Tin/Water Thermal Explosions in a Long Tube Geometry, Their Interpretation and Consequences for the Detonation Mode", Berkeley Nuclear Laboratories, California, US, FCI 4/P20.

17. Fry, C.J. and Robinson, C.H., (1979), "Experimental Observations of Propagating Thermal Interactions in Metal/Water Systems", Fourth CSNI Specialist Meeting on Fuel-Coolant Interactions, OECD, CSNI, Report No. 37, Vol. 2, pp. 330-362.

18. Fry, C.J. and Robinson, C.H., (1980), "Results from Selected Experiments Performed in the Thermic Facility at AEE Winfrith", CSNI Joint Interpretation Exercise on Fuel Coolant Interactions AEEW-M-1778, UK.

19. Board, S.J. and Hall, R.W., (1976), Proc. 3rd Specialists Meeting Sodium/Fuel Interaction in Fast Reactors, pp. 249-end.

20. Buxton, L.D. and Benedick, W.B., (1979), "Steam Explosion Efficiency Studies", NUREG/CR-0947, SAND79-1399, Sandia National Laboratory, Albuquerque, US.

21. Mitchell, D.E., Corradini, M.L. and Tarbell, W.W., (1981), "Intermediate Scale Steam Explosion Phenomena Experiments and Analysis", NUREG/CR-2145, SAND81-0124, Sandia National Laboratory, US.

22. Mitchell, D.E. and Evans, N.A., (1982). Proc. Thermal Reactor Safety Meeting, August 29, Chicago, pp. 1011-1025.

23. Marshall, B.W. Jr., Berman, M. and Krein, M.S., (1986), "Recent Intermediate Scale Experiments on Fuel-Coolant Interactions in an Open Geometry (EXO-FITS)", Proc. International ANS/ENS Meeting on Thermal Reactor Safety, SANDIEGO, California, USA, February.

24. Asher, R.C., Davies, D., Dandiah, S.K. and Worthington, A.J., (1976a), "The Effect of Ambient Pressure on a Vapour Explosion", AERE-M-2862, Harwell, UK.

25. Shoji, M. and Takagi, N., (1983), Bulletin of the JSME, Vol. 26, No. 215, May.

26. Shoji, M. and Takagi, N., (1984), "Small Scale Vapour Explosions on a Surface of Stationary Molten Tin Cooled by Flowing Water", Bulletin of the JSME, Vol. 27, No. 228, June.

27. Mijazaki, K., et al., (1984), J. Nucl. Sci. Technology, Vol. 21, pp. 907-918.

28. Tso, C.P., Teh, S.K., Sim, C. and Kew, C.S., (1986), PCH, Physical Chemical Hydrodynamics, Vol. 7, No. 2/3, pp. 111-123.

29. Fröhlich, G., Muller, G. and Unger, H., (1980a), "Entrapment Experiments of Small Water Amounts and Various Melts", Jahrestagung Kerntechnile 80, p. 347.

30. Fröhlich, G. and Müller, K., (1983), "Entrapment Experiments in Hot Tin Melt with Variation of the Injection Velocity and Water Outlet", Institut für Kernergetik and Energiesystem, Universitat Stuttgart, Federal Republic of Germany, IKE 2-65.

31. Asher, R.C., Davies, D. and Jones, P.G., (1976), "Fuel Coolant Interactions: Preliminary Experiments on the Effect of Gases Dissolved in the Coolant", AERE-M2861, Harwell, UK.

32. Fröhlich, G. and Andale, M., (1980b), "Experiments for Studying the Initiation Mechanisms for Steam Explosions", Institut für Kernergetik and Energiesystem, Universitat Stuttgart, Federal Republic of Germany, IKE 2-51.

33. Fröhlich, G. and Alisch, S., (1982), "Optical Registration of the Interaction of Molten Tin Jets with Water Triggered Spontaneously and by Shock Waves", Institut für Kernergetik and Energiesystem, Universitat Stuttgart, Federal Republic of Germany, IKE 2-58.

34. Anderson, R. and Armstrong, D.R., (1981), "Experimental Study of Small Scale Explosions in an Aluminum-Water System", Am. Soc. Mech. Eng. Heat Transfer Division, Vol. 19, pp. 31-40.

36. Nelson, L.S., (1983), "Steam Explosion Studies with Single Drops of Corium-Related Melts: Ferrous Metals and U and Zr Containing Oxides", Proc. International Meeting on Lightwater Reactor Severe Accident Evaluation, August 28, Cambridge, MA., No. Ts-6-7.

37. Nelson, L.S. and Buxton, L.D., (1980), "Steam Explosion Triggering Phenomena; Part 2, Corium-A and Corium-E Simulants and Oxides of Iron and Cobalt Studied with a Floodable Arc-Melting Apparatus", Sandia Laboratories, SAND 79-0260, NUREG/CR-0633, May.

38. Nelson, L.S. and Duda, P.M., (1982), "Steam Explosion Experiments with Single Drops of Iron Oxide Melted with a CO_2 Laser", J. High Temperatures - High Pressures, Vol. 14, pp. 259-281.

39. Nelson, L.S. and Duda, P.M., (1985), "Steam Explosion Experiments with Single drops of Iron Oxide Melted with a CO_2 Laser Part II Parametric Studies", NUREG/CR-2718, SAN82-1105, April, Sandia National Laboratory, US.

40. Nelson, L.S., (1980), "Steam Explosion Studies with Single Drops of Molten Refractory Materials". Proc. ANS Thermal Reactor Safety Meeting, Knoxville, TN.

TABLE I

SUMMARY OF EXPERIMENTS WITH TIN/WATER INVOLVING PROPAGATION THERMAL INTERACTIONS BY HALL ET AL. [16]*

EXPERIMENT	VESSEL	METAL CHARGE (ml)	METAL TEMPERATURE (°C)	P_{max} (MPa)	$P_{plateau}$ (MPa)	TRIGGER
T2	steel tube	75	705	9	∿4	detonator, 0.1 g PETN
T4	steel tube	75	660	8	∿4	spontaneous, cold, 20°C, water
T5	steel tube	180	720	11	∿4	spontaneous, cold, 20°C, water
T7	glass tube	180	720	--	--	spontaneous, cold, 20°C, water
T8	glass tube	180	620	--	--	spontaneous, cold, 20°C, water

* water temperature ∿90°C; pressure rise time ∿50 μs; front or shock propagation velocity 300 m/s near bottom slowing down to ∿60 m/s near top of tube

TABLE II

SUMMARY OF EXPERIMENTS WITH TIN/WATER MIXTURES
INVOLVING PROPAGATING THERMAL INTERACTIONS AT WINFRITH
BY FRY AND ROBINSON [17, 18]

VESSEL	METAL CHARGE kg	METAL TEMP °C	WATER TEMP °C	SHOCK PROPAGATION VELOCITY m/s	MAXIMUM PRESSURE MPa	PRESSURE RISE TIME µs	TRIGGER
thin tank 450 mm x 400 mm x 80 mm	6	800	85	81	1.7	320	one detonator, detonator pulse at Figure 6 is 1.1 MPa.
	6	800	86	120	3.4	320	two detonators (no delay)

TABLE III

SUMMARY OF EXPERIMENTS WITH Aℓ/WATER MIXTURES INVOLVING PROPAGATING THERMAL INTERACTIONS AT WINFRITH BY FRY AND ROBINSON [17, 18]

VESSEL	METAL CHARGE kg	METAL TEMP °C	WATER TEMP °C	SHOCK PROPAGATION VELOCITY m/s	MAX PRESSURE MPa	PRESSURE RISE TIME μs	TRIGGER
Rectangular 300 mm x 300 mm x 200 mm	7	802	10	120	6	800	spontaneous
Rectangular 300 mm x 300 mm x 200 mm	3	806	8	76	1.2	1600	spontaneous
Metal cylinder 300 mm radius 200 mm high	7	790	6	409	40	90	detonator
Perspex cylinder 300 mm radius 200 mm high	7	800	14	301	21	106	detonator
Thin tank 450 mm x 400 mm x 80 mm	5 5	820 807	28 24	∿350 ∿360	40 ∿60	160 ∿90	detonator detonator

TABLE IV

SUMMARY OF STRONG PROPAGATING THERMAL EXPLOSIONS

STUDY	METAL CHARGE	METAL TEMP °C	WATER TEMP °C	SHOCK VELOCITY m/s	MAXIMUM PRESSURE MPa	RISETIME μs	DEBRIS SURFACE AREA m^2/kg	REMARKS
Fry & Robinson (1979) [17,18] Aℓ/water, steel cylinder: 300 mm diameter, 200 mm high	7 kg	790	6	409	40	90	∿1000	Detonator at base. Pressure transducer ∿10 cm away from center of apparatus.
Hall et al. (1979) [16] tin/water, steel tube: 28 mm diameter, 85 cm long	75 ml	705	90	60-300	9	≤50	10-200	Detonator at base (0.1 g PETN). Water 85-95°C. Molten globule size 0.3 to 0.5 cm in diameter. Plateaus at ∿4 MPa.
Mitchell et al. (1981) [21] $FeAℓ_2O_3$/water, square lucite vessel (600 mm x 600 mm x 760 mm)	5.38 kg	2727	∿24	200-600	130	100-900	5000-25000	Detonator (0.6 g PETN). Molten globule size 1-2 cm in diameter. Plateaus at ∿10 MPa.

TABLE V

MINIMUM INITIATING PRESSURE PULSE FOR TRIGGERED SINGLE DROP EXPLOSIONS

STUDY	METAL CHARGE	METAL TEMP °C	WATER TEMP °C	MINIMUM TRIGGER PULSE MPa	REMARKS
Anderson & Armstrong (1981) [34] Argonne Laboratory Aℓ/water	28 g	800°C	30	5	Aℓ collected on bottom trigger 5-10 cm away.
Nelson (1980) [40] Sandia Laboratory $Aℓ_2O_3$/water	2.4 mm diam	∿2054°C	--	1-2	Trigger ∿12.5 cm away.
Nelson & Duda (1982) [38] Sandia Laboratory $FeO_{1.19}$/water	0.055 g	∿1954°C	25	0.4	For prompt explosions at 1 atm. Trigger 5 cm below drop. Pressure transducer 5 cm to the side of the drop (laser melting apparatus).

TABLE VI
SUMMARY OF STRONG SINGLE DROP THERMAL EXPLOSIONS

STUDY	METAL CHARGE	METAL TEMP °C	WATER TEMP °C	TRIGGER ENERGY joule	TRIGGER PRESSURE MPa	MAXIMUM PRESSURE MPa	REMARKS
Anderson & Armstrong (1981) [34] Aℓ/water	28 g	800	30	1500	>15	22	Small steel water vessel (3 cm deep). Droplet collected on vessel base. Trigger and pressure transducer ∿2.5 cm away.
	28 g	800	∿30	80	>5	4.5	Larger steel vessel (10 cm deep). Droplet collected on vessel base. Trigger and pressure transducer ∿5-10 cm away from drop.
Nelson & Buxton (1978) [12] Fe/water	∿25 g	∿1493	7-47	-	1-20	no explosion	Arc-melting apparatus. Fragmentation but no explosion. More extensive fragmentation if drop heated in argon/steam. Trigger and pressure transducer 5 and 8 cm away from drop.
Nelson (1980) [40] $Aℓ_2O_3$/water	2.4 mm diam. sphere	∿2327 small superheat	-	-	1-2	≤2	Laser melting apparatus. Larger debris. Trigger 5 cm below drop and pressure transducer ∿5 cm to the side of drop.
Shoji & Takagi (1983) [25] tin/water	5 g	800	∿20	-	spontaneous	0.3	Pressure transducer ∿3 cm below explosion center.
Nelson & Duda (1982) [38] $FeO_{1.19}$/water	0.055 g	∿1955	∿25	-	∿0.71	2-3 at pressure transducer or 30 at drop	Laser melting apparatus. Trigger ∿7 cm below drop Pressure transducer ∿5 cm to the side of molten drop.

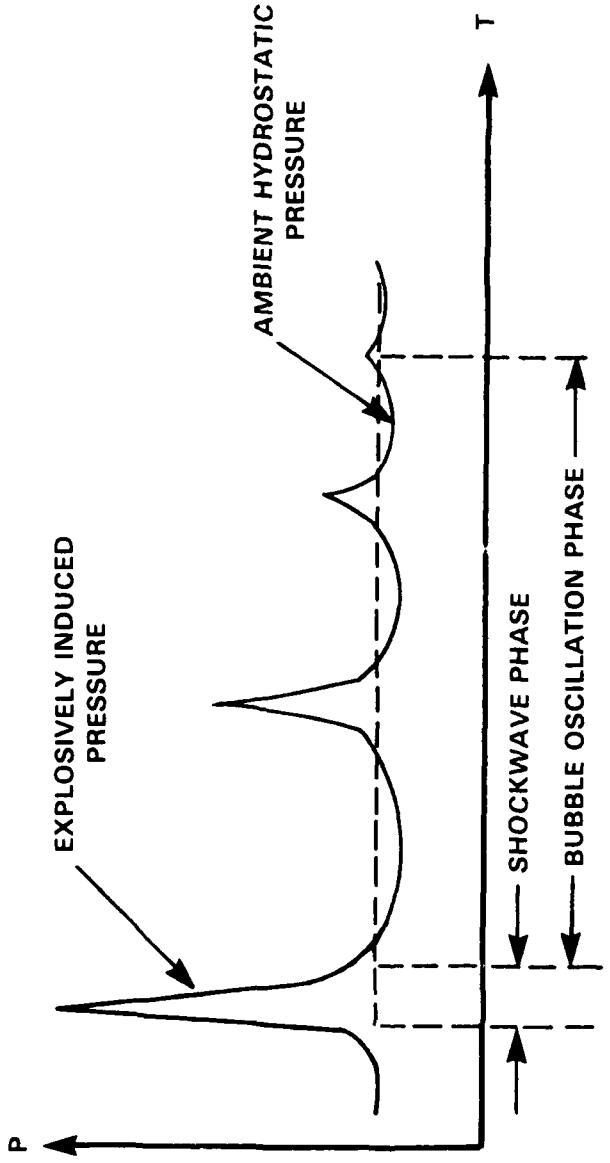

Figure 1

TYPICAL PRESSURE-TIME HISTORY CURVE FOR AN UNDERWATER EXPLOSION USING CONVENTIONAL HIGH EXPLOSIVES

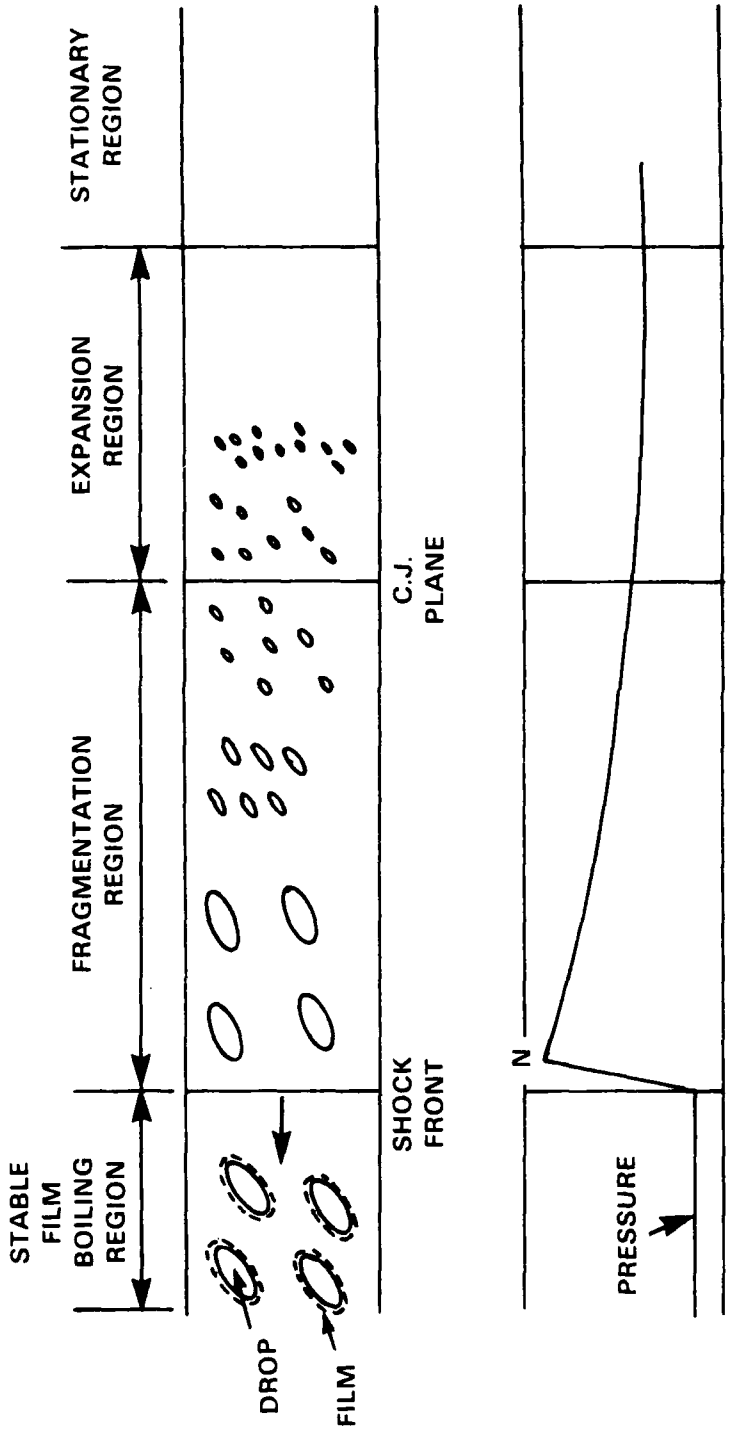

Figure 2

SKETCH OF A THERMAL DETONATION PROPAGATING IN MOLTEN METAL DROPS DISPERSED IN WATER [1]

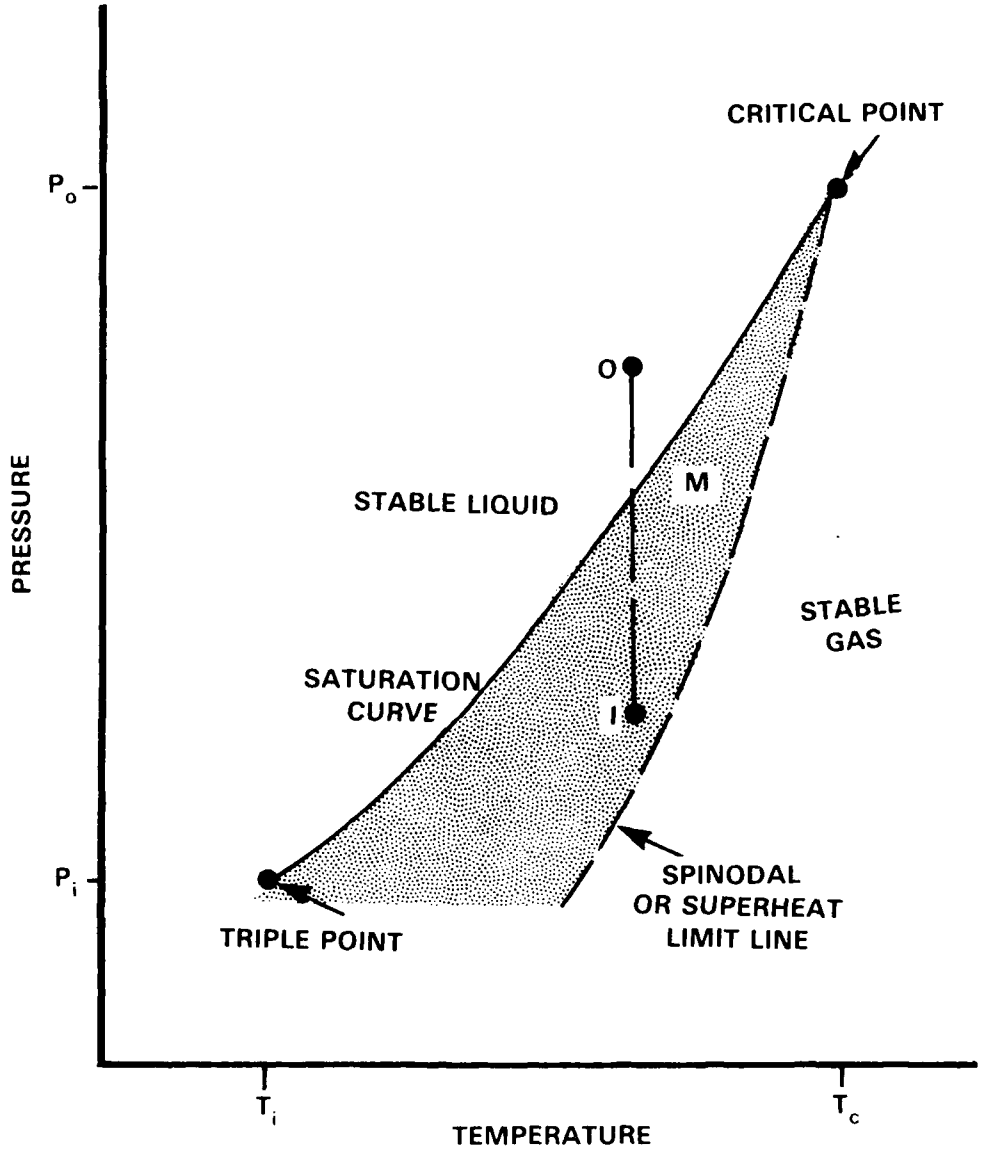

Figure 3

LIQUID-VAPOUR SATURATION AND NUCLEATION CURVES CURVE IN THE P-T PLANE

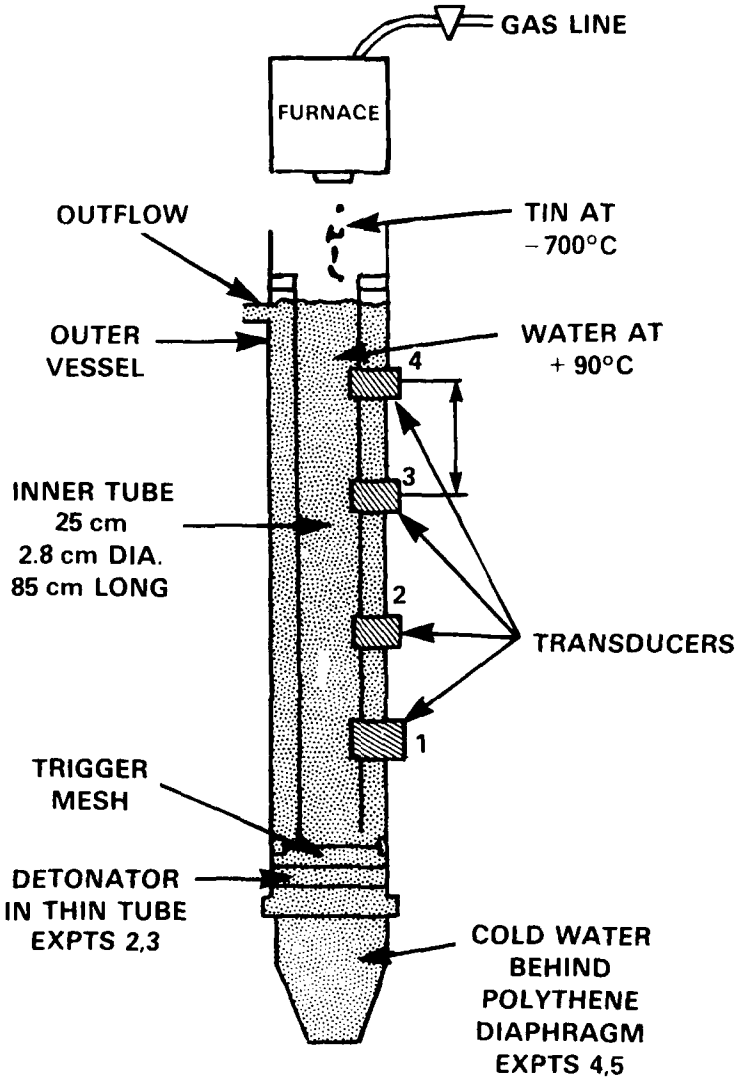

Figure 4

SCHEMATIC DIAGRAM OF THE APPARATUS FOR TIN/WATER EXPERIMENTS ON PROPAGATING THERMAL EXPLOSIONS [16]

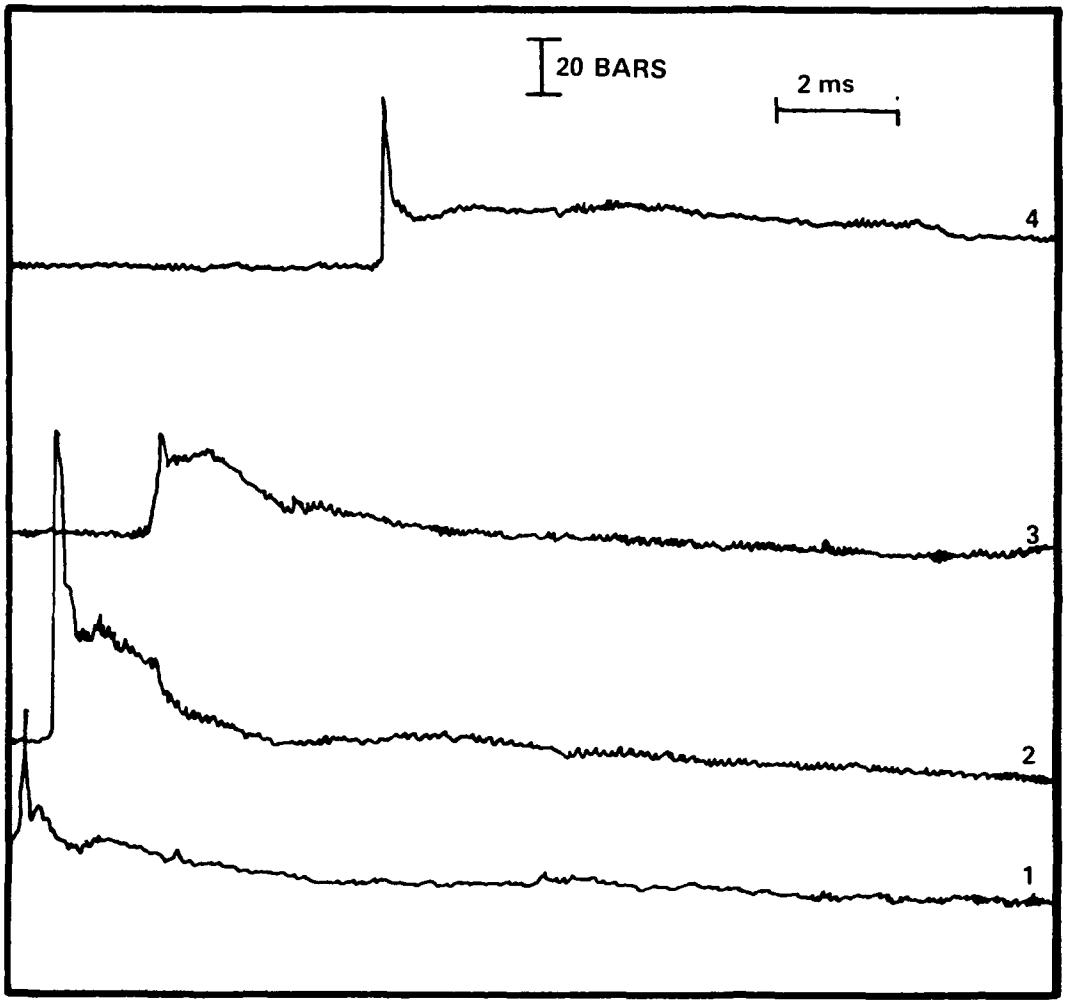

Figure 5

TRANSDUCER PRESSURE TRACE FOR TIN/WATER EXPERIMENT [16]

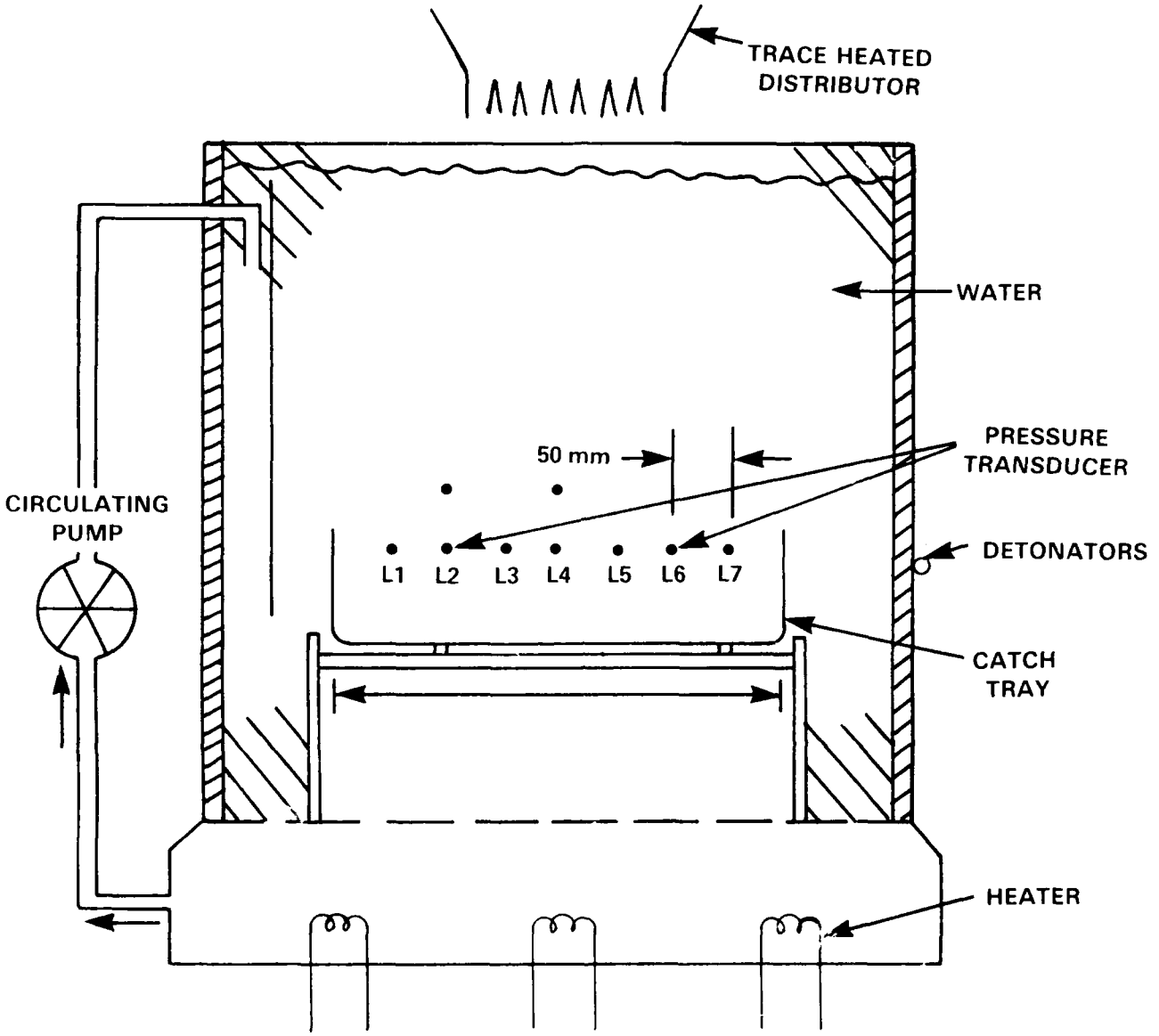

Figure 6

LARGE NARROW THERMIR VESSEL OF WINFRITH Al/WATER AND TIN/WATER EXPERIMENTS ON PROPAGATING THERMAL EXPLOSIONS [17]

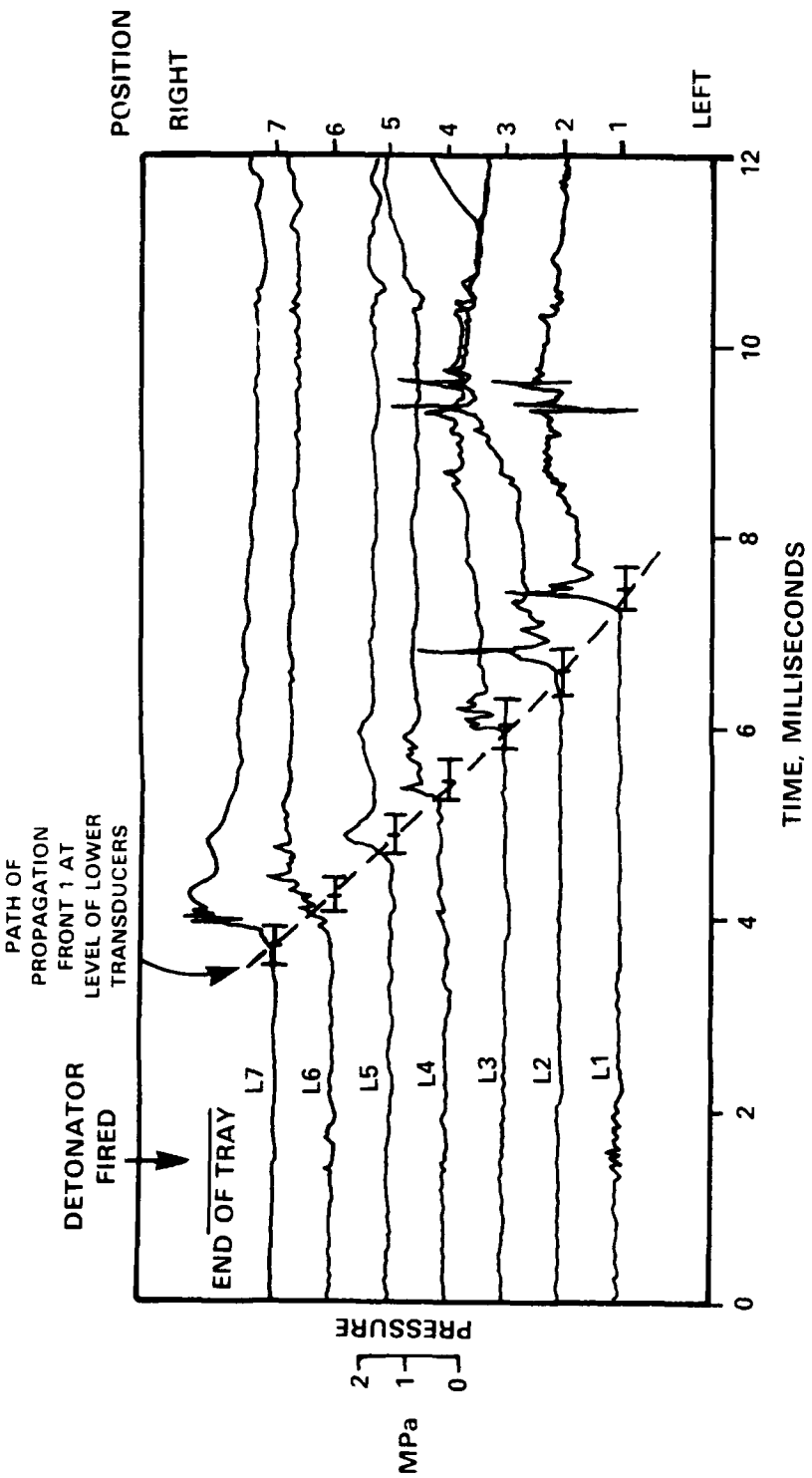

Figure 7
PRESSURE RECORDS SHOWING OBSERVED PROPAGATION FRONT IN WINFRITH TIN/WATER EXPERIMENT T107 [17]

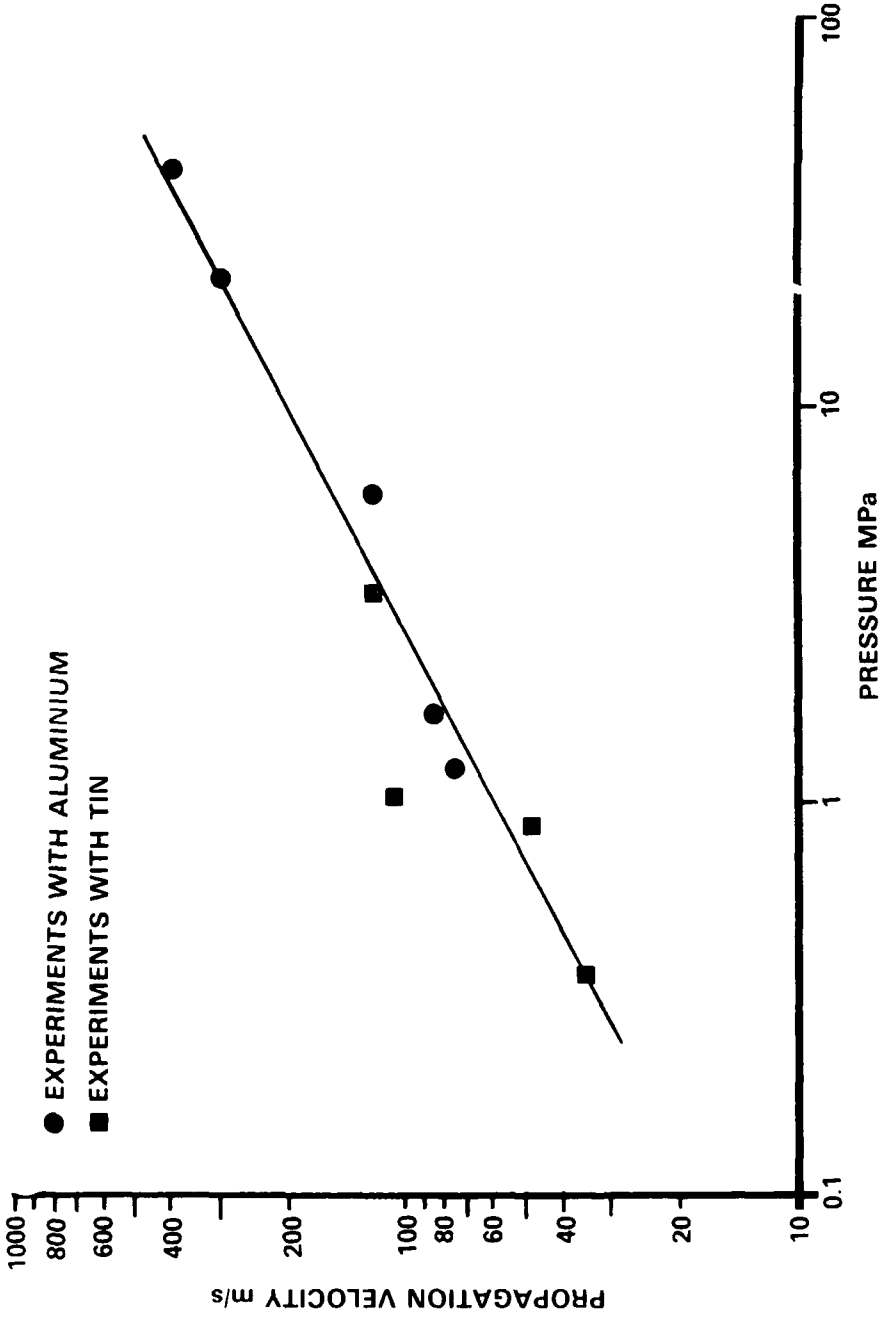

Figure 8

VARIATION OF PROPAGATION VELOCITY WITH PEAK PRESSURE IN WINFRITH Al/WATER AND TIN/WATER EXPERIMENTS ON PROPAGATING THERMAL EXPLOSIONS [17]

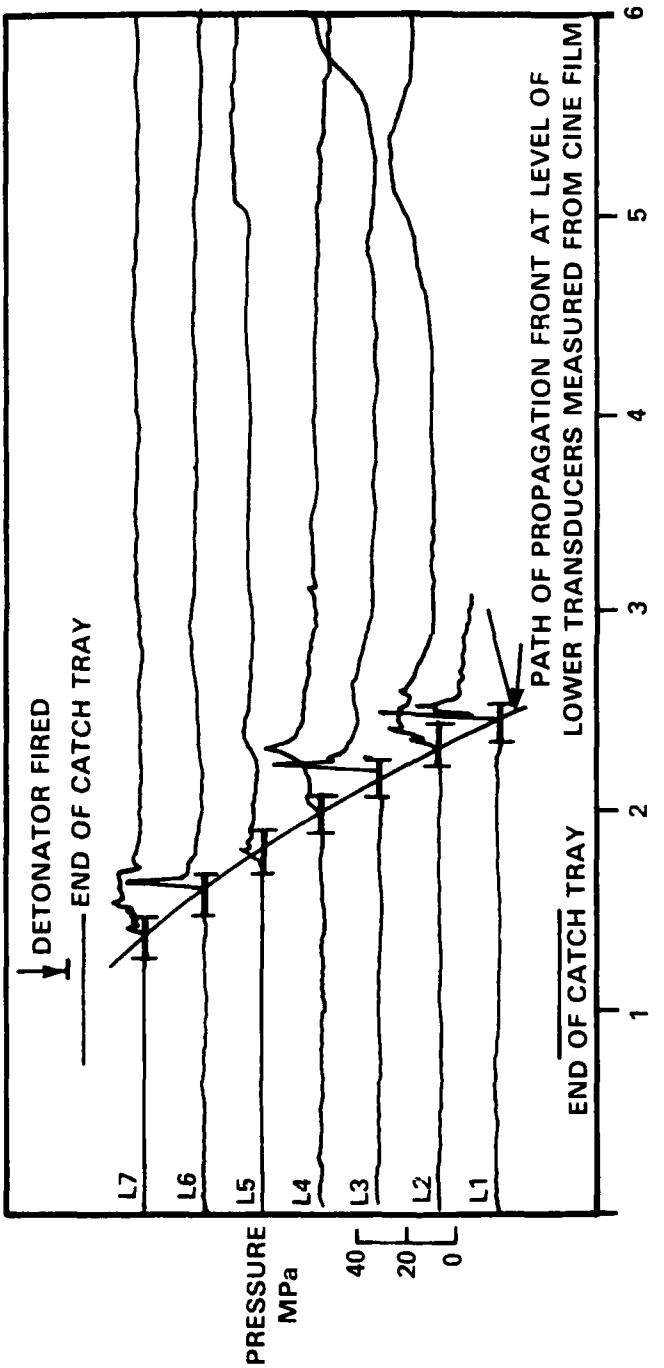

Figure 9

COMBINATION PLOT OF DATA FROM LOWER PRESSURE TRANSDUCERS OF WINFRITH Aℓ/WATER EXPERIMENT T120 [18]

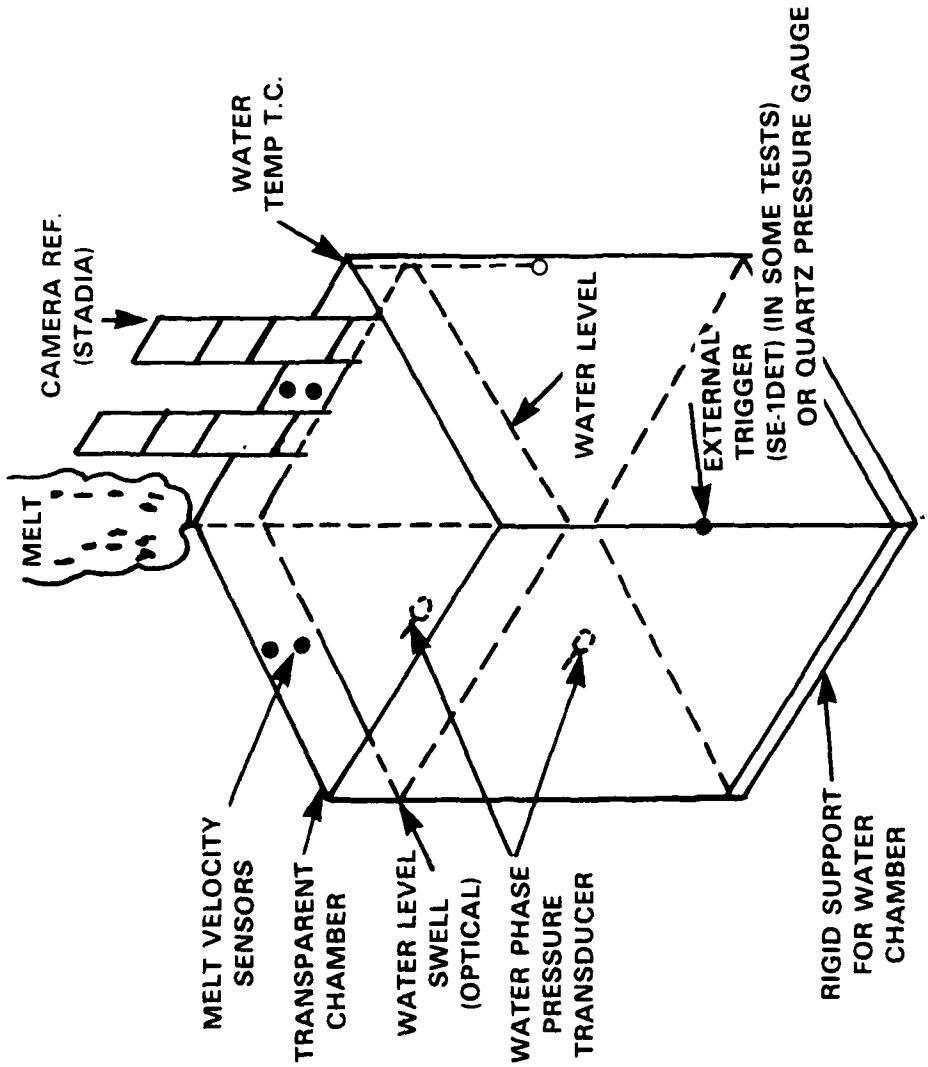

Figure 10
INSTRUMENTED WATER CHAMBER [21]

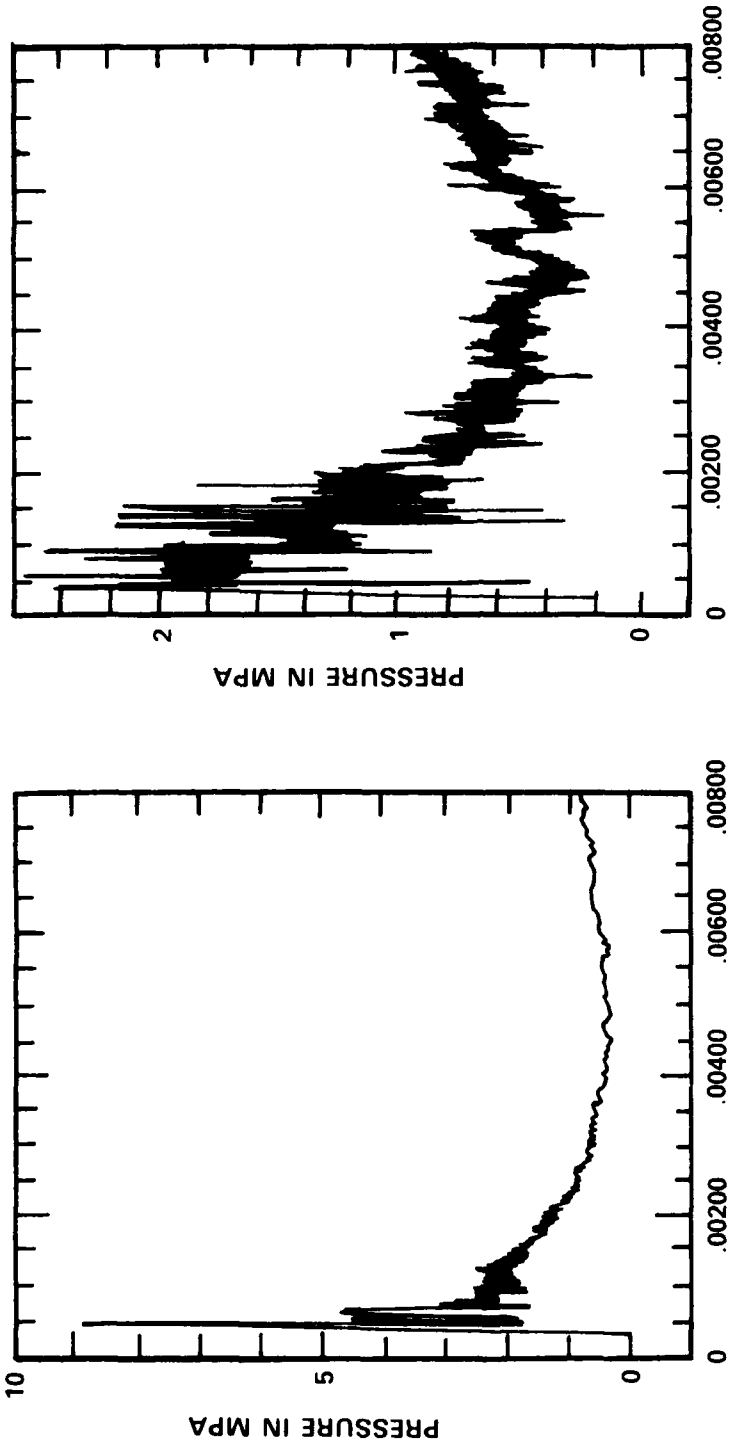

Figure 11

WATER PHASE PRESSURE FOR EXPERIMENT MD-18, ON PROPAGATING THERMAL EXPLOSIONS IN ($Fe{\cdot}Al_2O_3$) /WATER SYSTEMS [21]

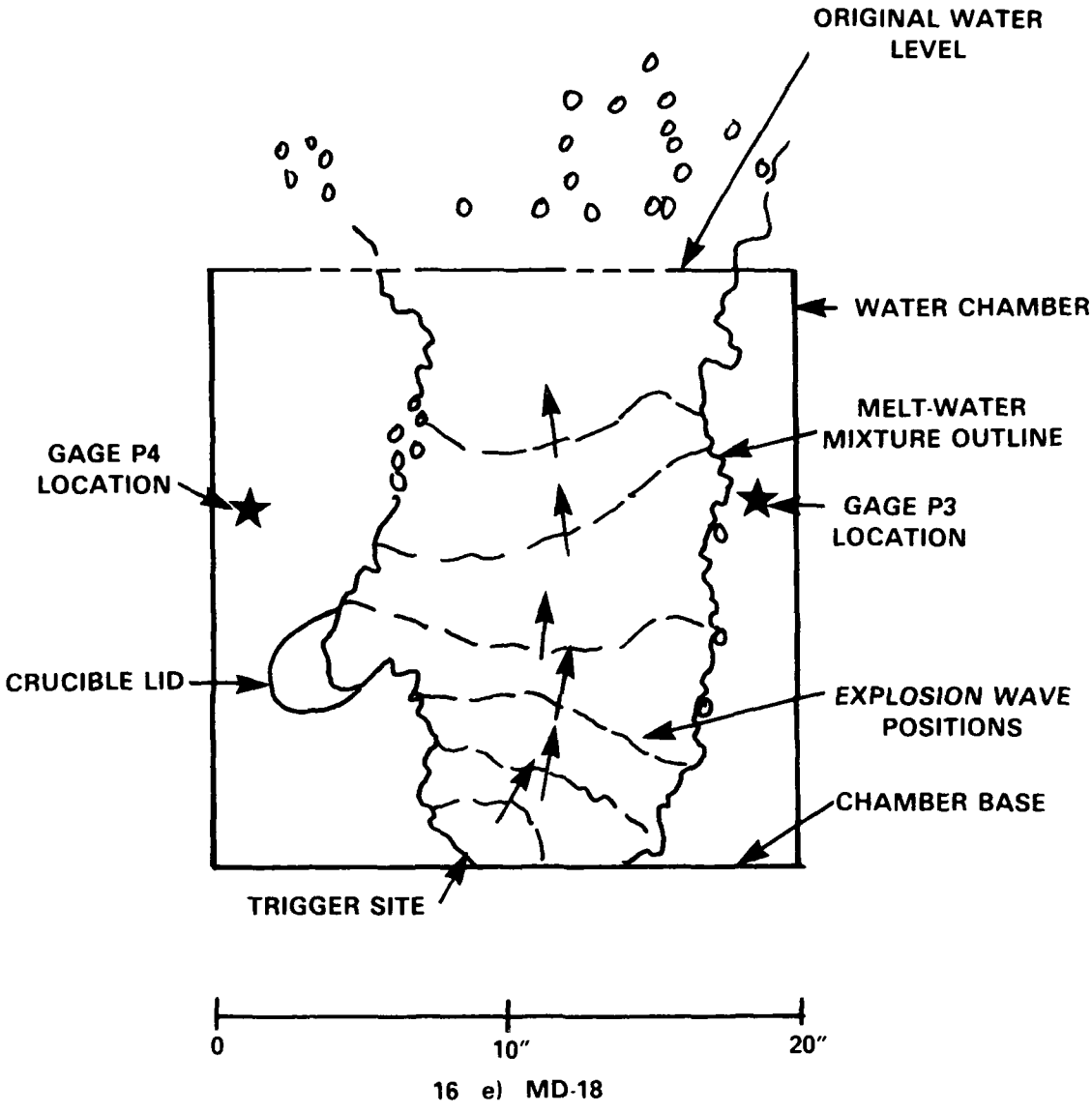

Figure 12

EXPLOSION WAVE PROPAGATION IN EXPERIMENT MD-18 ON PROPAGATING THERMAL EXPLOSIONS IN (Fe-Al_2O_3)/WATER SYSTEMS [21]

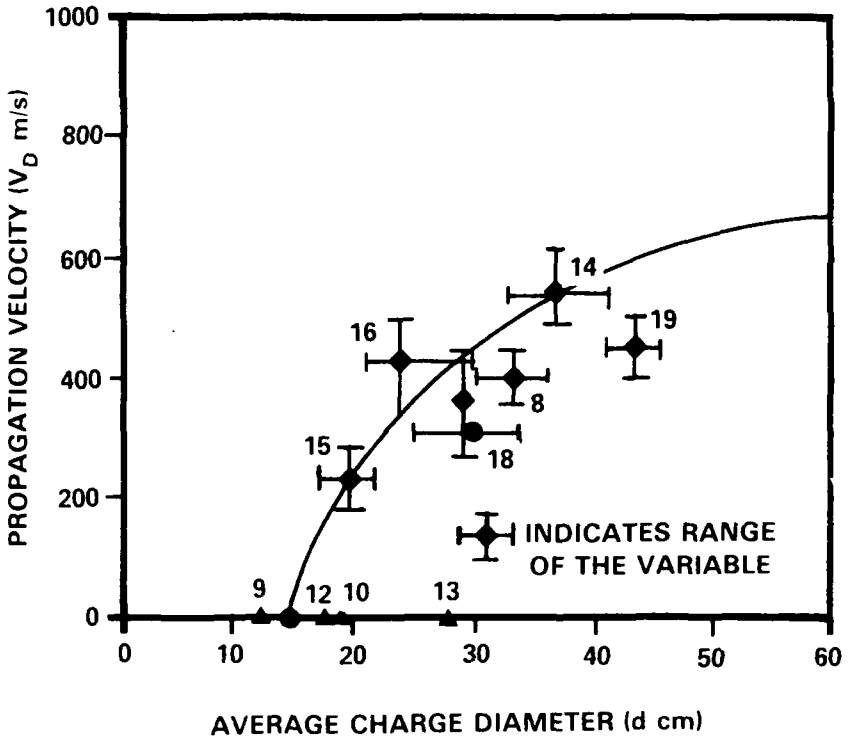

Figure 13

PROPAGATION VELOCITY VS MELT/WATER MIXTURE DIAMETER [21]

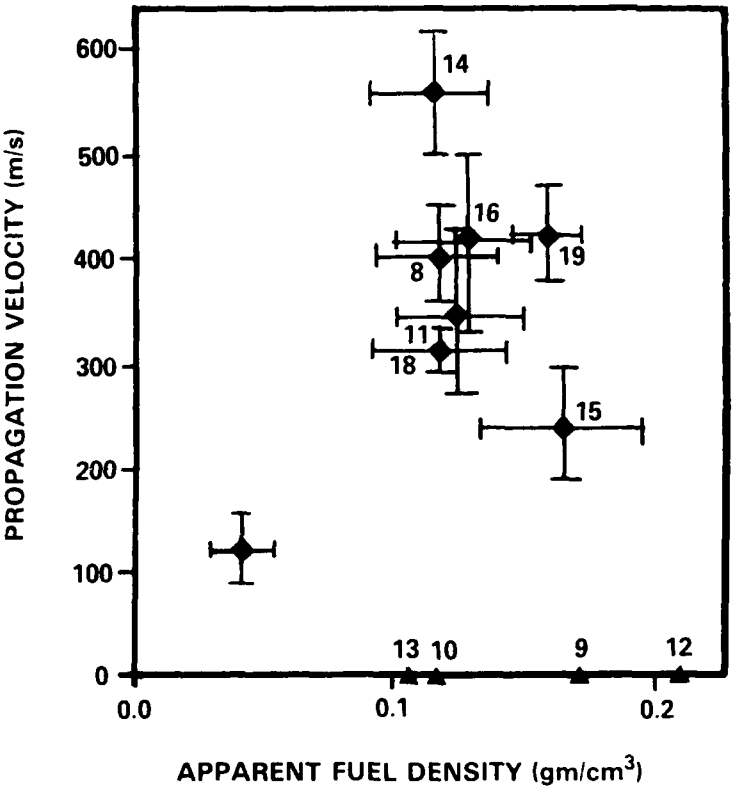

Figure 14

PROPAGATION VELOCITY VS MELT/WATER MIXTURE DENSITY [21]

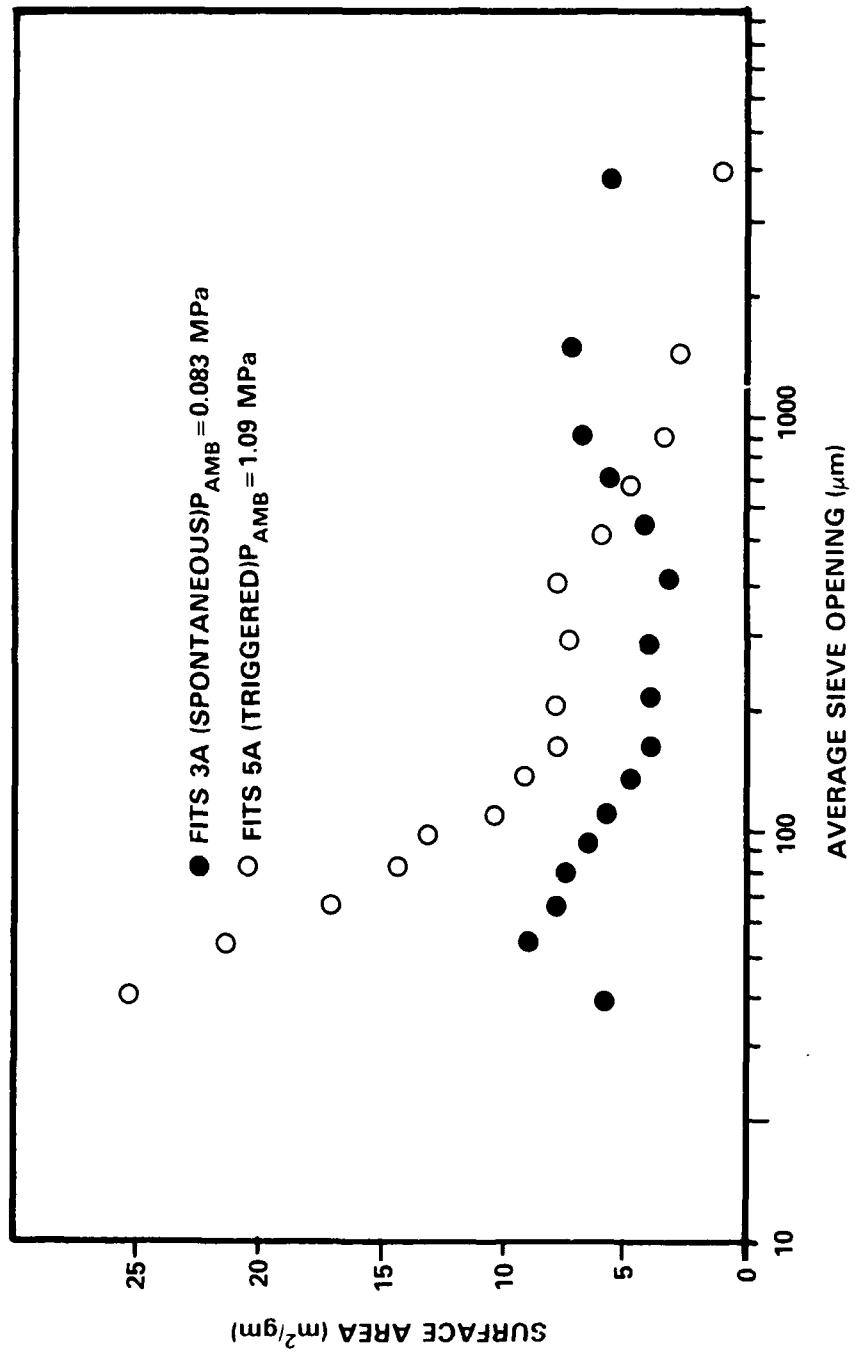

Figure 15

DEBRIS SURFACE AREA VS AVERAGE SIEVE OPENING FOR EXPERIMENTS FITS3A AND FITS5A

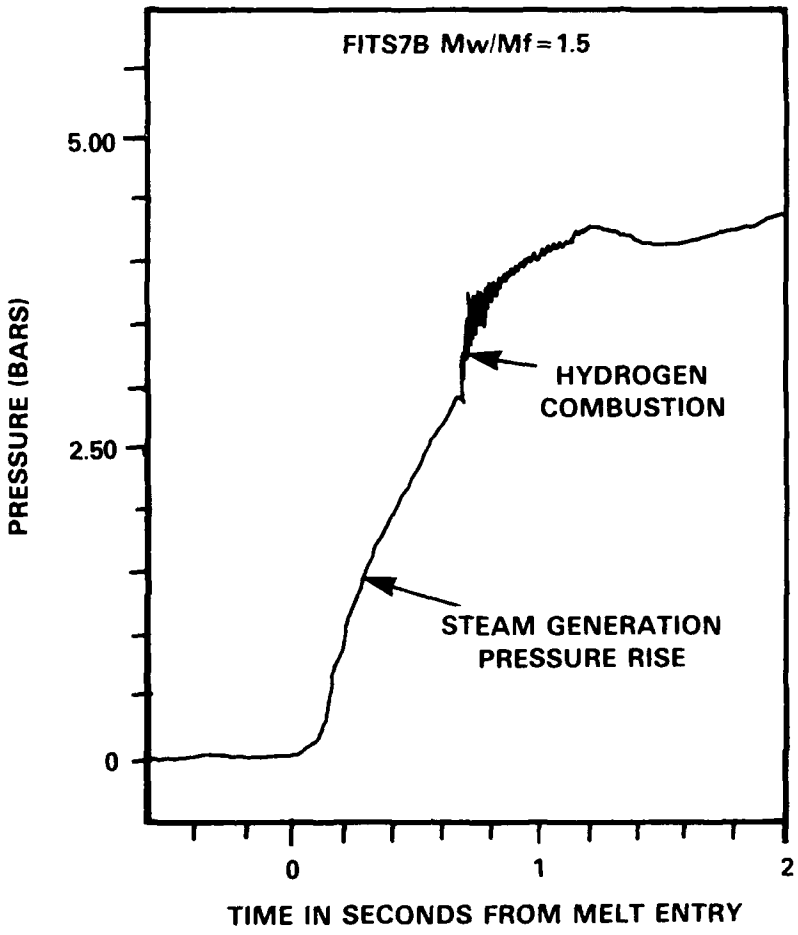

Figure 16

CHAMBER AIR PRESSURE IN FITS7B $M_w/M_f = 1.5$ [22]

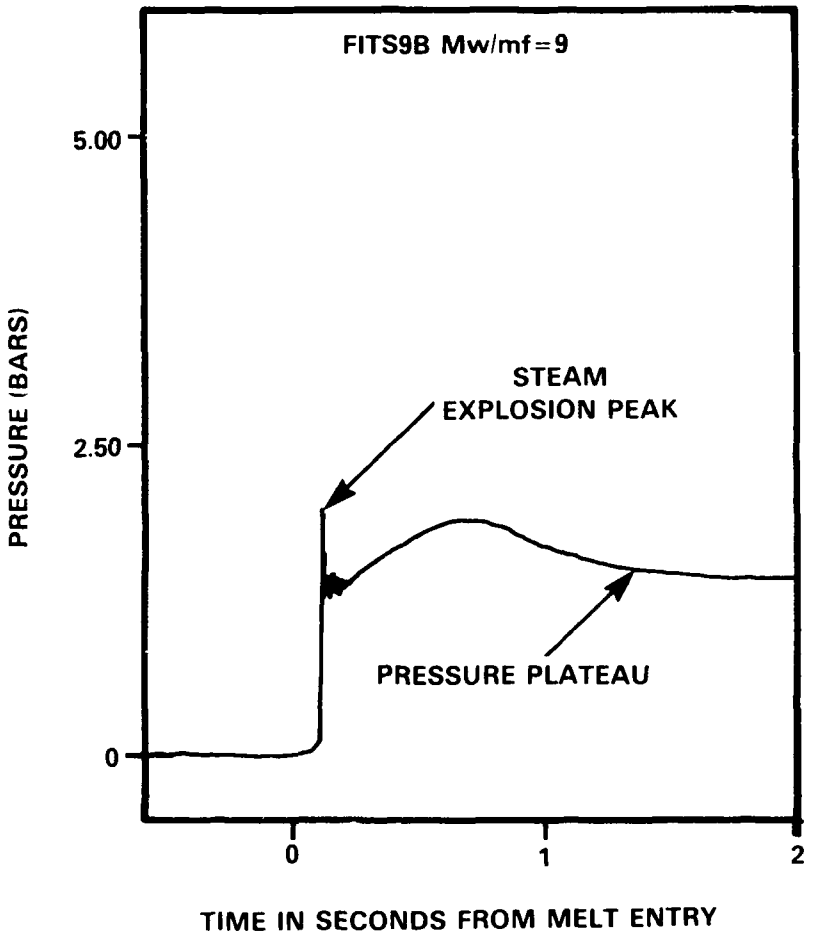

Figure 17

CHAMBER AIR PRESSURE IN FITS9B $M_w/M_f=9$ [22]

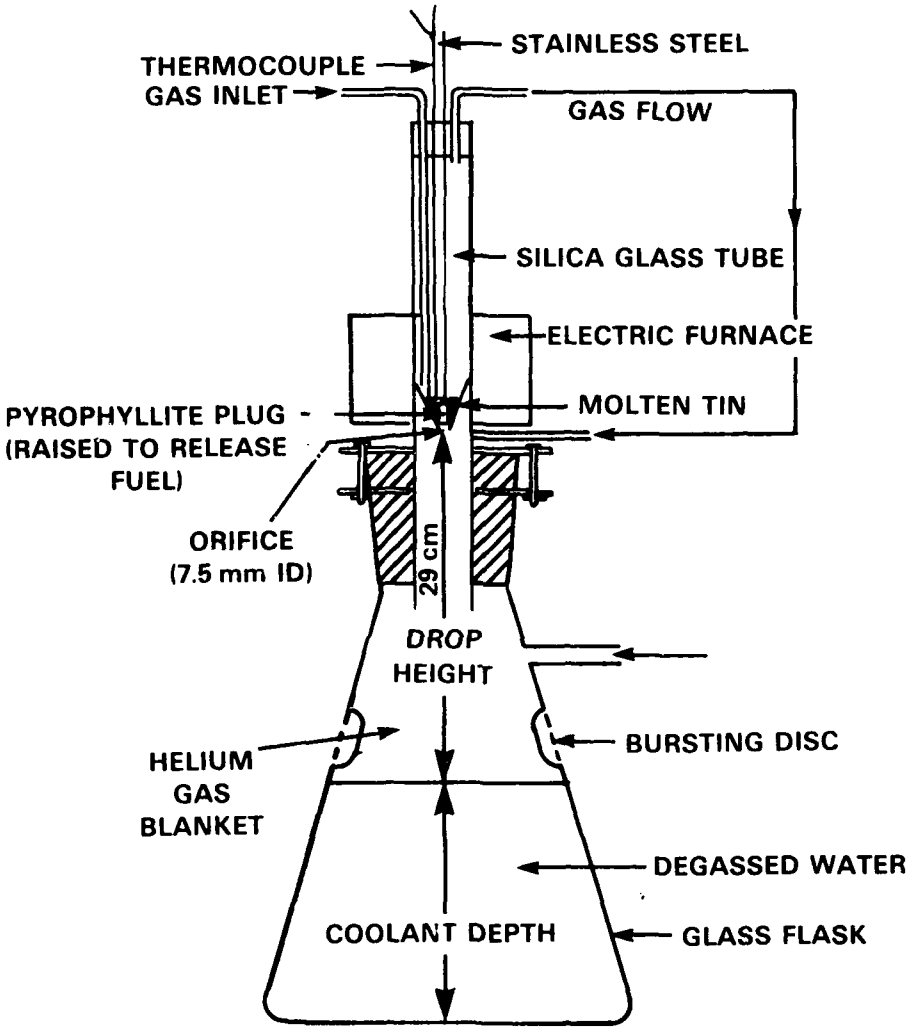

Figure 18

APPARATUS FOR STUDYING THE EFFECT OF AMBIENT PRESSURE ON SINGLE DROP THERMAL EXPLOSIONS [24]

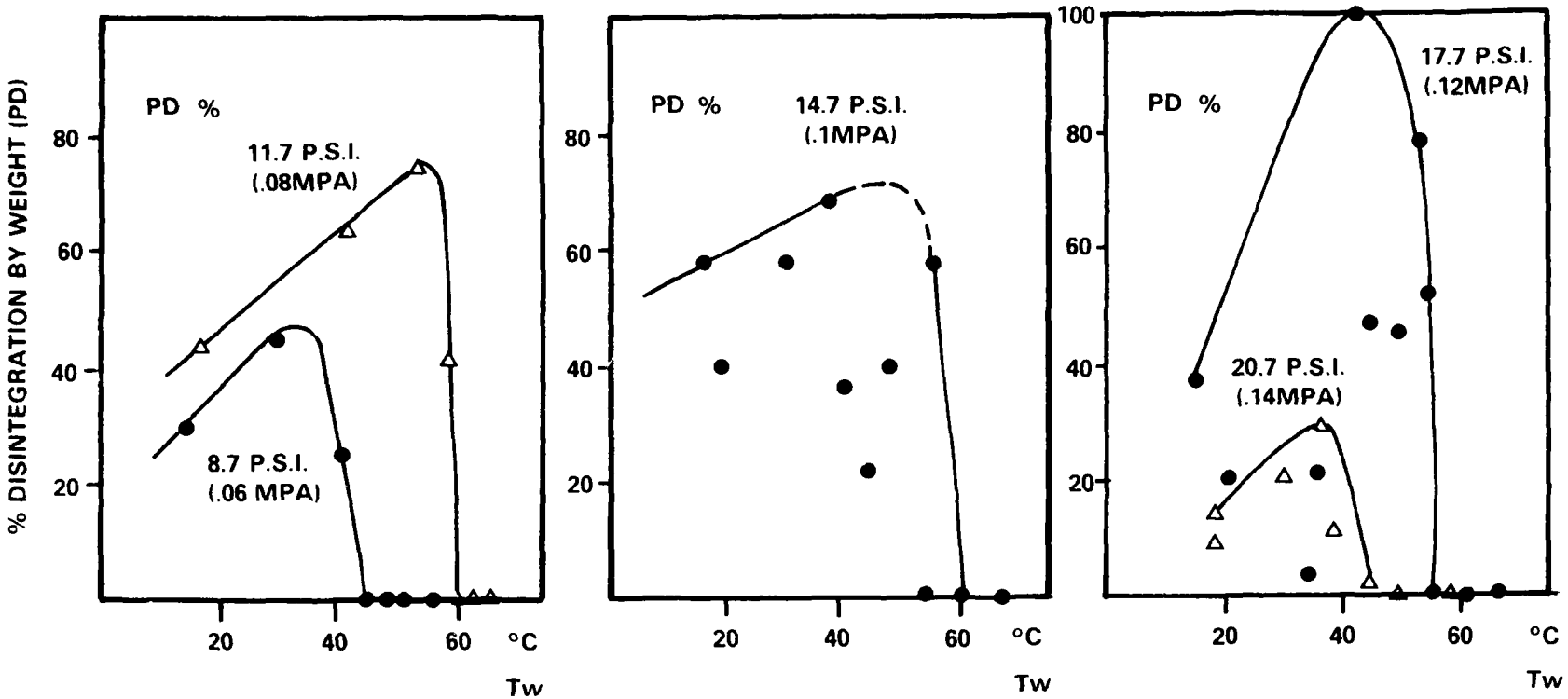

Figure 19

PERCENTAGE DISINTEGRATION (PD) AGAINST COOLANT TEMPERATURE AT VARIOUS AMBIENT PRESSURES FOR TIN/WATER, SINGLE DROP THERMAL EXPLOSIONS [24]

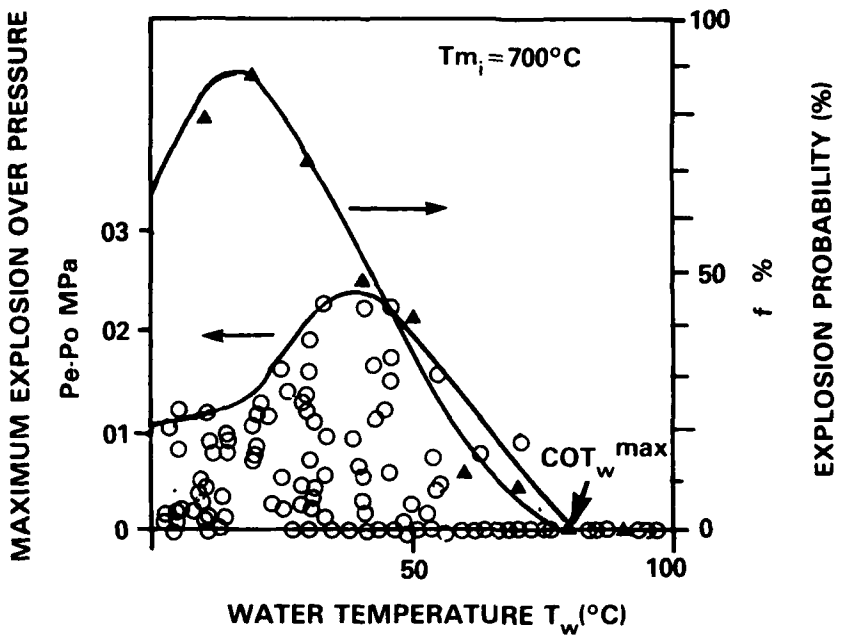

Figure 20

DEPENDENCE OF PROBABILITY AND INTENSITY OF TIN VAPOUR EXPLOSION ON WATER TEMPERATURE [25]

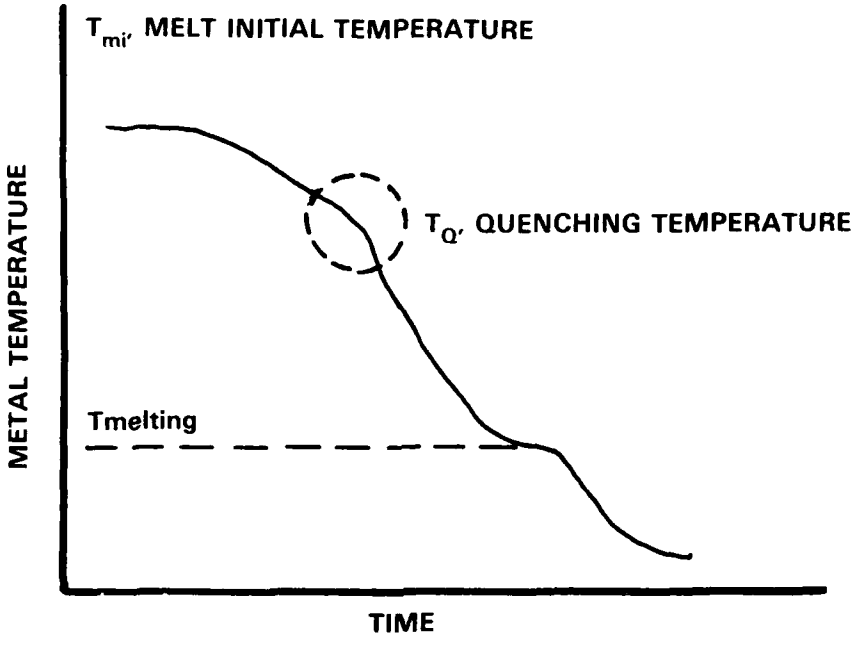

Figure 21

TYPICAL COOLING CURVE OF A MOLTEN TIN DROP WHEN QUENCHING TAKES PLACE [26]

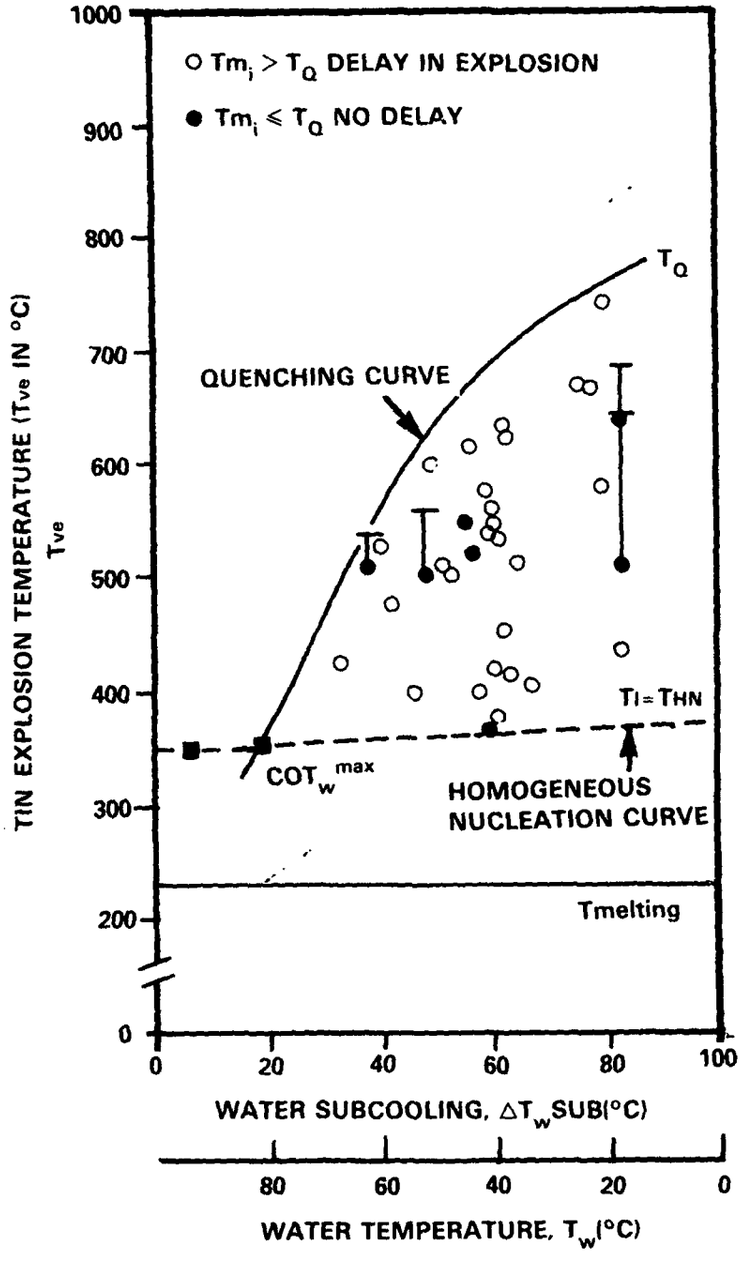

Figure 22

THE EFFECT OF THE DEGREE OF WATER SUBCOOLING ON THE TIN EXPLOSION TEMPERATURE

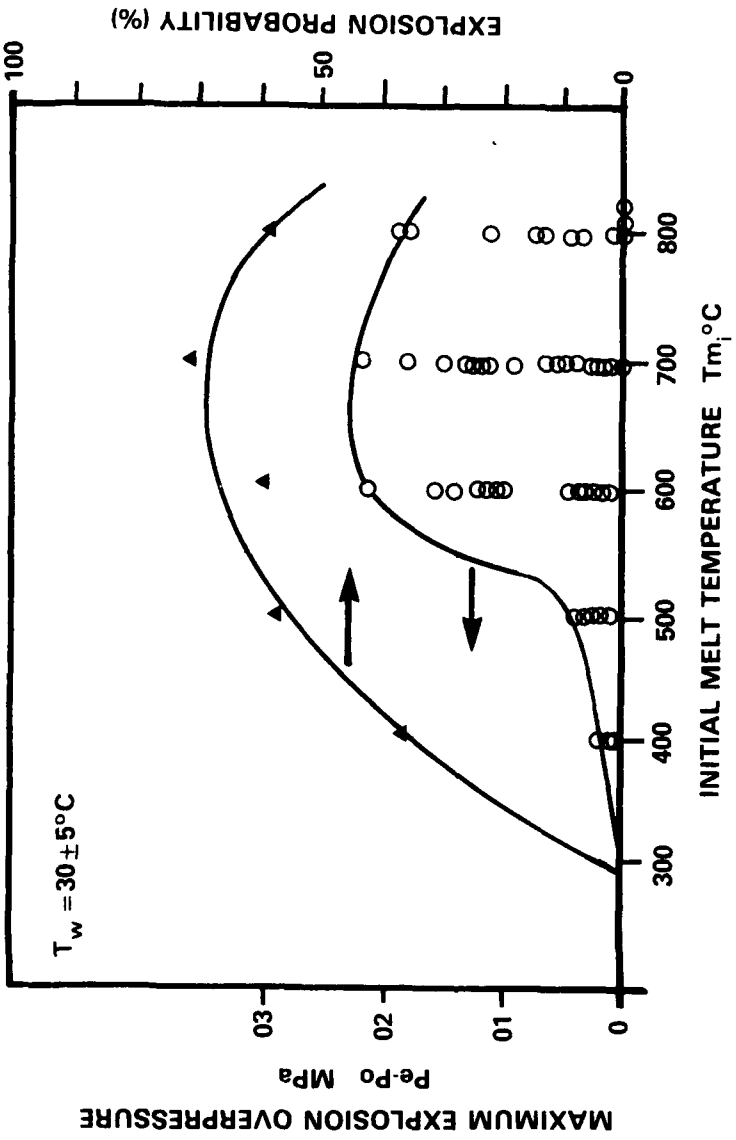

Figure 23

DEPENDENCE OF PROBABILITY AND INTENSITY OF VAPOUR EXPLOSION ON INITIAL TIN TEMPERATURE [25]

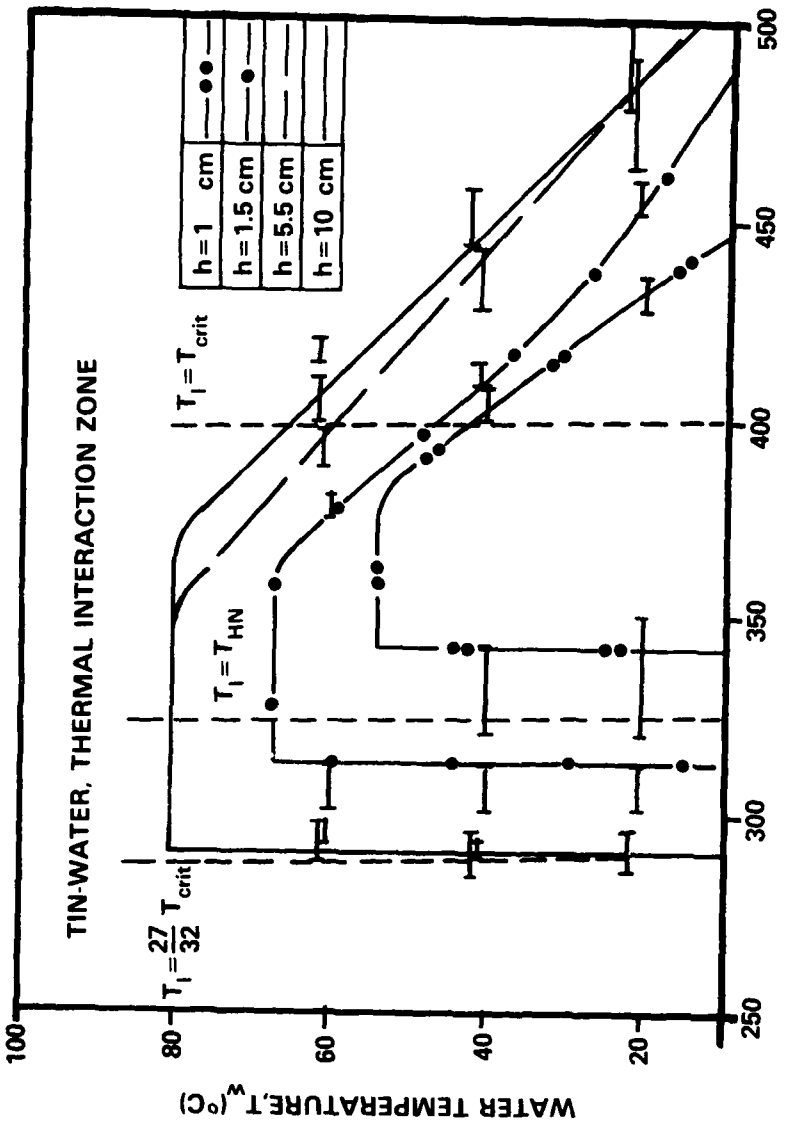

Figure 24

THERMAL INTERACTION ZONES (TIZ) AND WATER/TIN TEMPERATURE MAP FOR VARIOUS DROPPING HEIGHTS [27]

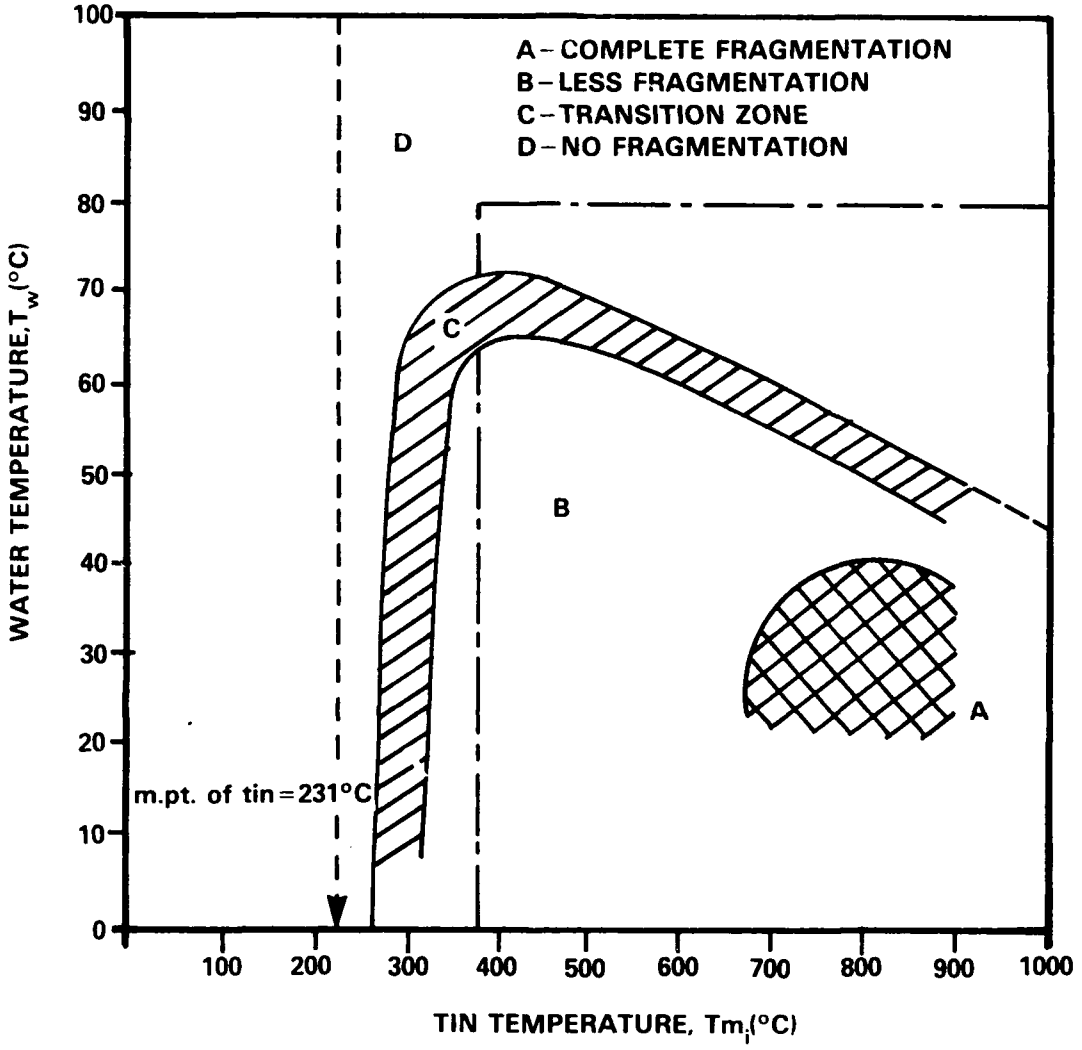

Figure 25

THE THERMAL INTERACTION AND FRAGMENTATION ZONES FOR TIN [28]

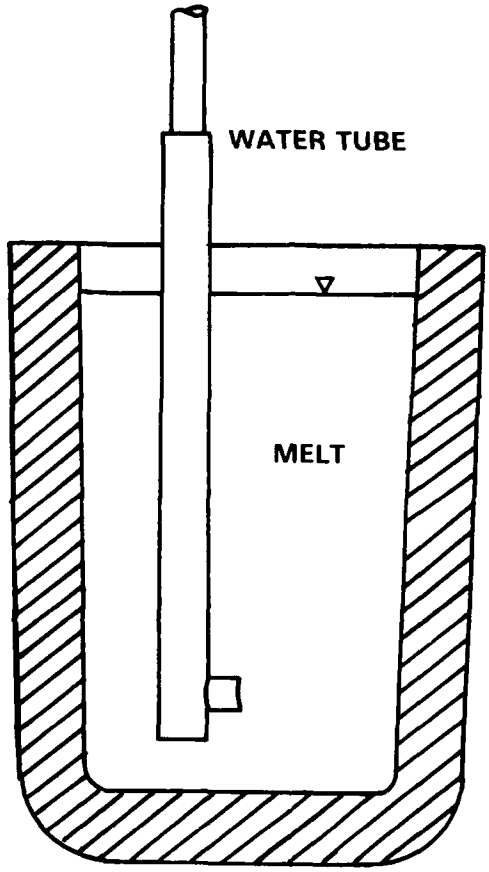

Figure 26

A SKETCH OF THE MAIN PART OF THE APPARATUS IN WHICH WATER WAS FORCED THROUGH A THERMALLY-INSULATED TUBE ON THE BOTTOM OF A CRUCIBLE FILLED WITH HOT TIN MELT [30]

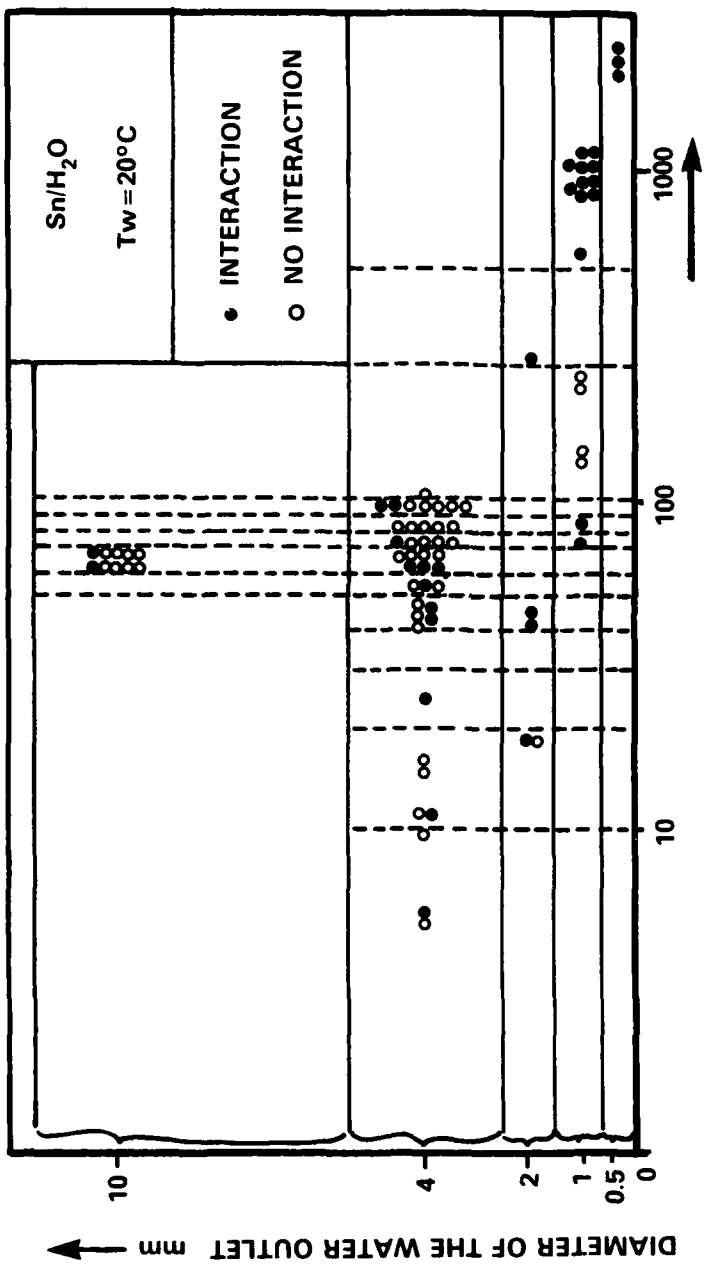

Figure 27

A SUMMARY OF ENTRAPMENT EXPERIMENTS PERFORMED WITH TIN AT 600 K AND WITH 1 g WATER AT 293 K WITH VARIATIONS IN VELOCITY OF INJECTION OF WATER AND DIAMETER OF WATER OUTLET [30]

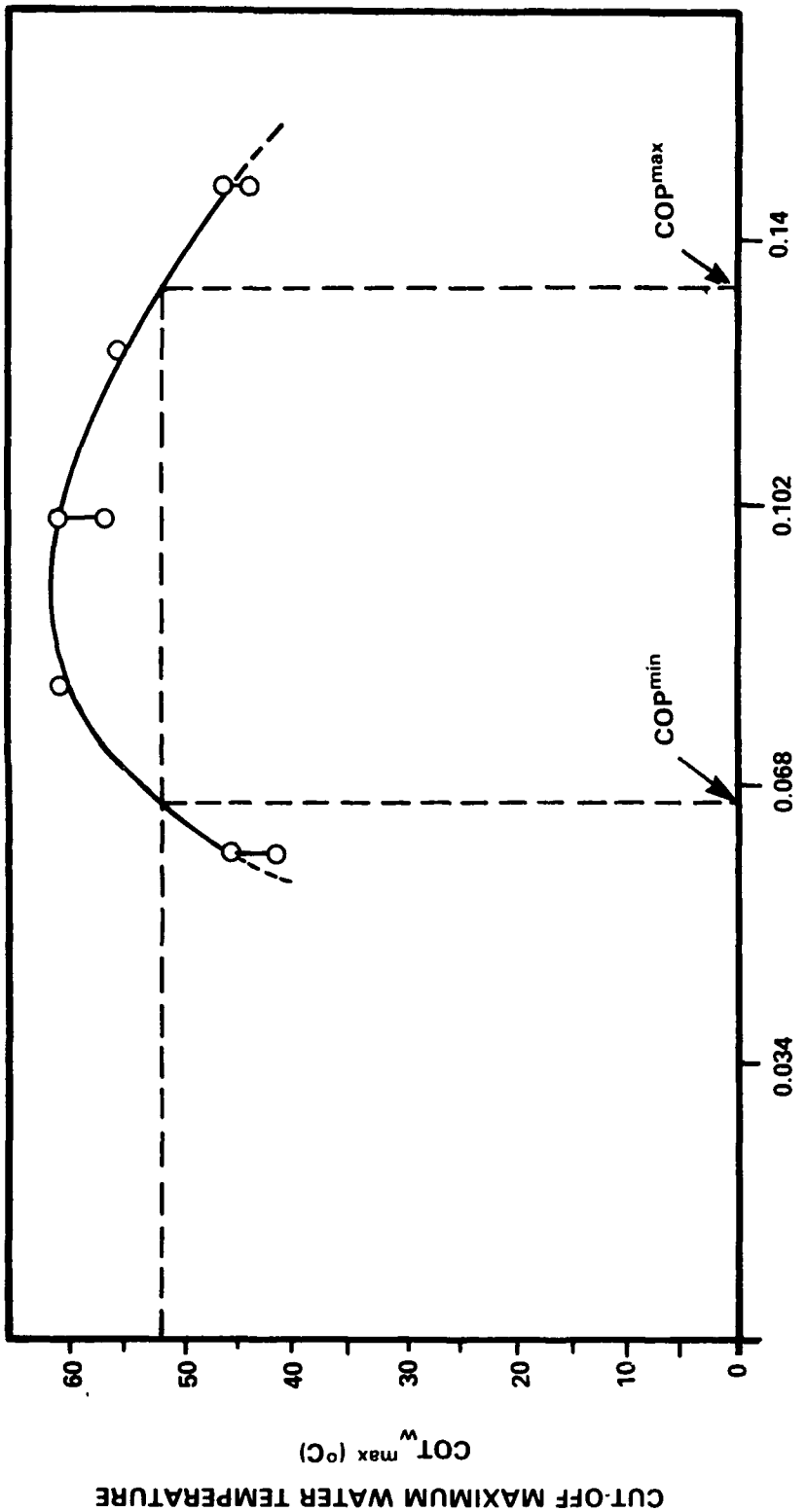

Figure 28

CUT-OFF MAXIMUM WATER TEMPERATURE AGAINST AMBIENT PRESSURE FOR TIN/WATER SINGLE DROP THERMAL EXPLOSIONS [24]

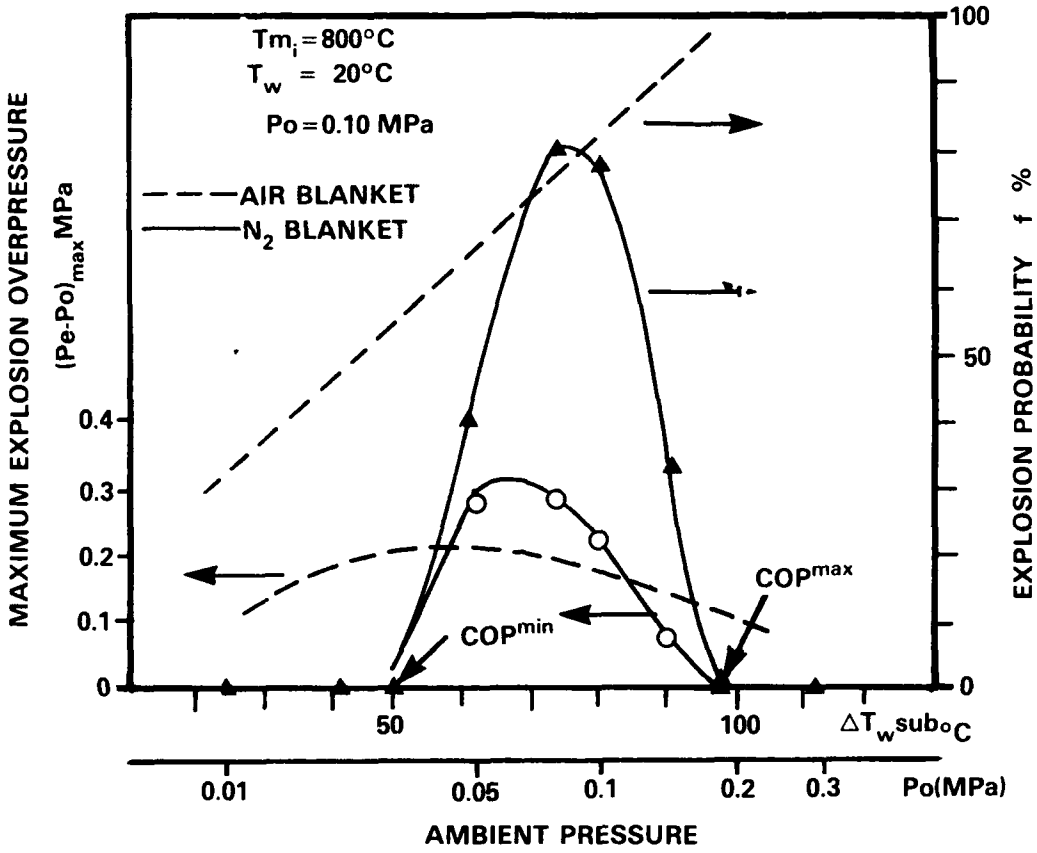

Figure 29

DEPENDENCE OF THE PROBABILITY AND INTENSITY OF TIN VAPOUR EXPLOSIONS ON THE AMBIENT PRESSURE [25]

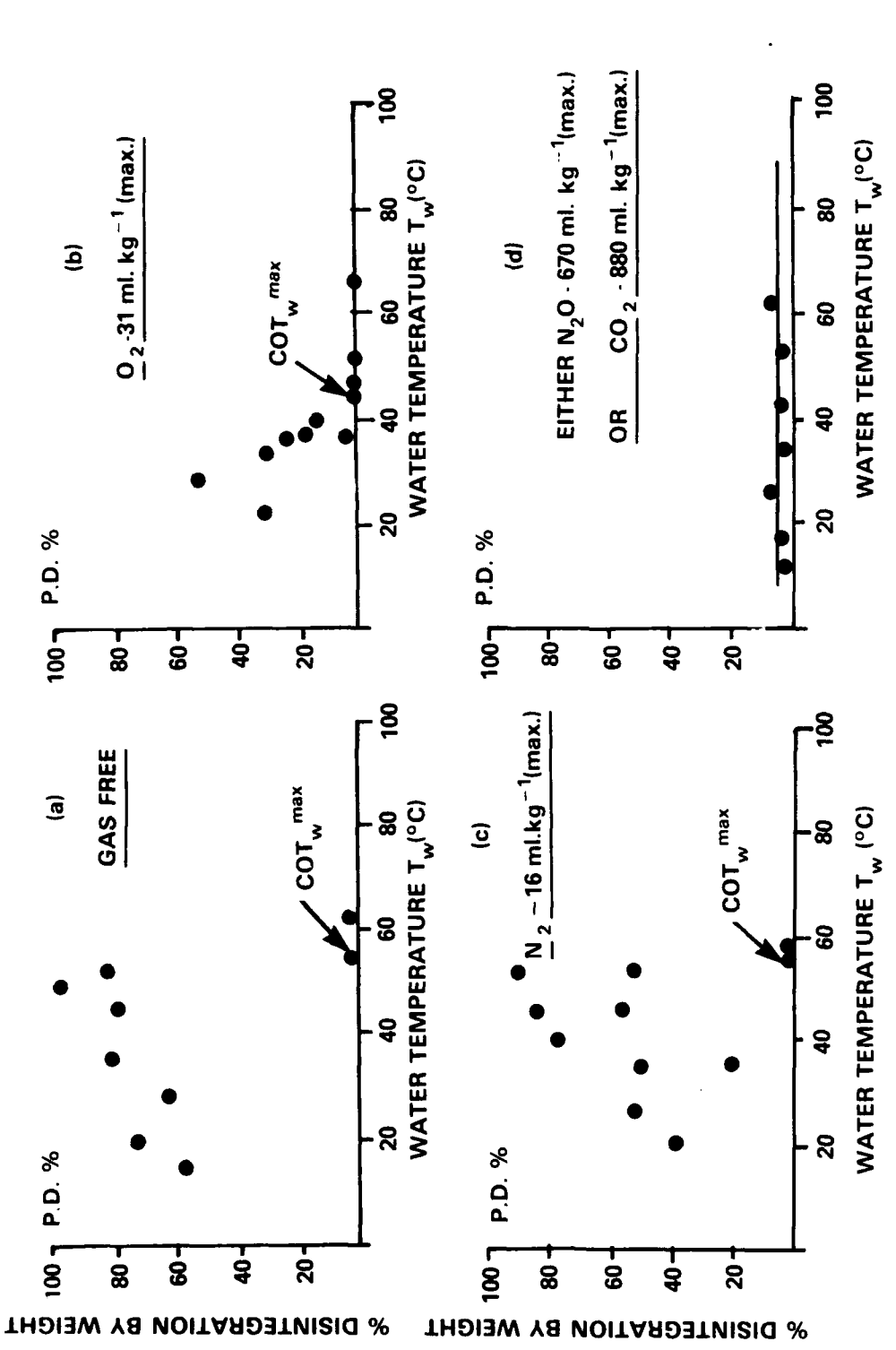

Figure 30

THE EFFECT OF DISSOLVED GASES ON TIN/WATER SINGLE DROP THERMAL EXPLOSIONS [31]

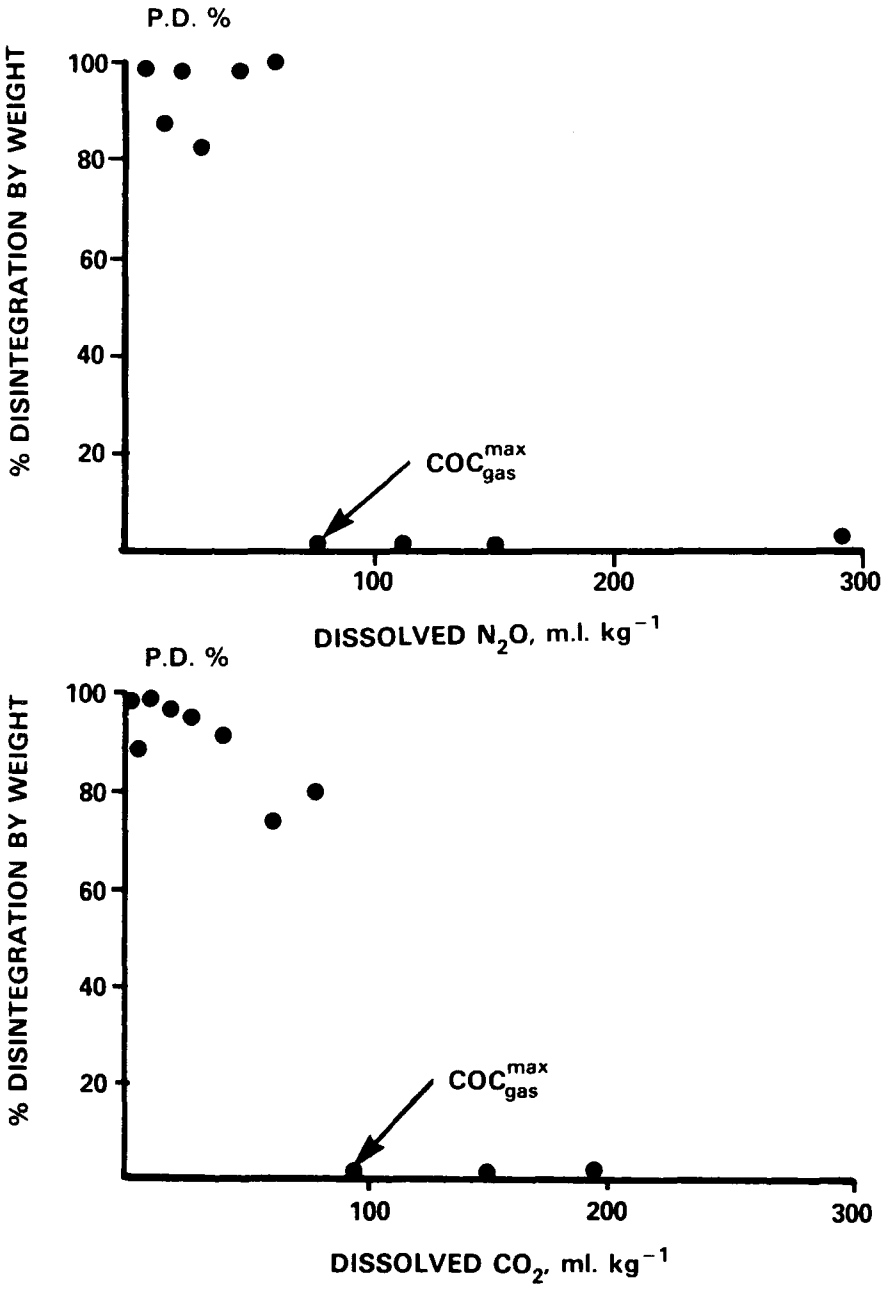

Figure 31

THE EFFECT OF DISSOLVED CO_2 AND N_2O ON TIN/WATER SINGLE DROP THERMAL EXPLOSIONS [31]

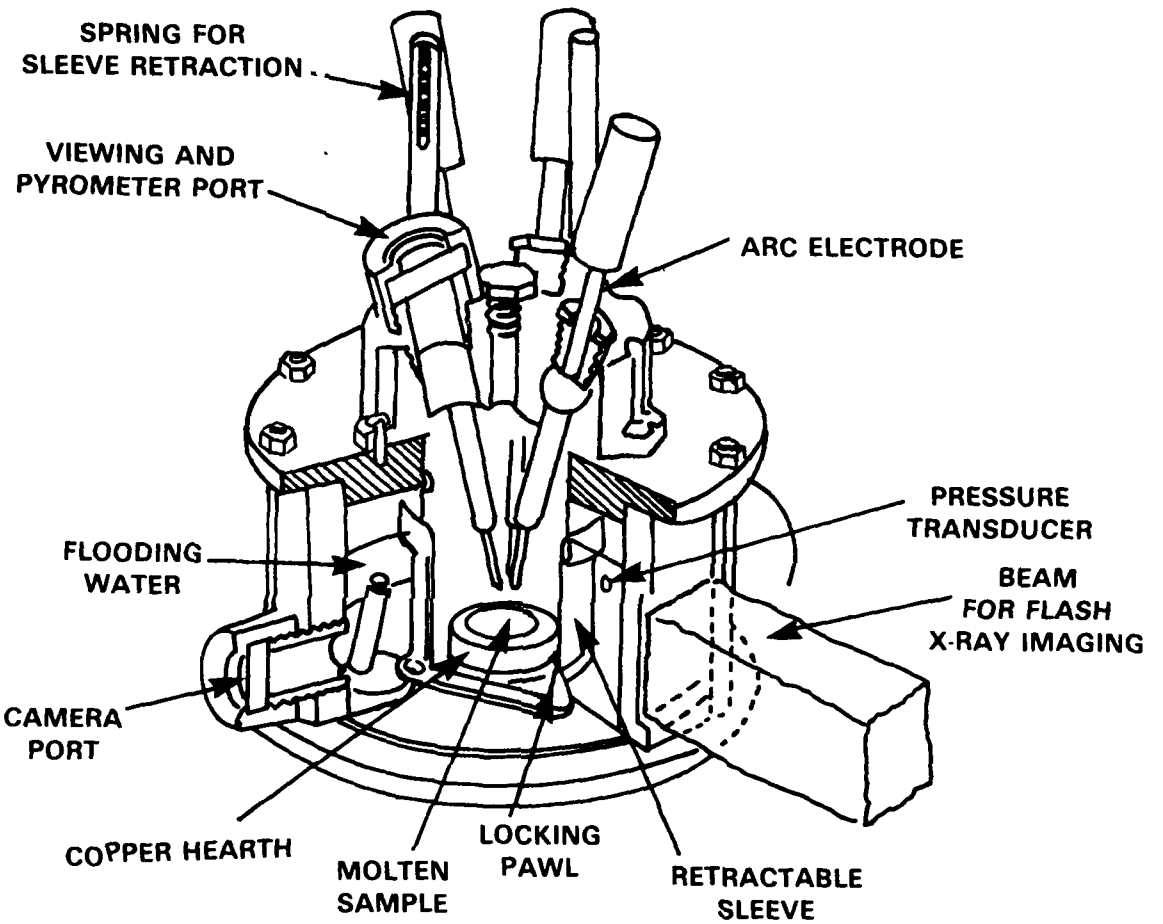

Figure 32

CUTAWAY DRAWING OF FLOODABLE ARC MELTER FOR SANDIA SMALL SCALE STEAM EXPLOSION TRIGGERING STUDIES [12]

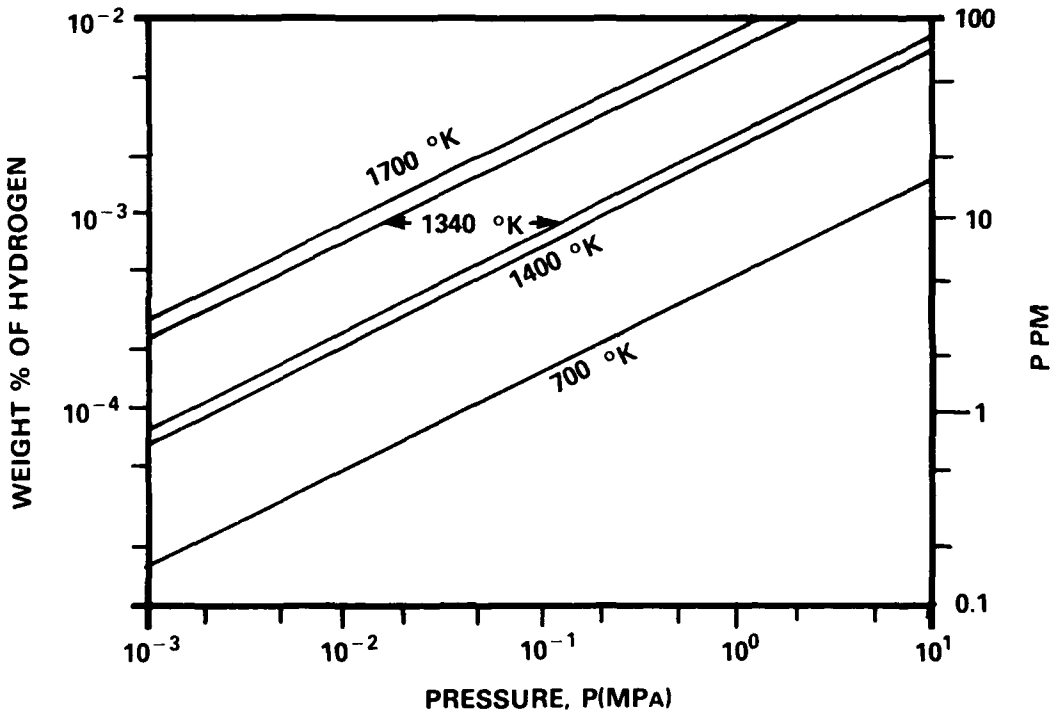

Figure 33

SIEVERT'S LAW RELATIONSHIPS FOR THE IRON-HYDROGEN SYSTEM [12]

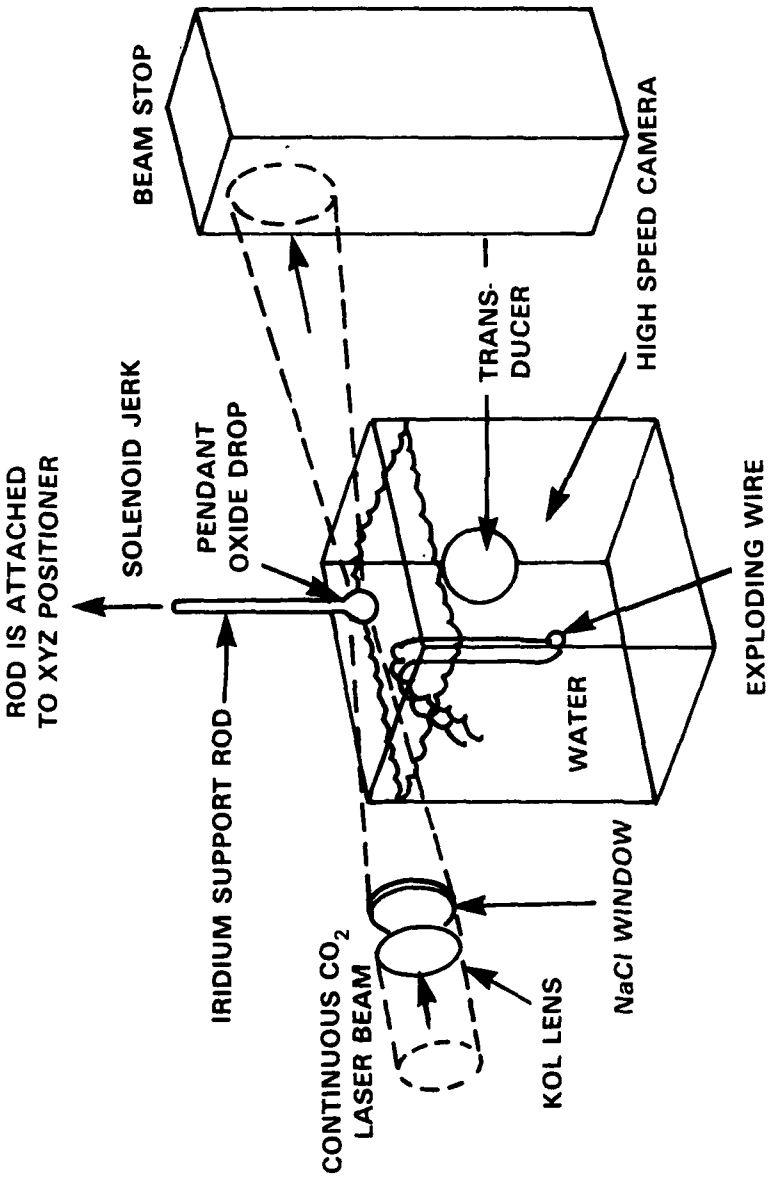

Figure 34

LASER MELTING APPARATUS [38]

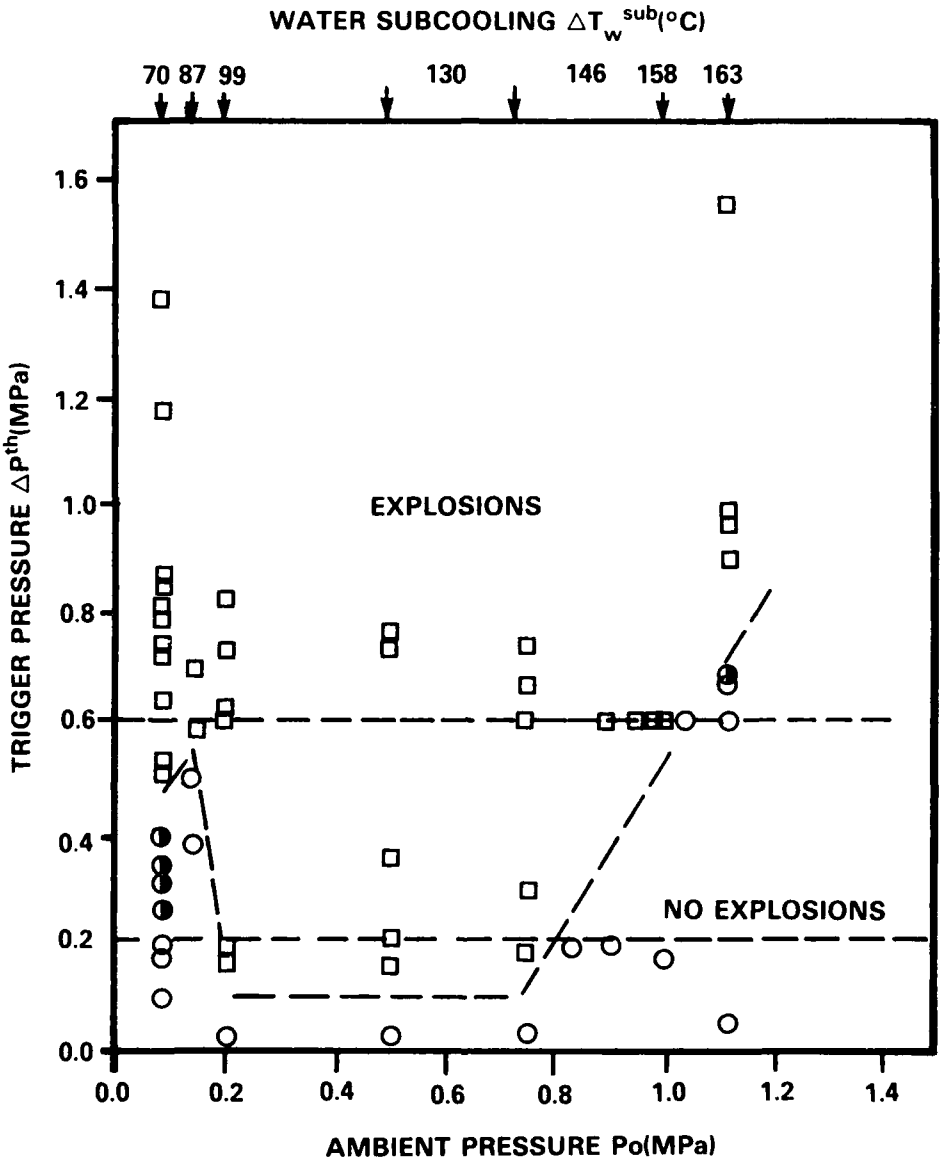

Figure 35

PEAK TRIGGERING PULSE PRESSURE VS AMBIENT PRESSURE FOR A MOLTEN IRON OXIDE DROP RELEASED INTO WATER [39]

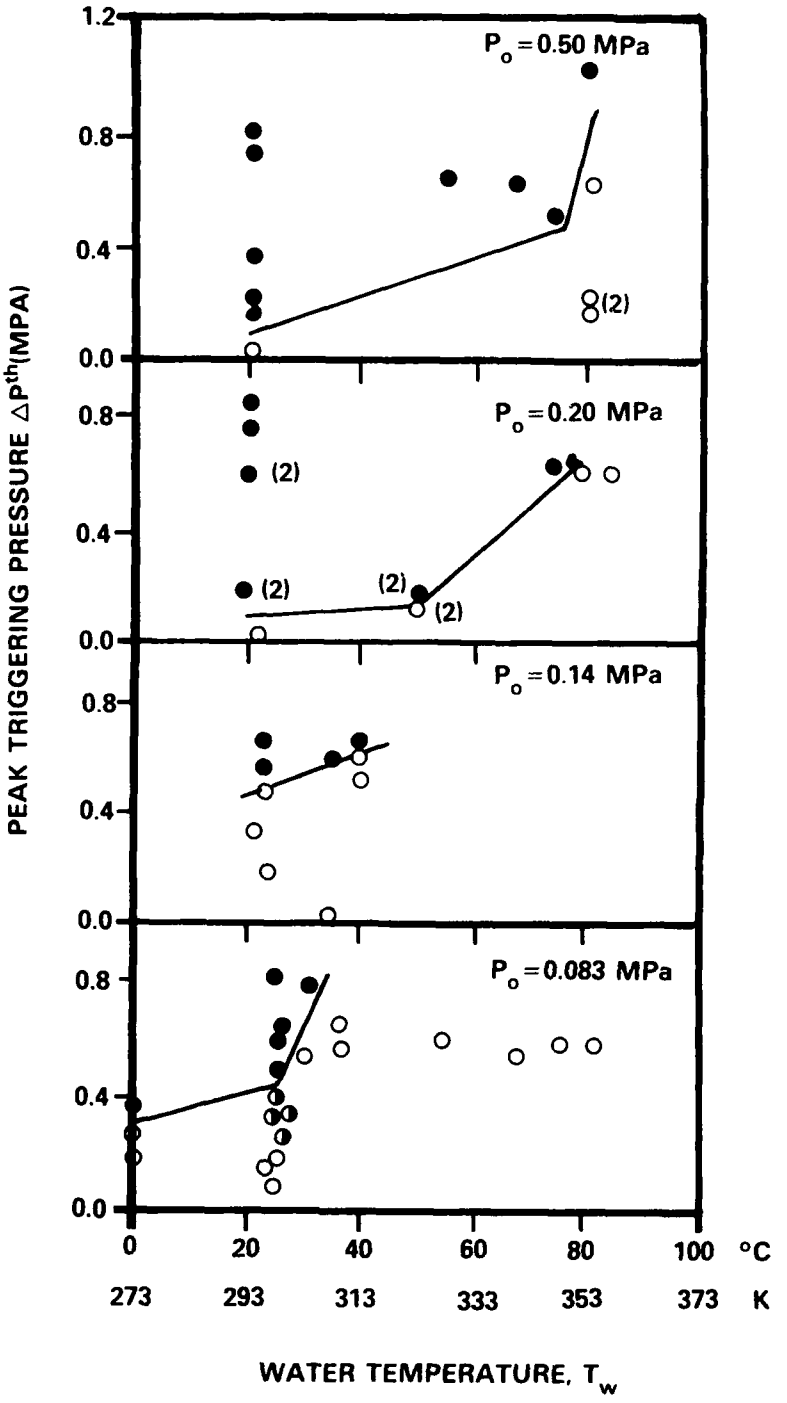

Figure 36

PEAK TRIGGERING PULSE PRESSURE VS WATER TEMPERATURE AT VARIOUS AMBIENT PRESSURES FOR AN IRON OXIDE DROP RELEASED INTO WATER [39]

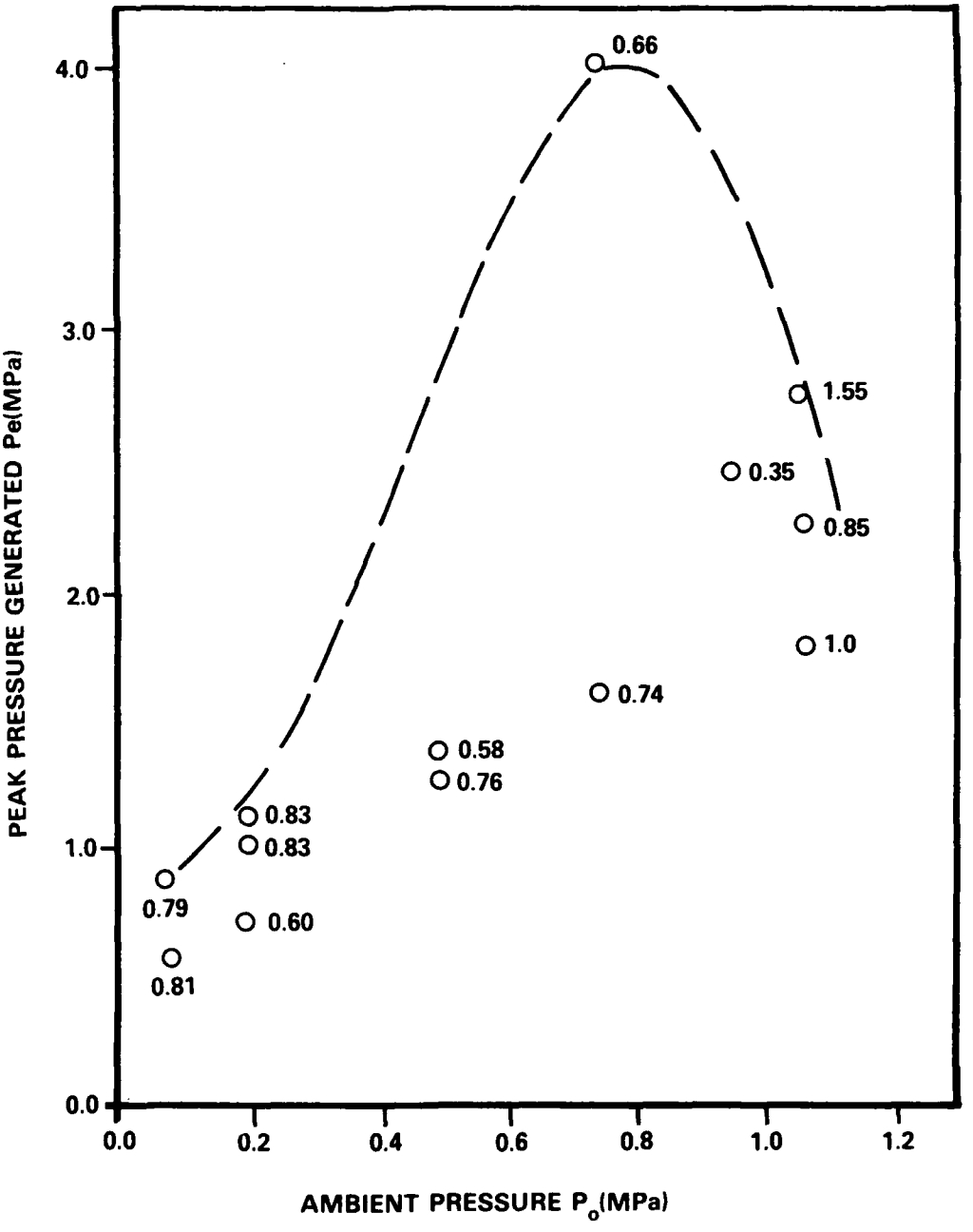

Figure 37

PEAK PRESSURE GENERATED AS THE MAJOR STEAM EXPLOSION BUBBLE CCLLAPSES VS AMBIENT PRESSURE FOR A MOLTEN IRON OXIDE DROP REALEASED INTO WATER [39]

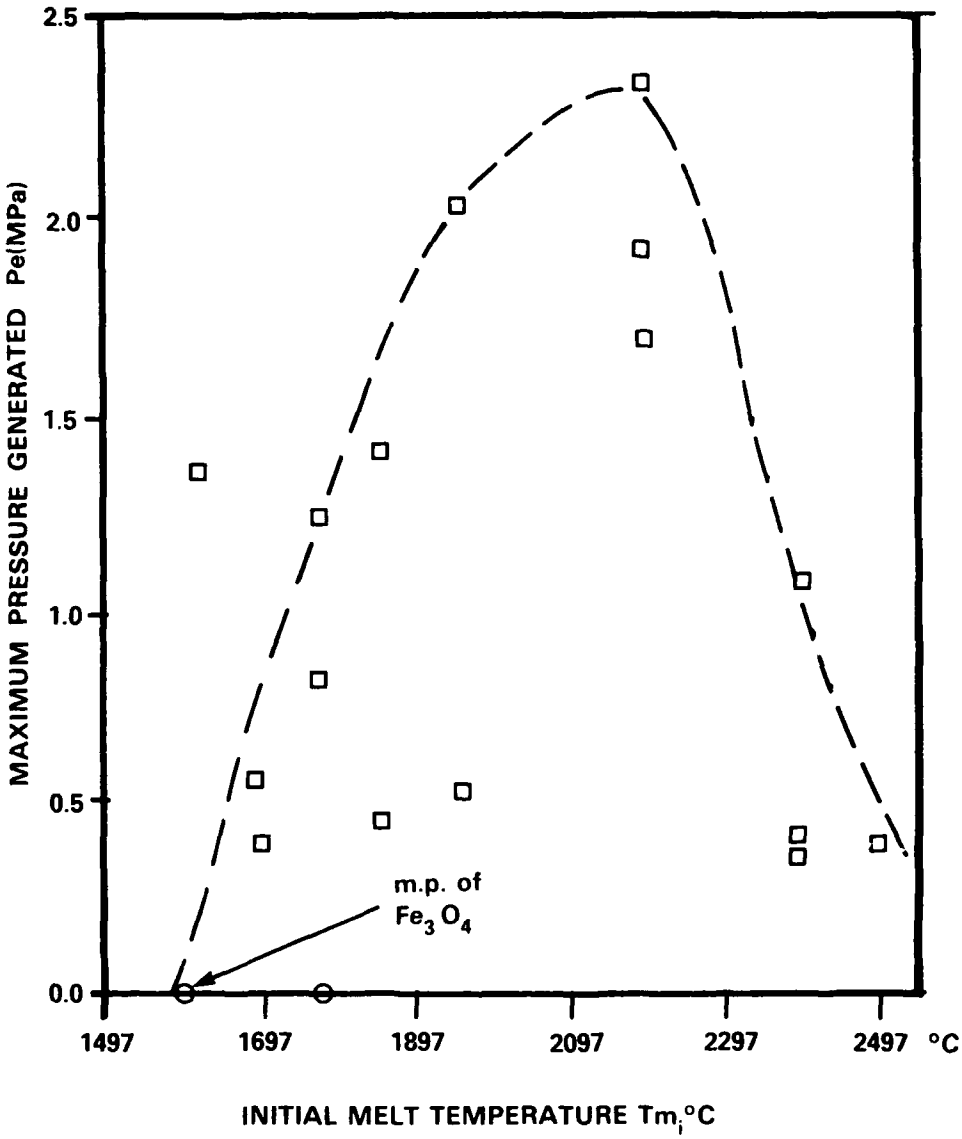

Figure 38

PEAK PRESSURE GENERATED AS THE MAJOR STEAM EXPLOSION BUBBLE COLLAPSES VS MELT TEMPERATURE FOR A MOLTEN IRON OXIDE DROP RELEASED INTO WATER [39]

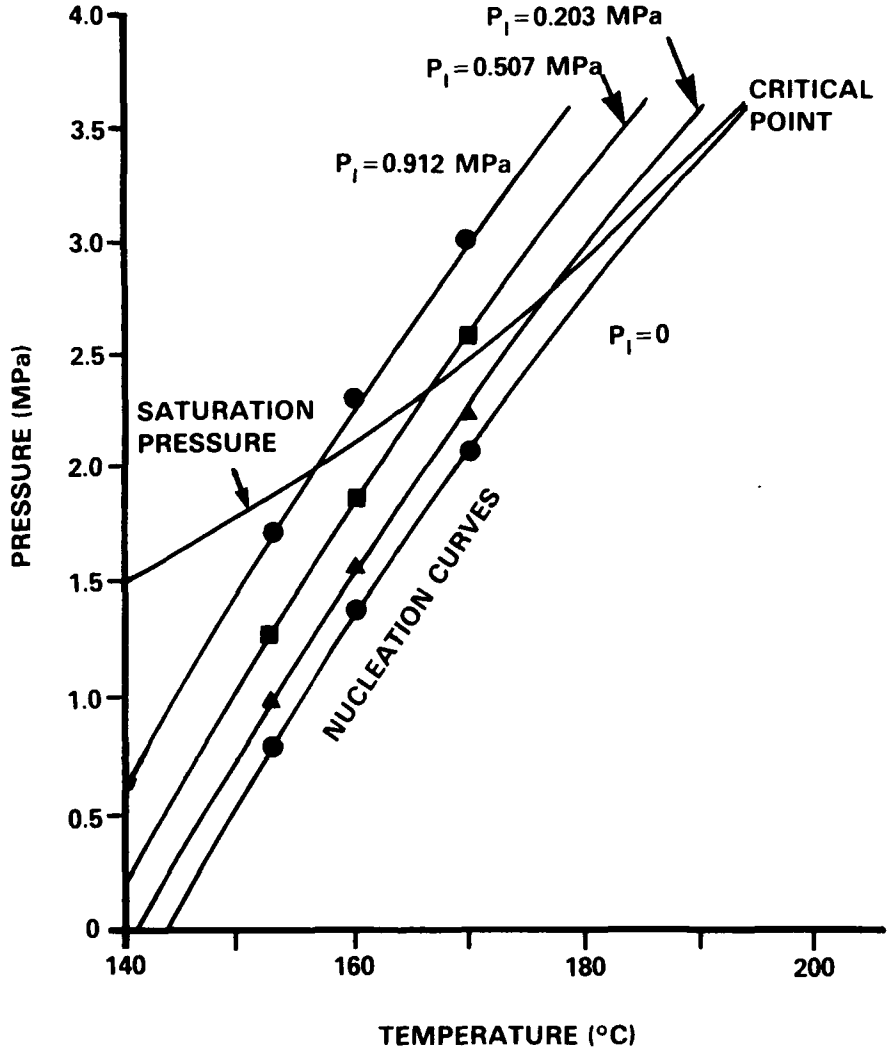

Figure 39

MEASURED AND PREDICTED NUCLEATION CURVES FOR SOLUTIONS OF NITROGEN IN ETHYL-ETHER [11]

DOCUMENT CONTROL DATA

(Security classification of title, body of abstract and indexing annotation must be entered when the overall document is classified)

1. ORIGINATOR (the name and address of the organization preparing the document. Organizations for whom the document was prepared, e.g. Establishment sponsoring a contractor's report, or tasking agency, are entered in section 8.)

Defence Research Establishment Suffield
Box 4000, Medicine Hat, AB
T1A 8K6

2. SECURITY CLASSIFICATION (overall security classification of the document. including special warning terms if applicable)

unclassified

3. TITLE (the complete document title as indicated on the title page. Its classification should be indicated by the appropriate abbreviation (S,C,R or U) in parentheses after the title.)

A REVIEW OF LARGE SCALE AND SMALL SCALE UNDERWATER THERMAL EXPLOSIONS

4. AUTHORS (Last name, first name, middle initial. If military, show rank, e.g. Doe, Maj. John E.)

Rizk, M.

5. DATE OF PUBLICATION (month and year of publication of document)

April 1990

6a. NO. OF PAGES (total containing information. Include Annexes, Appendices, etc.)

94

6b. NO. OF REFS (total cited in document)

40

6. DESCRIPTIVE NOTES (the category of the document, e.g. technical report, technical note or memorandum. If appropriate, enter the type of report, e.g. interim, progress, summary, annual or final. Give the inclusive dates when a specific reporting period is covered.)

Suffield Memorandum No. 1272

8. SPONSORING ACTIVITY (the name of the department project office or laboratory sponsoring the research and development. Include the address.)

CRAD/DRES

9a. PROJECT OR GRANT NO. (if appropriate, the applicable research and development project or grant number under which the document was written. Please specify whether project or grant)

011SA

9b. CONTRACT NO. (if appropriate, the applicable number under which the document was written)

10a. ORIGINATOR'S DOCUMENT NUMBER (the official document number by which the document is identified by the originating activity. This number must be unique to this document.)

SM 1272

10b. OTHER DOCUMENT NOS. (Any other numbers which may be assigned this document either by the originator or by the sponsor)

11. DOCUMENT AVAILABILITY (any limitations on further dissemination of the document, other than those imposed by security classification)

(X) Unlimited distribution
( ) Distribution limited to defence departments and defence contractors; further distribution only as approved
( ) Distribution limited to defence departments and Canadian defence contractors; further distribution only as approved
( ) Distribution limited to government departments and agencies; further distribution only as approved
( ) Distribution limited to defence departments; further distribution only as approved
( ) Other (please specify):

12. DOCUMENT ANNOUNCEMENT (any limitation to the bibliographic announcement of this document. This will normally correspond to the Document Availabilty (11). However, where further distribution (beyond the audience specified in 11) is possible, a wider announcement audience may be selected.)

13. ABSTRACT (a brief and factual summary of the document. It may also appear elsewhere in the body of the document itself. It is highly desirable that the abstract of classified documents be unclassified. Each paragraph of the abstract shall begin with an indication of the security classification of the information in the paragraph (unless the document itself is unclassified) represented as (S), (C), (R), or (U). It is not necessary to include here abstracts in both offical languages unless the text is bilingual).

This report contains a review of large scale propagating thermal explosions and small scale single drop explosions. The review of large scale propagating thermal explosions identifies potential thermal explosive systems, as well as the experimental conditions and geometrical configurations, conducive to the establishment of thermal detonations.

The review of small scale single drop explosions identifies experimental data relevant to the design of detonating systems of thermal explosives. In addition, the effect of various thermodynamic parameters on the strength of both spontaneous and triggered single drop explosions is predicted qualitatively based on two promising fragmentation mechanisms; a new vapour/gas melt supersaturation mechanism and the water entrapment mechanism. It is shown that the vapour destabilization and nucleation phenomena which constitute the heart of the two fragmentation mechanisms govern single drop thermal explosions. The experimental data, however, is neither conclusive nor sufficient for the development of a predictive model. For some molten metal water systems (Aℓ/water), the data was found to be incomplete and in the case of Fe-$Aℓ_2O_3$/water, a system of particular interest, there is no available data. Recommendations are made for new experimental studies to rigorously assess the two fragmentation mechanism and to obtain a better understanding of vapour explosion phenomenon in general.

14. KEYWORDS, DESCRIPTORS or IDENTIFIERS (technically meaningful terms or short phrases that characterize a document and could be helpful in cataloguing the document. They should be selected so that no security classification is required. Identifiers, such as equipment model designation, trade name, military project code name, geographic location may also be included. If possible keywords should be selected from a published thesaurus. e.g. Thesaurus of Engineering and Scientific Terms (TEST) and that thesaurus-identified. If it is not possible to select indexing terms which are Unclassified, the classification of each should be indicated as with the title.)

thermal
explosion
detonation
underwater